

**THE MORPHOLOGY AND PROPERTIES OF EVA/MALAYSIAN  
EMPTY FRUIT BUNCH COMPOSITES**

**by**

**JEREMIA SHALE SEFADI (B.Sc. Honours)**

**Submitted in accordance with the requirements for the degree**

**Master in Science (M.Sc.)**

**Department of Chemistry**

**Faculty of Natural and Agricultural Sciences**

**at the**

**UNIVERSITY OF THE FREE STATE (QWAQWA CAMPUS)**

**SUPERVISOR: PROF AS LUYT**

**07 December 2010**

## DECLARATION

We, the undersigned, hereby declare that the research in this thesis is Mr Sefadi's own original work and has not previously, in its entirety or in part, been submitted to any other university in order to obtain a degree.

---

J.S. Sefadi

---

Prof A.S. Luyt

## **DEDICATION**

The credit must be given to Almighty God for the strength and potential given to me throughout the entire piece of research work. This research work is dedicated to my beloved wife Ntebaleng Eva Molise-Sefadi and my son Kananelo Sefadi for their endless love, patience and well-displayed moral support. This thesis is also dedicated to my dear parents for their ever lasting love and encouragement during the tough times of this study.

## ABSTRACT

Composites based on ethylene vinyl acetate copolymers (EVA18 and EVA28) containing different vinyl acetate (18 and 28% VA) contents and empty fruit bunch (EFB) fibre were studied in this project. The EVA-EFB composites were prepared by melt mixing using a Brabender Plastograph mixer. The structure and morphology of the composites were characterized using scanning electron microscopy (SEM) and Fourier-transform infrared (FTIR) spectroscopy. The SEM results showed an improved extent of interfacial adhesion between the polymer and the fibre with an increase in the amount of vinyl acetate in the copolymers. The DSC results revealed that the melting and crystallization enthalpies decreased significantly with increasing VA content, while the presence of EFB fibre had very little influence on the melting and crystallization behaviour of both EVA18 and EVA28. The thermogravimetric analysis showed that EVA18 is more thermally stable than EVA28 due to the larger amount of VA in EVA28, which increases the amorphous phase in the semi-crystalline material. The decomposition of EFB fibre seems to be retarded when incorporated into the EVA copolymers. Dynamic mechanical analysis (DMA) revealed that both the storage modulus and loss modulus decreased significantly with an increase in vinyl acetate content, and that these two properties observably increased with the incorporation of the fibre. The glass transition temperature also increased observably with increasing fibre loading, and decreased with an increase in the vinyl acetate content. The stress and strain at break showed a similar decrease with increasing fibre content for both EVA18 and EVA28, while Young's modulus increased much more significantly with increasing fibre content for EVA28. The reasons for this are (i) the very low Young's modulus of EVA28 compared to that of EVA18, and (ii) the slightly better interaction between EVA28 and the fibre because of the higher VA content of this copolymer. Generally it seems as if the improvement in interaction between EVA28 and EFB was not significant enough to overcome the inherent weak properties of EVA28, and that in this case it is probably better to use EVA18 when EVA/EFB composites with good properties are needed.

## LIST OF ABBREVIATIONS

AC	Alternating current
ASTM	American Society for Testing and Materials
ATR-FTIR	Attenuated total reflectance Fourier-transform infrared spectroscopy
BSE	Back scattered electrons
DCP	Dicumyl peroxide
DMA	Dynamic mechanical analysis
DSC	Differential scanning calorimetry
3-D	Three dimensional
EFB	Empty fruit bunch
Eq	Equation
EVA	Ethylene vinyl acetate
EVA-GMA	Ethylene vinyl acetate-glycidyl methacrylate
EVAL	Ethylene vinyl alcohol
EVA-MA	Ethylene vinyl acetate grafted maleic anhydride
EWR	Eucalyptus wood residue
FRCs	Fibre reinforced composites
FRPCs	Fibre reinforced polymer composites
FTIR	Fourier transform infrared spectroscopy
GMA	Glycidyl methacrylate
HDPE	High density polyethylene
IR	Infrared
LDPE	Low-density polyethylene
LLDPE	Linear low-density polyethylene
MAPP	Maleic anhydride grafted polypropylene
MAPE	Maleic anhydride grafted polyethylene
MA-SEBS	MA-styrene-(ethylene-co-butylene)-styrene
MFI	Melt flow index
MLDPE	Maleated low density polyethylene
NaOH	Sodium hydroxide
NFs	Natural fibres

N-66	Nylon-66
PE	Polyethylene
PEGMA	Poly(ethylene-co-glycidyl methacrylate)
PET	Poly(ethylene terephthalate)
PMMA	Poly(methyl methacrylate)
PP	Polypropylene
PRCs	Particle reinforced composites
PS	Polystyrene
PVC	Polyvinyl chloride
RHF	Rice husk flour
SCB	Sugarcane bagasse
SCs	Structural composites
SE	Secondary electrons
SEM	Scanning electron microscopy
SF	Sisal fibre
SFs	Synthetic fibres
TC-PBT	Titanate coupling-polybutylene terephthalate
TC-POT	Titanate coupling-polyoxide terephthalate
TGA	Thermogravimetric analysis
TPMC	Thermoplastic matrix composite
TPCs	Thermoplastic composites
USA	United States of America
VA	Vinyl acetate
WF	Wood fibres/flour
WPMMA	Wood poly(methyl methacrylate)
WP	Wood powder
WSF	Wheat straw flour

## LIST OF SYMBOLS

E	Young's modulus
E'	Storage modulus
E''	Loss modulus
F	Force applied in N
$\epsilon_b$	Elongation at break
$\sigma_b$	Stress at break
$\rho$	Density of the material
Hz	Hertz
$\Delta H_m$	Specific enthalpy of melting
$\Delta H_m^0$	Specific enthalpy of melting for 100% crystalline PE
$\Delta H_m^{obs}$	Observed melting enthalpy
$\Delta H_m^{calc}$	Calculated melting enthalpy
L	Extension in the gauge
M	Middle lamella
P	Primary wall (fibril position unarranged)
S	Secondary wall
S <sub>1</sub>	Secondary wall I (two or more fibrillar layers crossing one another and positioned spirally along the fibre axis)
S <sub>2</sub>	Secondary wall II (fibrils wound spirally around the fibre axis)
S <sub>3</sub>	Secondary wall III (fibrils tightly interlaced)
T <sub>c</sub>	Crystallization temperature
T <sub>d</sub>	Decomposition temperature
T <sub>g</sub>	Glass transition temperature
T <sub>m</sub>	Melting temperature
T <sub>o,m</sub>	Onset temperature of melting
T <sub>p,m</sub>	Peak temperature of melting
w	Weight
w <sub>EVA</sub>	Weight fraction
w/w	Weight by weight
$\chi_c$	Degree of crystallinity

## TABLE OF CONTENTS

	<b>Page</b>
<b>DECLARATION</b>	i
<b>DEDICATION</b>	ii
<b>ABSTRACT</b>	iii
<b>LIST OF ABBREVIATIONS</b>	iv
<b>LIST OF SYMBOLS</b>	vi
<b>TABLE OF CONTENTS</b>	vii
<b>LIST OF TABLES</b>	x
<b>LIST OF FIGURES</b>	xi
<b>CHAPTER 1: INTRODUCTION</b>	1
1.1 Background	1
1.2 Objective of the study	5
1.3 Structure of the thesis	6
1.4 References	7
<b>CHAPTER 2: LITERATURE SURVEY</b>	11
2.1 Introduction	11
2.2 Natural fibres	12
2.2.1 Composition and structure	12
2.2.2 Cellulose	13
2.2.3 Hemicellulose	14
2.2.4 Lignin	15
2.2.5 Structure of natural fibres	16
2.2.6 Classification of natural fibres	17
2.2.7 Empty fruit bunch (EFB) fibre	18
2.3 Matrix material	18
2.3.1 Ethylene vinyl acetate (EVA)	19
2.4 PE/natural fibre composites	20
2.4.1 Preparation and morphology	20
2.4.2 Thermal properties	24
2.4.2.1 Melting and crystallization	24



2.4.2.2	Thermal stability	25
2.4.3	Thermo-mechanical and mechanical properties	27
2.4.3.1	Thermo-mechanical properties	27
2.4.3.2	Mechanical properties	30
2.5	References	32
<b>CHAPTER 3: EXPERIMENTAL</b>		<b>44</b>
3.1	Materials	44
3.1.1	Ethylene vinyl acetate (EVA)	44
3.1.2	Empty fruit bunch (EFB) fibre	44
3.2	Methods	44
3.2.1	Preliminary work on EFB fibre	44
3.2.2	Preparation of composites	45
3.3	Characterization and analysis	45
3.3.1	Scanning electron microscopy (SEM)	45
3.3.2	Differential scanning calorimetry (DSC)	46
3.3.3	Thermogravimetric analysis (TGA)	47
3.3.4	Dynamic mechanical analysis (DMA)	47
3.3.5	Tensile testing	49
3.3.6	Fourier transform infrared (FTIR) spectroscopy	50
3.4	References	50
<b>CHAPTER 4: RESULTS AND DISCUSSION</b>		<b>52</b>
4.1	Scanning electron microscopy (SEM)	52
4.2	Attenuated total reflectance Fourier-transform infrared spectroscopy (ATR-FTIR)	54
4.3	Differential scanning calorimetry (DSC)	59
4.4	Thermogravimetric analysis (TGA)	66
4.5	Dynamic mechanical analysis (DMA)	69
4.6	Tensile testing	78
4.7	References	82
<b>CHAPTER 5: CONCLUSIONS</b>		<b>88</b>
5.1	Comparison of the EVA copolymers	88

5.2	EVA/EFB composites	89
5.3	Final conclusion	90
<b>ACKNOWLEDGEMENTS</b>		91
<b>APPENDIX</b>		95

## LIST OF TABLES

		<b>Page</b>
Table 2.1	Chemical composition of some common lignocellulosic fibres	13
Table 2.2	Comparison of the properties of some natural fibres with those of conventional fibres	13
Table 3.1	List of the samples and compositions used in the present study	45
Table 3.2	Summary of DMA analysis conditions	48
Table 3.3	Tensile testing analysis conditions	50
Table 4.1	Some important peaks in the FTIR spectra of the EVA copolymers, EFB and the EVA/EFB composites	58
Table 4.2	DSC heating results for all the investigated samples	60
Table 4.3	DSC cooling results for all the investigated samples	62
Table 4.4	TGA results for all the investigated samples	67
Table 4.5	Relaxation temperatures for the EVA copolymers and the EVA/EFB composites as determined from the $\tan \delta$ curves	72
Table 4.6	Summary of mechanical properties for the samples	79

## LIST OF FIGURES

		Page
Figure 2.1	Molecular structure of cellulose	14
Figure 2.2	Structure of hemicellulose	15
Figure 2.3	Molecular structure of lignin	16
Figure 2.4	Internal structure of natural fibre	16
Figure 2.5	Classification of natural fibres	17
Figure 2.6	Unit structure of EVA copolymer	20
Figure 3.1	Dumbbell-shaped specimen used for tensile testing (sample thickness 2 mm)	49
Figure 4.1	SEM micrographs of 90/10 w/w EVA18/EFB ((a) 100x magnification & (b) 1000x magnification), and 70/30 w/w EVA18/EFB ((c) 100x magnification & (d) 300x magnification) composites	53
Figure 4.2	SEM micrographs of 90/10 w/w EVA28/EFB ((a) 100x magnification & (b) 300x magnification), and 70/30 w/w EVA28/EFB ((c) 100x magnification & (d) 300x magnification) composites	54
Figure 4.3	Comparison of the FTIR spectra of the pure EVA copolymers containing different VA contents	56
Figure 4.4	FTIR spectra of EFB, EVA18 and an EVA18/EFB composite	57
Figure 4.5	FTIR spectra of EFB, EVA28 and an EVA28/EFB composite	58
Figure 4.6	DSC heating curves for the EVA18 and EVA28 copolymers	59
Figure 4.7	DSC cooling curves for EVA18 copolymer and EVA28 copolymer	61
Figure 4.8	DSC heating curves for EVA18 and the EVA18/EFB composites	62
Figure 4.9	DSC cooling curves for EVA18 and the EVA18/EFB composites	63
Figure 4.10	DSC heating curves for EVA28 and the EVA28/EFB composites	64
Figure 4.11	DSC cooling curves for EVA28 and the EVA28/EFB composites	65
Figure 4.12	TGA curves for the different EVA copolymers	66
Figure 4.13	TGA curves for EFB, EVA18, and the EVA18/EFB composites	68
Figure 4.14	TGA curves for EFB, EVA28, and the EVA28/EFB composites	69
Figure 4.15	Comparison of the storage modulus as a function of temperature for the pure EVA18 and EVA28 copolymers	70
Figure 4.16	Comparison of the loss modulus as a function of temperature for the pure EVA18 and EVA28 copolymers	71

Figure 4.17	Comparison of $\tan \delta$ as a function of temperature for pure EVA18 and EVA28 copolymers	72
Figure 4.18	Storage modulus as a function of temperature for pure EVA18 and the EVA18/EFB composites	73
Figure 4.19	Loss modulus as a function of the temperature for pure EVA18 and the EVA18/EFB composites	74
Figure 4.20	Dissipation factor as a function of the temperature for pure EVA18 and the EVA18/EFB composites	75
Figure 4.21	Storage modulus as a function of the temperature for pure EVA28 and EVA28/EFB composites	76
Figure 4.22	Loss modulus as a function of the temperature for pure EVA28 and EVA28/EFB composites	76
Figure 4.23	$\tan \delta$ as a function of the temperature for pure EVA28 and EVA28/EFB composites	77
Figure 4.24	Stress at break of EVA18/EFB and EVA28/EFB as a function of EFB fibre content	80
Figure 4.25	Elongation at break of EVA18/EFB and EVA28/EFB as a function of EFB fibre loading	80
Figure 4.26	Young's modulus of the different composites as a function of EFB fibre content	81

# CHAPTER 1

## INTRODUCTION

### 1.1 Background

Polymer composites are defined as combinations of two or more constituent materials in which one of the materials is called the reinforcing phase and the other material is known as the matrix phase. The reinforcing material is in the form of fibres, sheets, or particles, and is embedded in the other material called the polymeric matrix. The reinforcing material and the matrix can be metal, ceramic, or polymer [1]. These composites were highly recognized in the last few decades by numerous researchers as the leading edge of materials technology [2]. This is due to a rapid development in the use of the materials in engineering applications, owing to their great usefulness and high performance [3,4]. The idea of using composite materials, however, is not a new or recent one but has been around for thousands of years. The Ancient Egyptians used chopped straw to reinforce mud bricks; and Mongol warriors used a composite consisting of bullock tendon, horn, bamboo strips, silk and pine resin to produce high-performance archery bows. Since the early 1960s there has been an increase in the demand for stronger, stiffer and more lightweight materials for use in the aerospace, transportation and construction industries. High performance demands on engineering materials have led to extensive research and development of new and improved materials, such as composites [5].

The properties of the new structure with an identifiable interface are dependent upon the properties of the constituent materials as well as the interface. This implies that composites have properties that could not be achieved by either of the constituent components alone such as being strong, stiff, and lightweight. Composites are used because their overall properties are more superior to those of the individual components. For example: polymer/ceramic composites have a greater modulus than the polymer component, but they are not as brittle as ceramic [1,3,6]. This often translates into some of the advantages displayed by the composite materials.

Composites offer several advantages over other materials like metal alloys [7]. Within the aerospace and marine industry where exceptional performance is required but weight is critical, composites become more and more important. The advantages of composites may be summarized as:

- ❖ High strength to weight ratio (low density, high tensile strength).
- ❖ High creep resistance
- ❖ High tensile strength at elevated temperatures
- ❖ High toughness

Although composite materials have certain advantages over conventional materials, they also have some disadvantages. In practice, these disadvantages are commonly summarized as (i) high cost compared to metals, and (ii) low fracture toughness and moisture absorption [7]. Despite these drawbacks, composite materials gained more interest from the research community and found more applications in industrial sectors.

There are many applications of composites in every day life. The composites are widely used in diverse fields such as appliances, spacecrafts and construction, transportation, military, industrial and biomedical applications mainly because of their excellent thermo-mechanical properties [8-12]. These applications lead to the composite materials being categorized or classified according to different functions and properties.

Composites can generally be classified into several major types or categories (particle-reinforced composites (PRCs), structural composites (SCs), and fibre-reinforced composites (FRCs)) depending on their geometry. The focus of this research is on the development of FRCs. Reinforcing fibres can be made of metals, ceramics, glasses, or polymers that have been turned into graphite that are known as carbon fibres [13,14]. They are used in some of the most advanced and therefore most expensive sports equipment, such as a time-trial racing bicycle frames that comprise of carbon fibres [15] in a thermoset polymer matrix. Body parts of race cars and some other vehicles are composites made of glass fibres in a thermoset matrix, with some currently replaced by natural fibre reinforcing materials coupled with a thermoplastic matrix as an alternative. There are many combinations of fillers and thermoplastics which are currently available commercially in various companies across the globe. Amongst them are combinations of thermoplastics with organic (natural) fillers and inorganic (synthetic) fillers.

Fibres/fillers are defined as materials that are added to a polymer formulation to lower the compound cost or to improve properties. They are generally added to commercial matrix resins for economic purposes and also to modify properties such as stiffness, tensile strength, heat distortion and mouldability [16]. Such materials can be in the form of solids, liquids or gases. Traditionally, fillers are regarded as additives due to their unfavourable geometrical features, surface area or surface chemical composition, which in essence could steadily increase the modulus of the polymer, while tensile and flexural strengths remain unchanged or decrease to a certain extent. The level of enhancement depends mainly on the type of filler, size, shape, fibre loading, and surface treatment which supports interaction between the filler and the polymer [17].

Generally there are several types of fibres used in fibre-reinforced polymer composites such as conventional fibres called non-renewable synthetic fibres, SFs (carbon, aramid, and glass) and organic fibres (natural fibres). The glass fibres are the most commonly used because they can be produced at a relatively low cost, are also heavier, and have the greatest flexibility. Aramid is a stiffer fibre and moderate in cost, which is the lightest one in weight. Carbon is moderate to high in price, slightly heavier than Kevlar but lighter than glass, and features certain varieties that have exceptionally high stiffness [18]. In this present work, the emphasis is on one of the natural fibres due to the advantages and properties demonstrated by the material.

Natural fibres (NFs) are a major renewable resource material throughout the world, particularly in the tropics. NFs exhibit a number of advantages compared with inorganic fibres; for example they are lower in density and cost, non-abrasive to processing equipment, relatively harmless, biodegradable and renewable. Typically, their mechanical properties such as relatively high strength, high stiffness, and low density are comparable to those of their inorganic counter parts [10-12,19-23]. Natural fibres seem to have little resistance towards environmental influences. Therefore, they can serve as reinforcements by strongly enhancing the strength and stiffness of the resulting material and can also be regarded as a substitute to SFs for use in a number of applications. In this study, a lignocellulosic-based fibre is used as a reinforcing agent because of its availability and properties.

The empty fruit bunch (EFB) fibre is one example of lignocellulosic materials, and it has received increased attention for price-driven applications. EFB is a by-product derived from



an oil palm tree called *Elaeis guineensis*. EFB is a cheap, biodegradable, non-toxic, and widely utilized natural fibre and abundantly available in Malaysia as well as other tropical forests of West Africa [22,24]. EFB is used as a raw material in various applications including power generation, composites formulation, and in the paper making industry. As a valuable biomass residue, it has an energy content of 3700 Kcal kg<sup>-1</sup> dry weight [25], and its use in polymer composites will remedy issues around environmental problems, especially those related to the disposal of oil palm wastes [22,26]. Several studies supported the incorporation of EFB into different types of polymer matrices to obtain cost reduction and reinforcement [2,28,43].

There are many polymer resin systems used as matrices in fibre-reinforced polymer composites (FRPCs). They can be classified into two types: thermoset and thermoplastic polymers. Thermoset materials are crosslinked polymers that cannot be melted once cured, and include resins such as epoxies, polyesters and phenolics. They generally have a higher resistance to heat than thermoplastics [27]. Thermoplastic polymers are long chain polymers that can be either amorphous in structure or semi-crystalline depending on their characteristic transition temperature. Molecules in thermoplastics are held together by relatively weak intermolecular forces so that the material softens when exposed to heat and then returns to its original condition when cooled. Common examples of thermoplastic polymers are polyethylene (PE), polypropylene (PP), polystyrene (PS), polyethylene terephthalate (PET), nylon (N-66), and polyvinyl chloride (PVC) [20]. The current study focused on a PE based thermoplastic matrix known as ethylene vinyl acetate (EVA) copolymer, which is very flexible and transparent.

Ethylene vinyl acetate (EVA) copolymers are randomly structured polymers, which in essence offer excellent ozone and weather resistance, and also good mechanical properties [28-30]. EVA is a semi-crystalline polyethylene (PE) material bearing polar functional groups known as vinyl acetate (VA) and it can readily be synthesized with various VA contents [31,32]. It is chosen to be mixed with empty fruit bunch (EFB) fibre because of its excellent properties and halogen-free [33,34] thermoplasticity in the cable industry. EVA is also suitable in drug control release systems or devices in the medical applications, and also it has been used for membrane preparation in various applications [35,36].

A thermoplastic matrix composite (TPMC) is a family of polymer reinforced structures which represent an important innovation in the field of composites. The properties of thermoplastic composites (TPCs) are generally influenced by the processing parameters such as a mixing time, rotor speed (rpm), and temperature in the compounding process [11]. Generally, there are many different methods used for the preparation of the composites including melt-mixing method and solution-mixing methods. The melt-mixing method is more advantageous in simplicity and cost effectiveness over other methods like solution mixing, which is too expensive and time consuming [37-39]. In this particular study, EVA thermoplastic composites were prepared by a melt-mixing method using a Brabender Plastograph internal mixer.

The purpose of mixing EFB fibre with an EVA thermoplastic material is to develop a material compound with a very low specific gravity, high flexibility, toughness, adhesion characteristics, stress-cracking resistance, high clarity and transparency as well as meeting the high initial modulus requirement. However, the major drawback associated with natural fibre polymer composites is the lack of thermal stability during processing, poor dispersion characteristics in the thermoplastic melt, and incompatibility exhibited between the hydrophobic polymeric matrix and the hydrophilic nature of the natural fibres [8,10,21]. This poor compatibility between the two components leads to weak interfacial adhesion, which results in poor mechanical properties [8,10,12]. Another common problem of natural fibre/polymer composites is the high sensitivity to water or poor resistance to moisture absorption [26,40]. All of these identified problems are often addressed by the use of adhesion-promoting agents such as a coupling agent or compatibilizer, or even fibre-surface modifying treatment [26,42]. In addition, it is also known that pre-impregnation of the fibre with the polyolefin solution will vitally improve adhesion [19,41]. In our work, the EVA copolymers have polar functional groups which should promote better adhesion and interaction between the EFB and the polymeric matrix, and therefore none of the components were modified or treated.

## **1.2 Objective of the study**

The objective of this study was to investigate composites based on EVA copolymers and Malaysian EFB fibre, and to study the effects of the fibre content and vinyl acetate (VA) content of the EVA copolymers on the thermal and mechanical properties. Another objective

is to explain these observations in terms of the morphology and possible interactions between the Malaysian EFB fibre and the EVA copolymer resin. In this work, EVA copolymers containing various VA contents (18 and 28% VA) were mixed with Malaysian EFB fibre. Different fibre loadings were used in these composites. The EFB fibre was prominently used as a filler and reinforcement to enhance the physical and mechanical properties of the polymeric matrix.

The specific activities of this research project are summarized as follows:

- ❖ Preparation of the EVA copolymer composites containing different amounts of vinyl acetate with Malaysian EFB fibre.
- ❖ To determine the morphologies of the different EVA copolymer samples using scanning electron microscopy (SEM).
- ❖ Determination of the melting and crystallization behaviour of the EVA composites using differential scanning calorimetry (DSC).
- ❖ To evaluate the influence of the Malaysian EFB fibre on the thermal stability of the samples using thermogravimetric analysis (TGA).
- ❖ Determination of the influence of the Malaysian EFB fibre on the dynamic mechanical behaviour of the samples using dynamic mechanical analysis (DMA).
- ❖ To measure the tensile properties of EVA/Malaysian EFB fibre in order to assess the performance of the end product.
- ❖ To determine possible chemical interaction between EVA copolymers and EFB fibres using FTIR microscopy.
- ❖ Explanation of the observed properties in terms of the compositions and morphologies of the composites.

### **1.3 Structure of the thesis**

This thesis consists of five chapters.

Chapter 1: Background and objectives

Chapter 2: Literature survey

Chapter 3: Experimental

Chapter 4: Results and discussion

Chapter 5: Conclusions

## 1.4 References

1. E.I.M. Asloun, M. Nardin, J. Schultz. Stress transfer in single-fibre composites: effect of adhesion, elastic modulus of fibre and matrix, and polymer chain mobility. *Journal of Materials Science* 1989; 24:1835-1844.
2. M.Z.M. Yusoff, M.S. Salit, N. Ismail. Tensile properties of single oil palm empty fruit (OPEFB) fibre. *Sains Malaysian* 2009; 38:525-529.
3. T.H.D. Sydenstricker, S. Mochnaz, S.C. Amico. Pull-out and other evaluations in sisal-reinforced polyester biocomposites. *Polymer Testing* 2003; 22:375-380.
4. I. Baroulaki, J.A. Mergos, G. Pappa, P.A. Tarantili, D. Economides, K. Magoulas, C.T. Dervos. Performance of polyolefin composites containing recycled paper fibres. *Polymers for Advanced Technologies* 2006; 17:954-966.  
DOI: 10.1002/pat.827
5. <http://www.epp.goodrich.com/why.shtml> (September 2008).
6. H.D. Rozman, B.K. Kon, A. Abusamah, R.N. Kumar, Z.A. Mohd. Ishak. Rubberwood-high density polyethylene composites: effect of filler size and coupling agents on mechanical properties. *Journal of Applied Polymer Science* 1998; 69:1993-2004.  
DOI: 0021-8995/98/101993-12
7. E.C. Botelho, R.A. Silva, L.C. Pardini, M.C. Rezende. A review on the development and properties of continuous fibre/epoxy/aluminum hybrid composites for aircraft structures. *Materials Research* 2006; 9:247-256.
8. R.A. Khan, M.A. Khan. Mechanical, degradation, and interfacial properties of synthetic degradable fibre reinforced polypropylene composites. *Journal of Reinforced Plastics and Composites* 2010; 29:466-476.
9. D.N. Saheb, J.P. Jog. Natural fibre polymer composites: A review. *Advances in Polymer Technology* 1999; 18:351-363.  
DOI: 0730-6679/99/040351-13
10. Y. Habibi, W.K. El-Zawawy, M.M. Ibrahim, A. Dufresne. Processing and characterization of reinforced polyethylene composites made with lignocellulosic fibres from Egyptian agro-industrial residues. *Composites Science and Technology* 2008; 68:1877-1885.  
DOI: 10.1016/j.compscitech.2008.01.008

11. K. Joseph, R.D.T. Filho, B. James, S. Thomas, L.H. De Carvalho. A review on sisal fibre reinforced polymer composites. *Revista Brasileira de Engenharia Agricola e Ambiental* 1999; 3:367-379.
12. M. Khalid, A. Salmiation, C.T. Ratnam, C.A. Luqman. Effect of trimethylolpropane triacrylate (TMPTA) on the mechanical properties of palm fibre empty fruit bunch and cellulose fibre biocomposite. *Journal of Engineering Science and Technology* 2008; 3:153-162.
13. C.J.R. Verbeek. The influence of interfacial adhesion, particle size and size distribution on the predicted mechanical properties of particulate thermoplastic composites. *Materials Letters* 2003; 57:1919-1924.
14. A. Kalam, B.B. Sahari, Y.A. Khalid, S.V. Wong. Fatigue behaviour of oil palm fruit bunch fibre/epoxy and carbon fibre/epoxy composites. *Composite Structures* 2005; 71:34-44.
15. Q.H. Zhang, D.J. Chen. Percolation threshold and morphology of composites of conducting carbon black/polypropylene/EVA. *Journal of Materials Science* 2004; 39:1751-1757.
16. H. Unal. Morphology and mechanical properties of composites based on polyamide 6 and mineral additives. *Materials and Design* 2004; 25:483-487.
17. D.G. Dikobe, A.S. Luyt. Morphology and properties of polypropylene/ethylene vinyl acetate copolymer/wood powder blend composites. *eXPRESS Polymer Letters* 2009; 3:190-199.
18. A.K. Mohanty, M. Misra, G. Hinrichsen. Biofibers, biodegradable polymers and biocomposites: An overview. *Macromolecular Materials and Engineering* 2000; 276/277:1-24.
19. P.J. Herrera-Franco, A. Valadez-González. Mechanical properties of continuous natural fibre-reinforced polymer composites. *Composites: Part A* 2004; 35:339-345.
20. M.E. Malunka, A.S. Luyt, H. Krump. Preparation and characterization of EVA-sisal fibre composites. *Journal of Applied Polymer Science* 2006; 100:1607-1617.
21. R. Dweiri, C.H. Azhari. Thermal and flow property-morphology relationship of sugarcane bagasse fibre-filled polyamide 6 blends. *Journal of Applied Polymer Science* 2004; 92:3744-3754.
22. H.D. Rozman, G.S. Tay, A. Abubakar, R.N. Kumar. Tensile properties of oil palm empty fruit bunch-polyurethane composites. *European Polymer Journal* 2001; 37:1759-1765.

23. H.D. Rozman, A.R. Rozyanty, G.S. Tay, R.N. Kumar. The effect of glycidyl methacrylate treatment of empty fruit bunch (EFB) on the properties of ultra-violet radiation cured EFB-unsaturated polyester composite. *Journal of Applied Polymer Science* 2010; 115:2677-2682.
24. M.S. Sreekala, M.G. Kumaran, S. Thomas. Oil palm fibres: Morphology, chemical composition, surface modification, and mechanical properties. *Journal of Applied Polymer Science* 1997; 66:821-835.
25. R.M. Soom, W.H.W. Hassan, A.B. Gapor MD-Top, K. Hassan. Thermal properties of oil palm fibre, cellulose and its derivatives. *Journal of Oil Palm Research* 2006; 18:272-277.
26. M.J. John, B. Francis, K.T. Varughese, S. Thomas. Effect of chemical modification on properties of hybrid fibre biocomposites. *Composites: Part A* 2008; 39:352-363.
27. M. Xanthos, D.B. Todd. "Plastics processing", *Kirk-Othmer Encyclopedia of Chemical Technology*, 4<sup>th</sup> Ed., John Wiley & Sons, New York, 1996;19:1-16.
28. M. González Alriols, A. Tejado, M. Blanco, I. Mondragon, J. Labidi. Agricultural palm oil tree residues as raw material for cellulose, lignin and hemicelluloses production by ethylene glycol pulping process. *Chemical Engineering Journal* 2009; 148:106-114.
29. S. Chen, J. Zhang, J. Su. Effect of damp-heat aging on the properties of ethylene vinyl acetate copolymer and ethylene acrylic acid copolymer blends. *Journal of Applied Polymer Science* 2009; 114:3110-3117.
30. G. Takidis, D.N. Bikiaris, G.Z. Papageorgiou, D.S. Achilias, I. Sideridou. Compatibility of low-density polyethylene/poly(ethylene-co-vinyl acetate) binary blends prepared by melt mixing. *Journal of Applied polymer Science* 2003; 90:841-852.
31. T. Jeevananda, Siddaramaiah. Thermal and morphological studies on ethylene vinyl acetate copolymer-polyaniline blends. *Thermochimica Acta* 2001; 376:51-61.
32. I.S. Suh, S.H. Ryu, J.H. Bae, Y.W. Chang. Effects of compatibilizer on the layered silicate/ethylene vinyl acetate nanocomposite. *Journal of Applied Polymer Science* 2004; 94:1057-1061.
33. D. Wei-hua, G. Zhang, Z. Zhu-Di, Y. Peng. Ethylene vinyl acetate copolymer/carbon fibre conductive composite: effect of polymer-filler interaction on its electrical properties. *Polymer International* 2004; 53:449-454.

34. B. Ramaraj, K.R. Yoon. Thermal and physicomechanical properties of ethylene vinyl acetate copolymer and layered double hydroxide composites. *Journal of Applied Polymer Science* 2008; 108:4090-4095.
35. Y. Bai, J. Qian, A. Quanfu, Z. Zhu, P. Zhang. Pervaporation characteristics of ethylene vinyl acetate copolymer membranes with different composition for recovery of ethyl acetate from aqueous solution. *Journal of Membrane Science* 2007; 305:152-159.
36. M. Sadeghi, G. Khanbabaei, A.H.S. Dehaghani, M. Sadeghi, M.A. Aravand, M. Akbarzade, S. Khatti. Gas permeation properties of ethylene vinyl acetate-silica nanocomposite membranes. *Journal of Membrane Science* 2008; 322:423-428.
37. B. Chul Chun, T.K Cho, M.H. Chong, Y.C. Chung, J. Chen, D. Martin, R.C. Cieslinski. Mechanical properties of polyurethane/montmorillonite nanocomposite prepared by melt mixing. *Journal of Applied Polymer Science* 2007; 106:712-721.
38. P.V. Joseph, K. Joseph, S. Thomas. Effect of processing variables on the mechanical properties of sisal-fibre-reinforced polypropylene composites. *Composites Science and Technology* 1999; 59:1625-1640.
39. R.H. Lin, Y.H. Liu, Y.H. Chen, A.C. Lee, T.H. Ho. Morphology controls of the melt blending in a novel highly crosslinked bismaleimide system. *European Polymer Journal* 2007; 43:4197-4209.
40. J.R. Araújo, W.R. Waldman, M.A. De Paoli. Thermal properties of high density polyethylene composites with natural fibres: coupling agent effect. *Polymer Degradation and Stability* 2008; 93:1770-1775.
41. A.K. Bledzki, J. Gassan. Composites reinforced with cellulose based fibres. *Progress in Polymer Science* 1999; 24:221-274.
42. H.D. Rozman, M.J. Saad, Z.A. Mohd Ishak. Modification of oil palm empty fruit bunches with maleic anhydride: the effect on the tensile and dimensional stability properties of empty fruit bunch/polypropylene composites. *Journal of Applied Polymer Science* 2003; 87:827-835.
43. M.Z.M. Yusoff, M.S. Salit, N. Ismail, R. Wirawan. Mechanical properties of short random oil palm fibre reinforced epoxy composites. *Sains Malaysiana* 2010; 39:87-92.

## CHAPTER 2

### LITERATURE SURVEY

#### 2.1 Introduction

Since the beginning of human existence people have developed plant fibre composites. These composites were used as a source of energy, to make shelters, clothes, construct tools and produce weapons [1-2]. In ancient Egypt, 3000 years ago, clay was reinforced by straw to build walls. They were produced in simple shapes and easy design structures by positioning the structural elements on top of each other to create the desired design. Some creative designs were made but limited by the shape and weight of the structural elements. Glue laminated beams were also introduced using a casein adhesive in 1893 in Basel, Switzerland. As early as 1908, the first composite materials were applied for the fabrication of large quantities of sheets, tubes and pipes for electric purposes (paper or cotton to reinforce sheets made of phenol- or melamine-formaldehyde resins). In general, all these composite products were produced in flat sheets and in two-dimensional designs. Many of our modern technologies require materials with remarkable combinations of properties that cannot be met by the conventional metals alloy, ceramics, and polymeric materials. This is especially true for materials that are needed for aerospace, underwater, and transportation materials. Materials property combination and ranges have been extended by the development of composite materials [3,4].

In the past five decades considerable attention has been devoted to composite materials. The advantage of composite materials over conventional materials stem largely from their higher specific strength, stiffness and fatigue characteristics, which enables structural design to be more versatile. By definition, composite materials consist of two or more constituents with significantly different mechanical properties and which remain separate and distinct phases within the finished structure [4,5]. However, only when the composite phase materials have notably different physical properties it is recognized as being a composite material. Composites are materials that comprise strong load carrying material (known as reinforcement) imbedded in weaker material (known as matrix). Reinforcement provides strength and rigidity, helping to support structural load. The matrix or binder (organic or



inorganic) maintains the position and orientation of the reinforcement. Constituents of the composites retain their individual physical and chemical properties; yet together they produce a combination of qualities which individual constituents would be incapable of producing alone. The reinforcement may be platelets, particles or fibres and are usually added to improve mechanical properties such as stiffness, strength and toughness of the matrix material [1,6,7].

Later on, the natural fibre composite lost much of its interest because more durable construction materials like metals were introduced. Engineering fibre composites were first used in 1940 when strong continuous filament glass fibre and unsaturated polyester resins became available. The rise of these composite materials began when glass fibre in combination with tough rigid resins could be produced on large scale. These fibres are used as reinforcing agents in both thermosetting and thermoplastic polymers in automotive, aeronautical and aerospace industries [8-10].

In recent years there has been a renewed interest in natural fibre as a substitute for glass fibre because of the potential advantages of weight saving, lower raw material price, recyclability and renewability. Natural fibre reinforced plastic composites have been utilised increasingly in quite widespread applications. For example, hemp, jute, flax, sisal and empty fruit bunch (EFB) fibres are already used in automotive and packaging industries. To reduce the cost of composite fabrication and to make them lightweight, wood flour and natural fibres were used as reinforcement or filler in early composites. In the 1980s, composites made of cellulosic fibres combined with thermoset resin began; in the 1990s, thermoplastic composites reinforced with wood flour were reported and extended to high-strength natural-fibre-reinforced thermoplastic composites [11,12].

## **2.2 Natural fibres**

### **2.2.1 Composition and structure**

Natural fibres are primarily composed of three main natural polymers: cellulose, non-cellulosic carbohydrates commonly known as hemicellulose, and lignin. These components are distributed throughout the cell wall with varying degrees of organization. The chemical compositions of a lignocellulosic fibre vary according to the species, growing conditions,

method of fibre preparations and many other factors [13,14]. Chemical compositions of lignocellulosic fibres and mechanical properties of some natural fibres as well as conventional fibres are shown in Tables 2.1 and 2.2.

**Table 2.1 Chemical composition of some common lignocellulosic fibres [13,14]**

Fibre	Cellulose / %	Hemicellulose / %	Lignin / %	Pectin / %
Empty fruit bunch (EFB)	35	25	18-23	-
Coir	32-43	0.15-0.25	40-45	2
Banana	63-64	19	5	-
Sisal	66-72	12	10-14	-
Jute	64.4	12	11.8	0.8
Pineapple	81.5	-	12.7	6.3
Flax	71.2	18.6	2.2	12.7

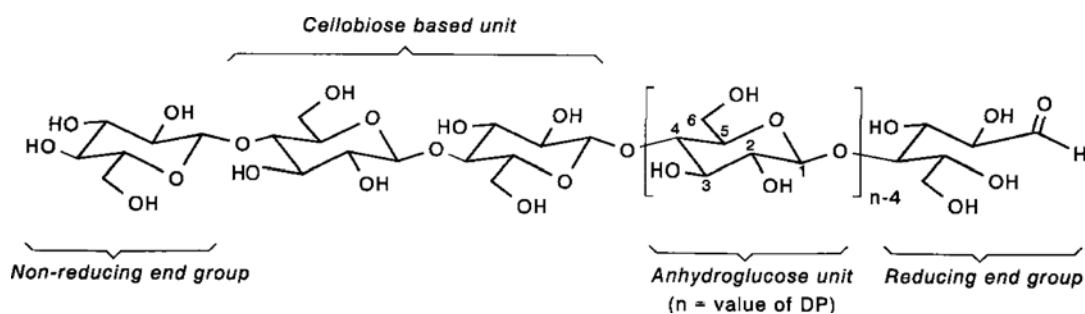
**Table 2.2 Comparison of the properties of some natural fibres with those of conventional fibres [3]**

Fibre	Density / g cm <sup>-3</sup>	Average diameter / mm	Tensile strength / MPa	Young's modulus / GPa	Elongation at break / %
EFB	0.75-0.93	0.15	215	17.3	11
Cotton	1.5-1.6	0.02	287-800	5.5-12.6	7.0-8.0
Jute	1.30	0.100	393-773	13-26.5	1.16-1.5
Flax	1.45	0.019	345-1100	27.6	2.7-3.2
Hemp	1.30	0.031	792	26.6	1.6
Ramie	1.16	0.034	560	24.5	1.2-3.8
Sisal	1.50	0.205	468-640	9.4-22.0	3-7
PALF	1.45	0.050	413-1627	34.5-82.51	14.5
Coir	1.2	0.01	131-175	4-6	30
Bamboo	0.80	0.187	465	18.0-55.0	-
Kenaf	1.04	0.078	448	24.6	1.6
E-glass	1.15	0.008-0.014	1400-2500	55.8-99.6	2.5
S-glass	2.50	-	4570	86	2.8
Aramid	2.5	-	3000-3150	63-67	3.3-3.7
Carbon	1.4	-	4000	230-240	1.4-1.8

### 2.2.2 Cellulose

Cellulose is the main component in lignocellulosic fibres and the reinforcing material within the cell wall. Cellulose is a linear crystalline condensation polymer consisting of D-anhydroglucopyranose units held together by  $\beta$ -1,4-glycosidic bonds (Figure 2.1). It is a high

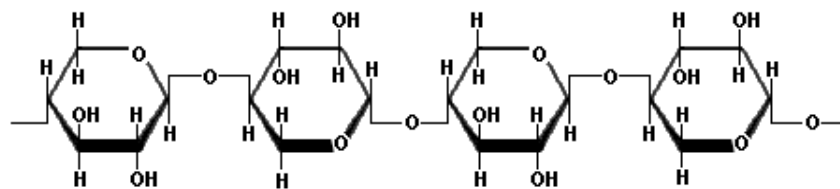
molecular weight homopolymer of glucose and it is laid down in microfibrils where extensive hydrogen bonding between the cellulose chains produces a strong crystalline structure [15,16]. The actual base unit, the cellobiose, consists of two molecules of glucose. The polymer chains are ordered in three-dimensional levels forming the supramolecular structure of cellulose. The linear polymeric chains (one dimension) form sheets that are held together with hydrogen bonds. These are connected by weak Van der Waals bonds generating microfibril crystalline structures. The overall structure of cellulose consists of crystalline and amorphous regions. The mechanical properties of cellulose depend on the proportion of each region and the spiral angle of microfibrils because of its geometrical conditions [17-19].



**Figure 2.1** Molecular structure of cellulose [15]

### 2.2.3 Hemicellulose

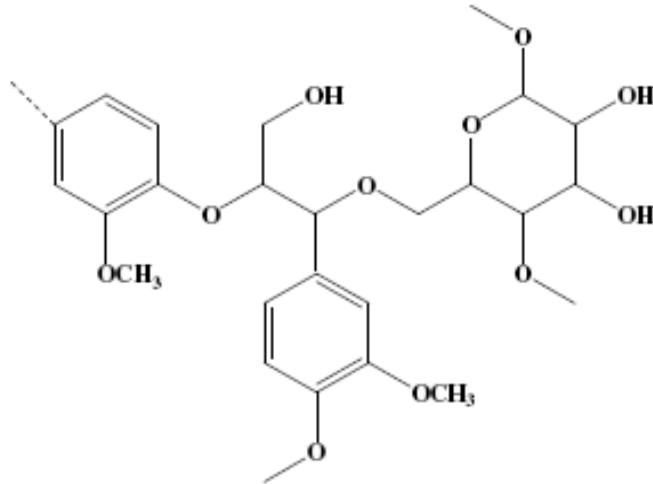
Hemicellulose is not a form of cellulose and is a copolymer of a group of polysaccharides consisting of glucose, mannose, xylose, galactose and arabinose. Hemicellulose is similar in structure to cellulose, but chains of hemicelluloses are shorter and less stable. Unlike cellulose, hemicelluloses is of low molecular weight, amorphous and exhibits chain branching. Owing to its amorphous morphology, hemicellulose is partially soluble in water and form gels. Besides that, the constituents of hemicelluloses vary from plant to plant [14,15].



**Figure 2.2** Structure of hemicellulose [14,15]

### 2.2.4 Lignin

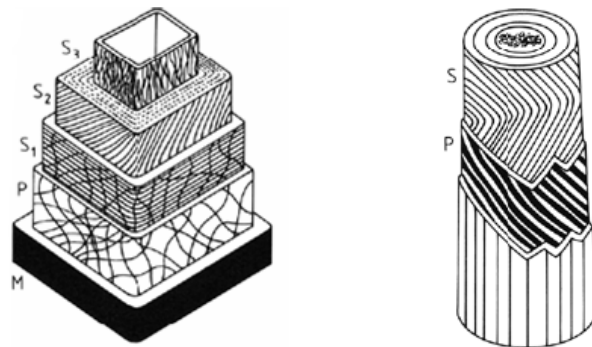
Lignin is a random polymer composed mainly of aromatic rings with short (up to three) aliphatic carbon chains connecting the rings. It has a disordered structure as shown in Figure 2.3, and is formed through ring opening polymerization of phenyl propane monomers. This also provides rigidity, hydrophobicity and decay resistance to the cell wall of lignocellulosic fibres. Lignin polymers are often found in most plant structures in association with cellulose. The structure of lignin is not well defined, but lignin appears to be made up of polymers of propylbenzene with hydroxyl and methoxy groups attached. Lignin is primarily hydrocarbon in nature and makes up a major portion of insoluble dietary fibre. It contains subunits derived from *p*-coumaryl alcohol, coniferyl alcohol, and sinapyl alcohol, and is unusual among biomolecules in that it is racemic i.e. it is not optically active. The lack of optical activity is because the polymerization of lignin occurs *via* free radical coupling reactions in which there is no preference for either configuration at a chiral centre [20-22].



**Figure 2.3** Molecular structure of lignin [15,20-22]

### 2.2.5 Structure of natural fibres

The supramolecular structure or texture of the cellulose is based on the elementary fibril. The elementary fibril is a strand of elementary crystals linked together by segments of long cellulose molecules (see Figure 2.4).



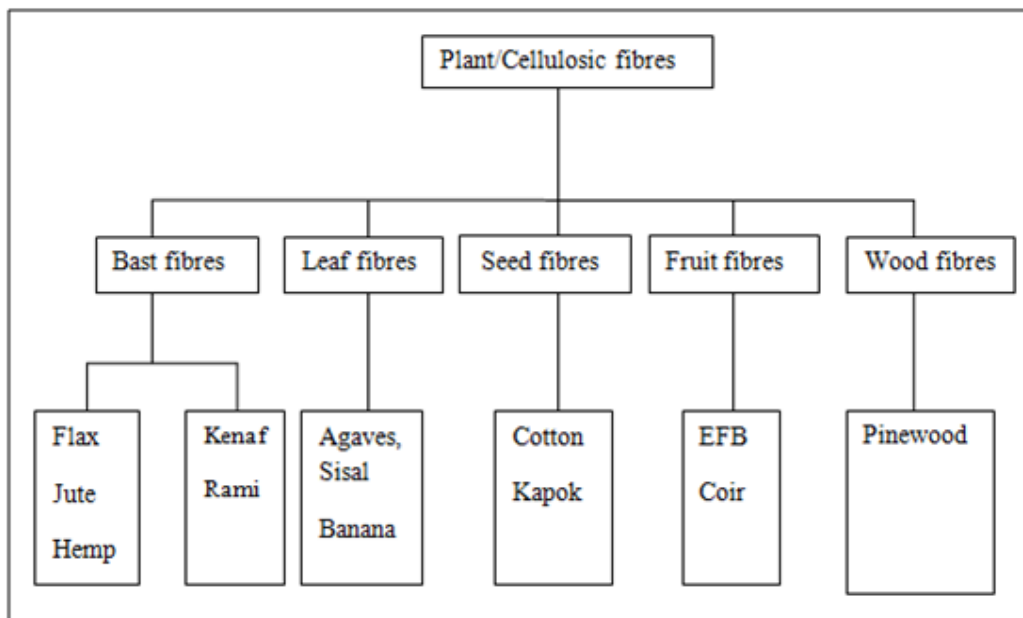
**Figure 2.4** Internal structure of natural fibre [14]

Figure 2.4 shows the positioning of the cellulose fibrils in wood (left). M is the middle lamella (lignin and hemicelluloses), P is the primary wall (fibril position unarranged), S<sub>1</sub> is

the secondary wall I (two or more fibrillar layers crossing one another and positioned spirally along the fibre axis),  $S_2$  is the secondary wall II (fibrils wound spirally around the fibre axis),  $S_3$  is the secondary wall III (fibrils tightly interlaced). In cotton fibres (right) P is the primary wall (interlaced fibrils) and S is the secondary wall (fibrils wound spirally around the fibre axis, in distinct distances along the fibre axis the spiral reverse direction) [14].

### 2.2.6 Classification of natural fibres

Natural fibres are subdivided based on their origin, either coming from plants, animals or minerals. They can be classified according to which part of the plant they are obtained from (Figure 2.5).



**Figure 2.5** Classification of natural fibres

### **2.2.7 Empty fruit bunch (EFB) fibre**

Empty fruit bunch (EFB) fibre is a valuable biomass material, which is a by-product derived from an oil palm tree called *Elaeis guineensis*. This *Elaeis guineensis* consists of two species of the Arecaceae, or palm family. Its mature trees are single-stemmed, and grow up to 20 m tall. The leaves are pinnate, and reach between 3 and 5 m long [25]. EFB is readily available in large quantities in Malaysia as well as in tropical forests of West Africa [26-28]. EFB is a cheap, biodegradable, non-toxic, and widely utilized natural fibre used in the development of composite materials. EFB is used as a raw material in various applications including power generation, composites formulation, and in the paper making industry. It is also used as a fuel and helps to control weeds, prevent erosion and maintain soil moisture. As a valuable biomass residue, it can also be converted into energy [29], and its use in polymer composites will remedy issues around environmental problems, especially those related to the disposal of oil palm wastes [30,31].

The total area of oil palm plantation in Malaysia is about 2.5 million hectares. The oil palm fruits are processed in mills and crude palm oil is extracted from these fruits. The oil palm industry in Malaysia produces about 10.5 million tones of crude palm oil per annum and produces a massive amount of biomass waste. One of the biomass wastes produced is the empty fruit bunches which are left behind after removal of oil palm fruits for the oil refining process. The empty fruit bunches are then used as boiler feedstock in the oil mill and are also left to mulch and degrade as soil fertilizers in the field while the majority of the empty fruit bunches are unutilized. It is disposed in the oil palm estates as soil fertilizers, and takes a long time to break down. During the rainy season it provides an ideal condition for fungi to grow, which is the main cause of the ganoderma disease. By using the oil palm empty fruit bunch fibres, that are extracted from the empty fruit bunches, as reinforcement in composite materials, the biomass waste generated by the oil palm industry can be significantly reduced [25,32].

### **2.3 Matrix material**

A matrix can be easily defined as a material in which the reinforcing part of a composite is embedded. The matrix serves as a binder which holds the reinforcing material in place. When

a composite is subjected to an applied load, the matrix deforms and transfers the external load uniformly to the fibres. The matrix also provides resistance to crack propagation and damage tolerance owing to the plastic flow at crack tips. The matrix also functions to protect the surface of fibres from adverse environmental effects and abrasion especially during composite processing. Plastic matrices can generally be classified into two major types which are thermoplastics and thermosets. The selection criteria of the matrices depend solely on the composite end use requirements. For example, if chemical resistance together with elevated temperature resistance is needed for a composite material, then thermoset matrices are preferred. If a composite material with high damage tolerance and recyclability is needed, then thermoplastics are preferred [1,33].

### **2.3.1 Ethylene vinyl acetate (EVA)**

Polyethylenes are the largest volume family of commercially important thermoplastic polymers. They have variations in the molecular structure due to branches and polar functional groups (polar copolymers). Polar copolymers usually exhibit lower crystallinity and yield strength. They are used for application requiring flexibility, toughness, stress-cracking resistance and adhesion to coatings, co-extruded film and laminates [34-39]. One such a PE copolymer contains vinyl acetate and is known as an ethylene vinyl acetate copolymer (EVA). Ethylene vinyl acetate (EVA) copolymers are randomly structured polymers which offer excellent ozone resistance, weather resistance and excellent mechanical properties [45-47]. EVA is one of the most widely used polymers for cable insulators. It is also frequently used as a long lasting life plasticizer to improve the mechanical and processing properties of PVC [45,48]. EVA is abundantly available as a plastic, thermoplastic elastomer, and rubber depending on the vinyl acetate content in the copolymer.

Crystallinity in an EVA copolymer is low, but not the density ( $0.930 - 0.955 \text{ g.cm}^{-3}$ ), because the vinyl acetate (VA) groups increase the density of the amorphous phase. Copolymers containing up to 20 wt% of VA are used in various extrusion and moulding applications. The EVA copolymers containing 2-5% VA behave similar to PE, but have better clarity, higher impact strength, better low temperature flexibility and lower heat seal temperatures. Those with 7.5-12% VA have greater flexibility, higher resistance and exceptional impact strength. They are used in high performance film applications. The EVA copolymers containing 15-



18% VA are almost soft and more resilient in nature than the ones with 7.5-12% VA content [40-44]. EVA containing 28% VA is a thermoplastic elastomer, and those containing 50% VA are rubbers [49]. Figure 2.6 represents the unit structure of the EVA copolymer.

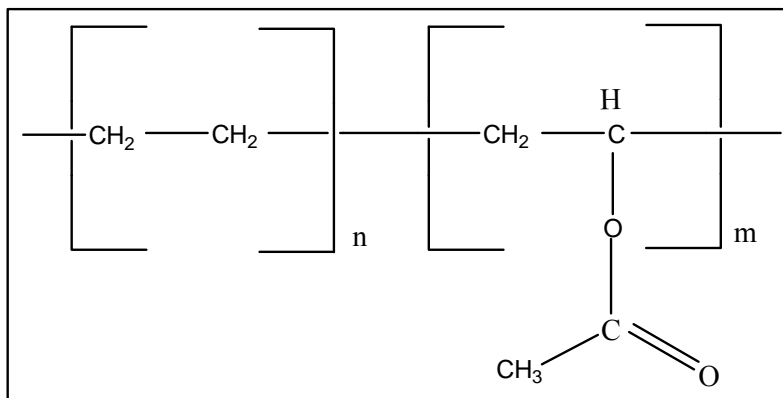


**Figure 2.6 Unit structure of EVA copolymer**

Other important features in EVA include toughness at low temperatures and good processability. As a result of these important properties, EVA copolymers have found several applications in sheeting, wire and cable coating, flexible tubing, shoe soles and food packaging. Besides their good properties, EVA copolymers can be used as compatibilizing agents or impact modifiers for PP, HDPE, and LDPE based polymer blends. The presence of acetate groups facilitates the generation of free radicals along the backbone, which enables promotion of grafting reactions in the presence of several monomers. Such graft copolymers can be readily prepared *in situ* during the blend preparation. The chemical modification of EVA by introducing a functional group that can act as a chain transfer agent is another elegant pathway for the synthesis of EVA-based graft copolymers [50-55].

## **2.4 PE/natural fibre composites**

### **2.4.1 Preparation and morphology**

Various methods are used to prepare polyethylene (PE)/natural fibre composite materials. These methods include solution mixing, roll milling, melt mixing, extrusion, as well as injection and compression moulding [7,19,31,55-73]. They differ in terms of their operating

principles and processing parameters, which may lead to different properties of the prepared composite materials. Many researchers have used polyethylene matrices as composite material with various natural fibres/fillers in their studies of polymer reinforcements. These natural fibres/fillers include abaca, alfa, bagasse, bamboo, banana, curaua, coir, cotton, flax, hemp, henequen, isora, jute, kapok, kenaf, kraft, maize, olive stone flour, piassava, pineapple, ramie, rice starch, sponge gourd, silk, sisal, straw (wheat), sun hemp, wood fibres/flour (WF), and wool [7,31,57,58,63,74]. The section below will emphasize the wide range of studies carried out by researchers based on both unmodified and modified natural fibre composites.

A lot of research work has been done on the preparation and morphology analysis of unmodified/uncoupled natural fibre/polyethylene composites [63,71-73,75-81]. Herrera *et al.* [63] reported on continuous henequen fibre reinforced high-density polyethylene (HDPE) composites prepared in a Brabender mill. The SEM results of the untreated composites showed a considerable fibre pull-out and smooth holes. There was no evidence or traces of matrix resin adhering to the fibre. Baroulaki *et al.* [71] studied composites based on high-density polyethylene (HDPE) and recycled paper fibre. These composites were prepared by using compression molding in the temperature range 200-240 °C, pressure range 50-170 bar, with heating and cooling times of 20 and 18 min. The SEM results of the HDPE/recycled paper fibre composites confirmed the poor interfacial adhesion because of the incompatibility of the two components. This is supported by gaps between the HDPE matrix and recycled paper fibre, fibre pull-out, and a relatively smooth surface on the recycled paper filler. In addition, fibre-fibre interaction was also observed with an increase in fibre loading. Lu *et al.* [72] and Mengelöglu *et al.* [73] respectively reinforced HDPE with WF and eucalyptus wood residue (EWR). The composite materials were prepared through single screw extrusion and injection moulding. Both authors obtained similar results as those discussed above [63,71], and all of them confirmed the existence of poor interfacial adhesion in untreated composites.

LDPE was also reinforced with natural fibres and the composite materials were characterized for their morphology. Baroulaki *et al.* [71] used recycled paper fibre, while Pasquini *et al.* [75] utilized sugar cane bagasse to reinforce LDPE. The composites were prepared by using melt mixing and compression moulding under different temperature conditions. The SEM results in both studies showed that the fibres were pulled out practically intact from the matrix. They also observed that only some areas of the fibres were covered by polymer, while there were gaps between the matrix and the fibre as well as walls with smooth surfaces. All of

these showed that there was a very poor interfacial adhesion between the two phases, which led to some properties deterioration. Similar behaviour was observed by other authors on HDPE based composites [63,71-73].

Virgin LLDPE was also reinforced with natural fibres and the composites were characterized for their morphology. Marcovich and Villar [76] and Liao *et al.* [77] used wood flour (WF), whereas Adhikari *et al.* [78] used coir fibre to reinforce LLDPE. The composites were prepared through extrusion and melt mixing methods. The SEM results for all the studies showed the existence of fibre pull-outs, gaps and no polymer matrix coating around the filler surfaces. Similar to the previous studies on HDPE and LDPE [63,71-73,75], the authors concluded that these confirmed the existence of poor interfacial adhesion for untreated LLDPE/natural fibre composites.

EVA was reinforced with natural fibres and the composites were characterized for their morphology. Stael *et al.* [55] used sugar cane bagasse fibre, whereas Dikobe and Luyt [79] used WF to reinforce EVA. The composites were prepared through melt mixing under different processing conditions. The SEM results for the EVA/WF composites show that there are obvious fibre pull out from the matrix indicating the poor interaction between them. The SEM photos of the fractured surfaces of the EVA/bagasse composites showed that the fibre was covered by the polymer. No gaps were observed at the interface and the lumens were almost closed. The broken bagasse still adhered to the EVA resin matrix, which means that good bagasse-EVA interaction occurred. In contrast to some other studies [63,71-73,75-79], these authors observed good adhesion between the bagasse fibre and the EVA matrix for non-treated composite systems. The good bagasse-EVA interaction could be attributed to the polar groups randomly distributed on the EVA macromolecular chains. This could also be interpreted as a sign that bagasse is really acting as reinforcement for the EVA matrix. Generally, most non-coupled/untreated natural fibre-polyethylene composites have poor interfacial adhesion, except for a rare case such as that of Stael *et al.* [55].

Some workers have also utilized polypropylene (PP) as the matrix component for polyolefin/natural fibre composites [58,80,81]. Rana *et al.* [58] used short jute fibre with a PP matrix, Rozman *et al.* [80] studied the physical properties of coconut fibre/PP composites, and Rozman *et al.* [81] utilized empty fruit bunch fibre and PP. These composite materials were prepared through injection molding, melt mixing and extrusion under different

processing conditions. The SEM results of these untreated composites showed fibre pull-outs, and the fibre scraped off left a smooth surface on the matrix indicating the occurrence of debonding through the weak interfacial interaction between the fibre and polymer matrix. There were also some irregularities in size and distribution of fibres which may affect the efficiency of stress transfer.

Dikobe and Luyt [57] investigated the influence of wood flour and EVA, in the presence and absence of poly (ethylene-co-glycidyl methacrylate) (EGMA) as compatibilizer, on the composite properties. The FTIR results revealed that there was no grafting reaction between the EVA and WF, even though there might have been hydrogen bonding between the –OH groups on the cellulose and the –C=O groups in the vinyl acetate. These authors suggested that there was probably a reaction between the epoxy groups in EGMA and the –OH groups in WF, giving a grafted product. Kim *et al.* [96] studied saw dust-reinforced LLDPE composites using an ethylene vinyl alcohol copolymer as adhesion promoter and their observations were similar to those of Dikobe and Luyt [57].

Generally it was found that treatment of the natural fibre or addition of a modifier into natural fibre composites showed improved interfacial adhesion. The modification may be achieved by physical or chemical methods (fibre surface or polymer treatment), and gives enhanced interfacial adhesion between the polymer matrix and the fibre, good fibre dispersion within the matrix and good fibre covering by the polymer. However, the level of interfacial adhesion between the composite components depends primarily on the chemical nature of the selected coupling agent [15]. A variety of coupling agents such as silane, organosilanes, maleic anhydride, maleic anhydride grafted polyethylene, acrylic acid grafted polyethylene, organic peroxide, and ethylene-vinyl alcohol (EVAL) copolymer (as adhesion promoters) were utilized to effectively and efficiently enhance the compatibility between natural fibres and thermoplastic resins [7,15,58,61,63,64,67,72-83]. The SEM results from these authors confirmed good compatibility and interfacial adhesion between the polyethylene matrices and the various natural fibres after modification of the composites. This was justified by the absence of gaps between fibres and matrices, reduction in fibre pull-outs resulting in small voids and holes, few cavities or closed lumen, improved fibres dispersion within polymer matrices, good fibre covering by polymers, insignificant fibres agglomeration and rough surfaces.

## 2.4.2 Thermal properties

### 2.4.2.1 Melting and crystallization

Several studies were conducted on the thermal properties of polyethylene/natural fibre composites and various features were observed [56,57,59,64,65,67,73,78,79,84-89]. These features were influenced mainly by the nature of the binding polyethylene matrix, coupling agent, or surface modification, and the choice of the fibre or filler. Araújo *et al.* [59], Mengeloglu *et al.* [73], and Karakus *et al.* [84] found a significant decreasing trend in the crystallinity of polyethylene in natural fibres (curaua, wheat straw flour, and eucalyptus wood residue)-reinforced polyethylene prepared in the presence of maleic anhydride as a coupling agent. This was attributed to the fact that the PE chains were immobilized by the coupling agent. Another reason given was that covering of part of the fibre surface by the coupling agent decreased the transcrystallinity effect. A slight increase in crystallinity of the matrix in polyethylene/rice husk flour (RHF) composites with increasing MAPP and MAPE content was noticed, but a decrease in the crystallinity of the matrix in LDPE/RHF fibre composites was observed by Kim *et al.* [85]. The RHF fibre loading led to a slight increase in melting temperature ( $T_m$ ) of LDPE/RHF composites compared to the  $T_m$  of pure LDPE, but the  $T_m$  of the composites was not significantly changed due to the addition of MAPP and MAPE [85]. Sailaja *et al.* [86] found that when wood pulp was grafted with polymethyl methacrylate (PMMA), there was not much of a difference between the melting temperatures of the composites. However, the presence of poly(ethylene-co-glycidyl methacrylate) (PEGMA) as compatibilizer showed a remarkable increase in crystallinity of the matrix, while the crystallinity of the matrix decreased as the filler loading increased in the absence of a compatibilizer. The reason given was that the presence of the inhibited the close packing of the LDPE chains [86].

Several authors such as Luyt *et al.* [56] and Dikobe and Luyt [79] reported on EVA-natural fibre composites. The expected enthalpies for EVA/sisal fibre composites were higher than the measured enthalpies. This was attributed to a decrease in the mobility of the EVA chains as a result of grafting. This also gave rise to the formation of thinner crystal lamellae, confirmed by the steady decrease in the melting temperatures, and a lower crystallinity [56]. Dikobe and Luyt [79] observed that wood fibre (WF) influenced the melting temperatures and crystallization behaviour of EVA in EVA/WF composites. The EVA part of the

composite crystallized fairly normal, even though the crystals were not as perfect as expected. The formation of perfect crystals was hindered by the presence of WF particles, which probably led to epitaxial crystallization on the surfaces of the WF particles that were well dispersed in the EVA matrix. Xie *et al.* [65] studied PP and PP/maleic anhydride grafted styrene-(ethylene-co-butylene)-styrene copolymer (MA-SEBS) sisal fibre (SF) composites. The DSC results showed that the  $T_m$  of the PP phase in the PP/MA-SEBS/SF composites slightly decreased with the incorporation of MA-SEBS. This means that there were some interactions between PP and MA-SEBS as well as between SF and MA-SEBS which improved the compatibility between the components. The crystallinity of PP also decreased quite noticeably with an increase in the MA-SEBS content [65]. Zhou *et al.* [67] evaluated the reinforcement of PP using sisal fibre grafted with PMMA. It was found that the  $T_m$  values of the PP matrix in the composites were almost the same, whereas the crystallization temperature was reduced in the PP/PMMA-g-SF composite compared to those of PP/untreated SF and PP/NaOH-treated SF. The crystallinity of the PP/PMMA-g-SF composite was lower than that of either the PP/untreated SF or the PP/NaOH-treated SF composite. This was due to the PMMA grafted onto the surface of SF enhancing the intermolecular interaction between PP and SF, and hence hindering the crystallization of the PP phase in the PP/PMMA-g-SF composite [67]. The DSC results by Nayak *et al.* [89] showed that the addition of bamboo fibre, glass fibre and MAPP did not significantly influence the  $T_m$  of a PP matrix. However, the introduction of these fibres and MAPP interrupted the linear crystallisable sequence of the PP phase and reduced the degree of crystallinity. The degree of crystallinity increased with the incorporation of both fibres. This was an indication that these fibres did act as a nucleating agents [89].

#### **2.4.2.2 Thermal stability**

The thermal stability of natural fibre-reinforced polyethylene composites depends heavily on the level of interaction between the polymeric matrix and fibres. This interaction is influenced by surface modifications introduced through physical and chemical methods, as well as coupling agents used to optimize the interface efficiency. In general, the thermal stability of natural fibres is considerably lower than that of neat polyethylene resins, but their incorporation into polyethylene matrices may lead to either a decrease or an increase in the thermal stabilities of the composites [56,57,59,67,70,73,76,79,84-86,89]. Araújo *et al.* [59] observed that the pure HDPE and HDPE/curaua composites were thermally more stable than

the HDPE/curaua/PE-g-MA composites. The compatibilized composites have more interfacial interaction due to reactions between the acid moieties on the maleic anhydride groups and the hydrophilic groups on the fibre surfaces. Mengeloglu *et al.* [73] found that the degradation temperature of recycled HDPE was around 300 °C, while HDPE/eucalyptus wood residue (EWR) composites degraded at 260 °C. It is clear that the addition of EWR into the HDPE matrix induced it to degrade thermally at low temperatures. This could be attributed to the fact that wood produced a higher concentration of free radicals which accelerate the thermal degradation of the PE matrix. The inclusion of MAPE as a coupling agent increased the thermal stability of the HDPE/EWR composites by 10-20 °C. Karakus *et al.* [84] comparatively evaluated the thermal stability of HDPE and HDPE/wheat straw flour (WSF) composites. The incorporation of WF showed a steady decrease in the thermal stability of HDPE.

Kim *et al.* [85] observed that the LDPE/untreated RHF composites have a higher thermal stability than neat LDPE, whereas the thermal stability of the treated composites were slightly increased with an increase in MAPE compatibilizer content. The improved thermal stability of the compatibilizing agent-treated composites was due to enhanced interfacial adhesion and additional intermolecular bonding which produced an esterification reaction between the hydroxyl groups in RHF and the functional groups in MAPE [85]. Sailaja *et al.* [86] investigated the thermal properties of LDPE/bleached kraft wood pulp grafted with polymethyl methacrylate (PMMA), with and without poly(ethylene-co-glycidyl methacrylate) (PEGMA). There was no significant change in the thermal behaviour for compatibilized and uncompatibilized composites with 20% wood pulp grafted with PMMA (WPMMA) loading. However, on increasing the WPMMA loading to 40%, the composites with the PEGMA compatibilizer showed a higher thermal stability than the uncompatibilized composites. Marcovich and Villar [76] found that natural fibres decreased the thermal stability of the composites in either unmodified, organic peroxide modified, or gamma radiation treated systems with the residual char increasing with fibre content. This was attributed to the polymers having more weak links due to the presence of organic peroxide, and an increase in concentration of free radicals.

Luyt *et al.* [57] observed that the fibre degraded before the EVA matrix and that the EVA/sisal composites were more thermally stable than both EVA and sisal fibre alone. These authors found that the composite stability did not depend on the amount of sisal, because in

most cases the sisal decomposed first followed by the decomposition of the EVA matrix. Similar trend in thermal stability was observed by Dikobe and Luyt [79] for EVA/WF composites. They also pointed out that the WF particle size did not substantially influence the degradation behaviour of the EVA/WF composites. Zhou *et al.* [67] investigated the thermal stability of PP/sisal fibre composites and found that the thermal stability of PP/SF composites was improved by grafting the sisal fibre surface with PMMA. This was because grafting of the PMMA chains enhanced the intermolecular interaction between PP and SF. Doan *et al.* [70] reported good thermal stabilities for jute fibre/PP composites compared to neat PP or fibre in both nitrogen and air atmospheres, due to the fibre-matrix interaction. Nayak *et al.* [89] found that the presence of MAPP enhanced the thermal stability of bamboo fibre in PP/short bamboo fibre composites.

### **2.4.3 Thermo-mechanical and mechanical properties**

#### **2.4.3.1 Thermo-mechanical properties**

Various studies were conducted on the thermo-mechanical properties of polyethylene/natural fibre composites [67,70,75,85,89-94]. Behzad *et al.* [92] studied the dynamic mechanical properties of wood flour (WF)-reinforced HDPE composites. The storage modulus of the HDPE/WF composites decreased rapidly with an increase in temperature, but there was no significant difference between the storage modulus of coupled and uncoupled composites in the case of 25% wood flour loading. In the case of 50% WF loading, a very significant improvement due to the addition of the compatibilizer could readily be observed. At higher temperatures the difference in storage modulus between coupled and uncoupled composites became negligible. The coupled composites had a higher loss modulus than the uncoupled composites. It was found that the alpha transition ( $\alpha$ -transition) peak significantly shifted to higher temperatures due to the addition of more fibres, but no pronounced shifting in the transition peaks was observed when the compatibilizer was added. It seemed that the  $\alpha$ -transition intensity was somewhat higher in the case of the coupled composites at 50% fibre content. It was also found that all the composites had relatively the same  $\tan \delta$  values below the  $\alpha$ -transition. Above the  $\alpha$ -transition the curves for the 50% fibre containing composites showed different  $\tan \delta$  values, while at 25% fibre content the curves showed similar values. It was concluded that the energy loss became more pronounced at temperatures above the  $\alpha$ -transition for the higher fibre content samples [92].



Kim *et al.* [85] observed that the storage modulus of LDPE substantially increased at higher temperatures due to the incorporation of RHF. With increasing coupling agent content, the  $E'$  values of the composites slightly increased compared to those of the untreated composites. The enhanced stiffness of the composites was mainly attributed to the improved compatibility between the RHF and LDPE. The  $T_g$  (-135 °C) of the treated composites slightly increased due to the existence of interfacial bonding between the components at the interface. The loss modulus ( $E''$ ) peak temperatures of LDPE and the treated composites were in the range of -23 to -19 °C, which may well be attributed to the  $\beta$ -relaxation. The  $\tan \delta$  values of the treated composites were lower than those of the untreated composites over the complete temperature range indicating that the energy dissipation of the modified composites was less than that of the uncoupled composites. Pasquini *et al.* [75] and Abdelmouleh *et al.* [94] observed similar behaviour in their investigation of LDPE/short bagasse and pine fibre composites.

Pracella *et al.* [95], in their investigation of EVA copolymers with cellulose fibres, observed that the storage modulus  $E'$  decreased systematically with an increase in temperature and that a pronounced relaxation of the virgin polymer and the composites was around -20 °C. This was associated with the glass transition temperature ( $T_g$ ) of the ethylene vinyl acetate (EVA) copolymer. The  $E'$  values of cellulose filled systems were higher than those of the pure polymers both in the glassy and rubbery regions. The  $E'$  values for the ethylene vinyl acetate-glycidyl methacrylate (EVA-GMA)/cellulose fibre composites were higher than those of the EVA/cellulose fibre and EVA grafted maleic anhydride (EVA-MA)/cellulose fibre composites. It was deduced that the cellulose fibre had a larger effect on the modulus above  $T_g$  than below it. The difference between the moduli of the glassy region and rubbery region was also smaller in the composites than in the neat polymers. This could be attributed to a combination of the hydrodynamic effects of the cellulose embedded in a viscoelastic medium, and to the mechanical restraint introduced by cellulose at high concentrations, which reduced the mobility and deformability of the matrix. The cellulose fibre incorporation reduced the  $\tan \delta$  peak height by restricting the movement of the polymer molecules. It was concluded that the  $T_g$  of EVA-MA was not affected by the incorporation of cellulose, whereas the  $T_g$  of EVA and EVA-GMA were changed markedly by the incorporation of cellulose.

Zhou *et al.* [67] found that the incorporation of sisal fibre into a PP matrix significantly increased the  $E'$  values. The NaOH-treated composites had more pronounced  $E'$  values than the untreated composites and neat PP. The  $\tan \delta$  curve for PP showed a peak at 17.5 °C, which corresponds to  $T_g$ . For all the sisal fibre reinforced composites, this peak was around 15 °C. There was an additional  $\tan \delta$  peak at about 90 °C only in the PP/PMMA-g-SF composites. The intensity of the transition decreased significantly when the SF was incorporated into the PP matrix. Doan *et al.* [70] found that with increasing jute fibre content, the storage modulus values increased. At the same fibre loading, the storage modulus of the jute/modified PP composite was slightly higher than that of the jute/unmodified PP composite over a wide temperature range. This indicated enhanced adhesion between the fibre and the matrix due to the coupling agent, leading to better stress transfer from the matrix to the fibre. It was observed that in the modified composite system the loss modulus increased with fibre content. The  $\tan \delta$  values dropped with an increase in the jute fibre loading for jute/modified PP composites. The reason for this was given as a restriction of the mobility of the PP chains by the fibres during the relaxation process. Nayak *et al.* [89] and Sanadi *et al.* [90] found similar trends in the storage modulus values in their investigation of PP/short bamboo and kenaf fibre composites. These authors observed three transition peaks ( $\alpha$ ,  $\beta$ , and  $\gamma$ ) at temperatures of -50, 20, and 90 °C. The  $\beta$ -transition peak of the MAPP treated PP/short bamboo fibre composites and the PP/kenaf fibre composites shifted to higher temperatures with increasing fibre content compared to the untreated composites and PP. This was attributed to restricted segmental motion of the amorphous PP chains at the fibre-matrix interface. The  $\tan \delta$  values for the PP/short bamboo fibre were lower than that of the pure PP, because of the lower weight fraction of the PP matrix that could dissipate the vibrational energy. The introduction the MAPP into the PP/short bamboo fibre composites seemed to decrease the  $\tan \delta$  values. This decline in the  $\tan \delta$  values indicates an improvement in the interfacial bonding of PP/short bamboo fibre composites, because the higher the damping at the interface, the poorer is the interface adhesion. In the case of the untreated composites, the mechanical loss factor remained high in the system due to poor interfacial adhesion.

### 2.4.3.2 Mechanical properties

The mechanical properties of thermoplastic/natural fibre composites were studied by several workers [56,57,63,72,79,92]. An increase in Young's modulus and tensile strength of HDPE filled with continuous henequen fibre was observed by Herrera *et al.* [63] with an increase in fibre loading. This increase was more pronounced for the treated composites as a result of the better compatibility between the components. Generally the HDPE composites had higher Young's modulus values because of the higher crystallinity of HDPE. It was also noticed that the flexural strength increased with increasing fibre loading in both directions compared to that of the pure matrix. The flexural modulus showed the same behaviour as the tensile modulus, and the values of stiffness were higher for silane-treated composites. Lu *et al.* [72] found that the tensile strength of HDPE/WF composites increased slightly at the low filler concentrations, but decreased at higher concentrations. Behzad *et al.* [92] investigated the effect of compatibilizer on the mechanical properties of HDPE/WF composites. They found an improvement in the properties such as tensile modulus, strength and flexural modulus due to the addition of the compatibilizer, and the differences were statistically significant. This was related to the effectiveness of the compatibilizer in enhancing the quality of the interface. This also resulted in higher tensile modulus values, improved stress transfer and eventually higher tensile strength. It was noticed that for uncoupled composites at higher fibre contents the tensile modulus and flexural modulus increased, while the tensile strength decreased.

Habibi *et al.* [19] observed that Young's modulus of the unfilled matrix was higher for maleated LDPE (MLDPE) than for LDPE as a result of its higher degree of crystallinity. The tensile strength clearly increased as the fibre content was further increased in the case of MLDPE, while in the case of LDPE it seemed to decrease. Maleic anhydride grafting improved the tensile strength because of better adhesion between the two components, and because of good stress transfer from the matrix to the fibre. The elongation at break of the unfilled matrix was higher for LDPE than for MLDPE. However, the elongation at break decreased upon fibre inclusion for both sets of composites regardless of the nature of the fibre (cotton stalk, rice straw, sugarcane and banana fibres). Marcovich and Villar [76] used wood flour to reinforce an LLDPE matrix and found that in all cases, the modulus increased with WF loading, but the increment was larger for organic peroxide and maleic anhydride modified samples. This increase in the tensile modulus could be explained by a good compatibility between the filler and matrix. The dispersion of the WF in the PE matrix was

also improved by matrix modification, and so the fibre-matrix interface was stronger, hence a more efficient reinforcing effect was obtained. Liao *et al.* [77] used two titanate coupling agents known as polyoxide terephthalate (TC-POT) and polybutylene terephthalate (TC-PBT) to modify WF to reinforce LLDPE, and they compared their mechanical properties with those of the untreated composites. They observed similar trends in the elongation, tensile modulus, and tensile strength properties as those discussed above [19,76]. Kim *et al.* [96] reported that ethylene vinyl alcohol, as a compatibilizer in saw-dust-reinforced LLDPE composites, led to better mechanical properties than ethylene vinyl acetate that showed poor properties. This behaviour improved with an increase in coupling agent content, and it was attributed to the compatibilizer's ability to chemically bond with saw-dust.

Luyt *et al.* [56] studied EVA-sisal fibre reinforced composites, and found that Young's modulus increased remarkably with an increase in the sisal fibre content. It was also observed that an increase in the sisal content as well as crosslinking and grafting gave rise to higher values of Young's modulus. A drastic decline in modulus values and stress at break was noticed for the neat EVA copolymer in the presence of dicumyl peroxide (DCP) as a crosslinking agent. This behaviour was expected since the crosslinking reduced the degree of crystallinity. There seemed to be a noticeable decrease in the values of stress at break for composites prepared in the presence and absence of DCP, especially at a very low sisal fibre loading. The reason could be attributed to the weak interaction between EVA and sisal, since there was no substantial grafting at this fibre loading. However, an increase in sisal content produced high stress at break values, especially for the samples prepared in the presence of DCP. This was attributed to a strong element of grafting and interaction between EVA and sisal fibre. The elongation at break decreased because of the crosslinking and grafting that restricted the chain movement. Similar trends were observed by Dikobe and Luyt [57,79] in their studies on wood flour- reinforced EVA composites.

Rana *et al.* [58] carried out work on short jute fibre-reinforced PP composites and observed a sharp increase in the tensile strength after introduction of the compatibilizer. This was explained as being due to the efficiency of stress transfer from the PP matrix to the jute fibre *via* the compatibilizer. The tensile strength of the composite materials prepared without compatibilizer showed a smaller improvement regardless of the amount of fibre present. This suggested that there was very little stress transfer from the matrix phase to the reinforcing/fibre component. The increase in the fibre content restrained the movement of the

PP chains and this was reflected in an increase in the tensile modulus values. A significant increase in the flexural strength and modulus values was observed in the presence of compatibilizer, while in the absence of compatibilizer there was practically no change in both these properties. The notched impact strength values were found to increase and the effect of the compatibilizer on these values was negligible with only a marginal improvement. This could have been due to the migration of too much compatibilizer around the fibres, causing self-entanglement among the compatibilizer instead of the PP matrix resulting in slippage. There was a sharp increase in the unnotched impact strength after addition of the compatibilizer. Khalid *et al.* [60] and Xie *et al.* [65] studied the mechanical properties of EFB and SF fibre-reinforced PP composites and found that the results which are in line with those in the study of the effect of compatibilizer on the short jute fibre-reinforced PP composites [58]. Rozman *et al.* [80] found that the flexural strength did not show significant changes as the percentage of fibre increased, and that the flexural modulus seemed to increase significantly as the lignin loading was increased. The overall tensile strength of the composites steadily decreased as the fibre loading increased and the incorporation of lignin did not change the tensile strength. A study of the effect on the tensile and dimensional stability properties of EFB fibre-reinforced PP composites was conducted by Rozman *et al.* [81]. They found that the tensile strength of the composites decreased, while the tensile modulus increased with increasing EFB filler loading. The composites with maleic anhydride treated filler showed significantly higher values of both tensile strength and modulus. This agreed well with the behaviour observed in other natural fibre-filled PP composites studies [58,60,65,80].

## 2.5 References

1. S. Taj, M.A. Munawar, S. Khan. Natural fibre-reinforced polymer composites. Proceedings – Pakistan Academy of Science 2007; 44(2):129-144.
2. L.Y. Mwaikambo, M.P. Ansell. Hemp fibre reinforced cashew nut shell liquid composites. Composites Science and Technology 2003; 63:1297-1305.  
DOI: 10.1016/S0266-3538(03)00101-5
3. E.C. Botelho, R.A. Silva, L.C. Pardini, M.C. Rezende. A review on the development and properties of continuous fibre/epoxy/aluminum hybrid composites for aircraft structures. Materials Research 2006; 9(3):247-256.

4. D.H. Mueller, A. Krobjilowski. New discovery in the properties of composites reinforced with natural fibres. *Journal of Industrial Textiles* 2003; 33(2):111-129.  
DOI: 10.1177/152808303039248
5. W.J. Work, K. Horie, M. Hess, R.F.T. Stepto. Definitions of terms related to polymer blends, composites, and multiphase polymeric materials. *Pure and Applied Chemistry* 2004; 76(11):1985-2007.
6. S.E. Selke, I. Wichman. Wood fibre/polyolefin composites. *Composites Part A* 2004; 35:321-326.  
DOI: 10.1016/j.compositesa.2003.09.010
7. B. Mano, J.R. Araújo, M.A.S. Spinacé, M.-A. De Paoli. Polyolefin composites with curaua fibres: Effect of the processing conditions on mechanical properties, morphology and fibres dimensions. *Composites Science and Technology* 2010; 70:29-35.  
DOI: 10.1016/j.compscitech.2009.09.002
8. R.D. Adams, M.M. Singh. The dynamic properties of fibre-reinforced polymers exposed to hot, wet conditions. *Composites Science and Technology* 1996; 56:977-997.  
DOI: S0266-3538(96)00065-6
9. M. Wollerdorfer, H. Bader. Influence of natural fibres on the mechanical properties of biodegradable polymers. *Industrial Crops and Products* 1998; 8:105-112.  
DOI: S0926-6690(97)10015-2
10. A. Kalam, B.B. Sahari, Y.A. Khalid, S.V. Wong. Fatigue behaviour of oil palm fruit bunch fibre/epoxy and carbon fibre/epoxy composites. *Composite Structures* 2005; 71:34-44.  
DOI: 10.1016/j.compstuct.2004.09.034
11. N. Lopattananon, K. Panawarangkul, K. Sahakaro, B. Ellis. Performance of pineapple leaf fibre-natural rubber composites: The effect of fibre surface treatments. *Journal of Applied Polymer Science* 2006; 102:1974-1984.  
DOI: 10.1002/app.24584
12. N. Lopattananon, Y. Payae, M. Seadan. Influence of fibre modification on interfacial adhesion and mechanical properties of pineapple leaf fibre-epoxy composites. *Journal of Applied Polymer Science* 2008; 110:433-443.  
DOI: 10.1002/app.28496
13. D.N. Saheb, J.P. Jog. Natural fibre polymer composites: A review. *Advances in Polymer Technology* 1999; 18:351-363.

- DOI: 0730-6679/99/040351-13
14. M.J. John, S. Thomas. Biofibres and biocomposites. *Carbohydrate Polymers* 2008; 71:343-364.  
DOI: 10.1016/j.carbpol.2007.05.040
  15. A.K. Bledzki, J. Gassan. Composites reinforced with cellulose based fibres. *Progress in Polymer Science* 1999; 24:221-274.  
DOI: S0079-6700(98)00018-5
  16. A.K. Mohanty, M. Misra, G. Hinrichsen. Biofibres, biodegradable polymers and biocomposites: An overview. *Macromolecular Materials and Engineering* 2000; 276/277:1-24.  
DOI: 1438-7492/2000/0103-0001
  17. S. Zakaria, H. Hamzah, J.A. Murshidi, M. Deraman. Chemical modification on lignocellulosic polymeric oil palm empty fruit bunch for advance material. *Advances in Polymer Technology* 2001; 20(4):289-295.  
DOI: IRPA 03-02-02-0059
  18. A.-A.M.A. Nada, M.Y. El-Kady, E.S.A. El-Sayed, F.M. Amine. Preparation and characterization of microcrystalline cellulose (MCC). *BioResources* 2009; 4(4):1359-1371.
  19. Y. Habibi, W.K. El-Zawawy, M.M. Ibrahim, A. Dufresne. Processing and characterization of reinforced polyethylene composites made with lignocellulosic fibres from Egyptian agro-industrial residues. *Composites Science and Technology* 2008; 68:1877-1885.  
DOI: 10.1016/j.compscitech.2008.01.008
  20. A. Habrant, C. Gaillard, M.-C. Ralet, D. Lairez, B. Cathala. Relation between chemical structure and supramolecular organization of synthetic lignin-pectin particles. *Biomacromolecules* 2009; 10:3151-3156.  
DOI: 10.1021/bm900950r
  21. M. Micic, K. Radotic, M. Jeremic, D. Djikanovic, S.B. Kämmer. Study of the lignin model compound supramolecular structure by combination of near-field scanning optical microscopy and atomic force microscopy. *Colloids and Surfaces B: Biointerfaces* 2004; 34:33-40.  
DOI: 10.1016/j.colsurfb.2003.10.018
  22. R. Hatfield, W. Vermerris. Lignin formation in plants. The dilemma of linkage specificity. *Plant Physiology* 2001; 126:1351-1357.

23. N.A. Ibrahim, W.M.Z. Wan-Yunus, F.A.F. Abu-Llaiwi, M.Z.A. Rahman, M.B. Ahmad, K.Z.M. Dahlan. Optimized condition for grafting reaction of poly (butyl acrylate) onto oil palm empty fruit bunch fibre. *Polymer International* 2003; 52:1119-1124.  
DOI: 10.1002/pi.1192
24. G. Chauve, L. Heux, R. Arouini, K. Mazeau. Cellulose poly (ethylene-co-vinyl acetate) nanocomposites studied by molecular modelling and mechanical spectroscopy. *Biomacromolecules* 2005; 6:2025-2031.  
DOI: 10.1021/bm0501205
25. S. Sumathi, S.P. Chai, A.R. Mohamed. Utilization of oil palm as a source of renewable energy in Malaysia. *Renewable and Sustainable Energy Reviews* 2008; 12:2404-2421.  
DOI: 10.1016/j.rser.2007.06.006
26. K.-N. Law, W.R.W. Daud, A. Ghazali. Morphological and chemical nature of fibre strands of oil palm empty fruit bunch (OPEFB). *BioResources* 2007; 2(3):351-362.
27. M.Y. Rosnah, A. Ghazali, W.D. Wan Rosli, Y.M. Dermawan. Influence of alkaline peroxide treatment duration on the pulpability of oil palm empty fruit bunch. *World Applied Sciences Journal* 2010; 8(2):185-192.
28. H.D. Rozman, K.R. Ahmadhilmi, A. Abubakar. Polyurethane (PU) oil palm empty fruit bunch (EFB) composites: the effect of EFBG reinforcement in mat form and isocyanate treatment on the mechanical properties. *Polymer Testing* 2004; 23:559-565.  
DOI: 10.1016/j.polymertesting.2003.11.004
29. R.M. Soom, W.H.W. Hassan, M.T. AB Gapor, K. Hassan. Thermal properties of oil palm fibre, cellulose and its derivatives. *Journal of Oil Palm Research* 2006; 18:272-277.
30. H.D. Rozman, G.S. Tay, A. Abubakar, R.N. Kumar. Tensile properties of oil palm empty fruit bunch-polyurethane composites. *European Polymer Journal* 2001; 37:1759-1765.  
DOI: S0014-3057(01)00063-5
31. M.J. John, B. Francis, K.T. Varughese, S. Thomas. Effect of chemical modification on properties of hybrid fibre biocomposites. *Composites Part A* 2008; 39:352-363.  
DOI: 10.1016/j.compositesa.2007.10.002
32. J. Ratnasingam, T.C. Tek, S.R. Farrokhpayam. Tool wear characteristics of oil palm empty fruit bunch particleboard. *Journal of Applied Sciences* 2008; 8(8):1594-1596.



33. C.J.R. Verbeek. The influence of interfacial adhesion, particle size and size distribution on the predicted mechanical properties of particulate thermoplastic composites. *Materials Letters* 2003; 57:1919-1924.  
DOI: 10.1016/S0167-577X(02)01105-9
34. M. Wu, B. Bao, J. Chen. Study on antithrombosis dialytic membrane prepared by preirradiation grafting. *Journal of Applied Polymer Science* 2000; 78:1321-1327.
35. J. Jin, S.J. Chen, J. Zhang. Non-isothermal crystallization kinetics of partially miscible ethylene-vinyl acetate copolymer/low density polyethylene blends. *eXPRESS Polymer Letters* 2010; 4(3):141-152.  
DOI: 10.3144/expresspolymlett.2010.19
36. S. Bistac, P. Kunemann, J. Schultz. Crystalline modifications of ethylene vinyl acetate copolymers induced by a tensile drawing: effect of the molecular weight. *Polymer* 1998; 39(20):4875-4881.  
DOI: S0032-3861(97)10328-7
37. J. Jin, S. Chen, J. Zhang. UV aging behaviour of ethylene-vinyl acetate copolymers (EVA) with different vinyl acetate contents. *Polymer Degradation and Stability* 2010; 95:725-732.  
DOI: 10.1016/j.polymdegradstab.2010.02.020
38. M.D. Watson, K.B. Wagener. Ethylene/vinyl acetate copolymers via acyclic diene metathesis polymerization. Examining the effect of “long” precise ethylene run lengths. *Macromolecules* 2000; 33:5411-5417.  
DOI: 10.1021/ma9920689
39. A. Marcilla, A. Gómez-Siurana, S. Menargues, R. Ruiz-Femenia, J.C. García-Quesada. Oxidative degradation of EVA copolymers in the presence of MCM-41. *Journal of Analytical and Applied Pyrolysis* 2006; 76:138-143.  
DOI: 10.1016/j.jaap.2005.10.004
40. S.P. Tambe, S.K. Singh, M. Patri, D. Kumar. Ethylene vinyl acetate and ethylene vinyl alcohol copolymer for thermal spray coating application. *Progress in Organic Coatings* 2008; 62:382-386.
41. A. Arsac, C. Carrot, J. Guillet. Determination of primary relaxation temperatures and melting points of ethylene vinyl acetate copolymers. *Journal of Thermal Analysis and Calorimetry* 2000; 61:681-685.

42. N.S. Allen, M. Edge, M. Rodriguez, C.M. Liauw, E. Fontan. Aspects of the thermal oxidation of ethylene vinyl acetate copolymer. *Polymer Degradation and Stability* 2000; 68:363-371.  
DOI: S0141-3910(00)00020-3
43. Y.-J. Park, H.-J. Kim. Hot-melt adhesive properties of EVA/aromatic hydrocarbon resin blend. *International Journal of Adhesion & Adhesives* 2003; 23:383-392.  
DOI: 10.1016/S0143-7496(03)0009-1
44. A. Arsac, C. Carrot, J. Guillet. Rheological characterization of ethylene vinyl acetate copolymers. *Journal of Applied Polymer Science* 1999; 74:2625-2630.  
DOI: 0021-8995/99/112625-06
45. M. Zurina, H. Ismail, C.T. Ratnam. The effect of HVA-2 on properties of irradiated epoxidized natural rubber (ENR-50), ethylene vinyl acetate (EVA), and ENR-50/EVA blend. *Polymer Testing* 2008; 27:480-490.  
DOI: 10.1016/j.polymertesting.2008.02.001
46. Y.T. Sung, C.K. Kum, H.S. Lee, J.S. Kim, H.G. Yoon, W.N. Kim. Effects of crystallinity and crosslinking on the thermal and rheological properties of ethylene vinyl acetate copolymer. *Polymer* 2005; 46:11844-11848.  
DOI: 10.1016/j.polymer.2005.09.080
47. R.L. Mcevoy, S. Krause. Interfacial interactions between polyethylene and polypropylene and some ethylene-containing copolymers. *Macromolecules* 1996; 29:4258-4266.  
DOI: S0024-9297(95)01768-2
48. M. Rodríguez-Vázquez, C.M. Liauw, N.S. Allen, M. Edge, E. Fontan. Degradation and stabilisation of poly (ethylene-stat-vinyl acetate): 1 – Spectroscopic and rheological examination of thermal and thermo-oxidative degradation mechanisms. *Polymer Degradation and Stability* 2006; 91:154-164.  
DOI: 10.1016/j.polymdegradstab.2005.04.034
49. X.M. Shi, J. Zhang, J. Jin, S.J. Chen. Non-isothermal crystallization and melting of ethylene vinyl acetate copolymers with different vinyl acetate contents. *eXPRESS Polymer Letters* 2008; 2(9):623-629.  
DOI: 10.3144/expresspolymlett.2008.75
50. M.A. Rodríguez-Pérez, A. Duijsens, J.A. De Saja. Effect of addition of EVA on the technical properties of extruded foam profiles of low-density polyethylene/EVA blends. *Journal of Applied Polymer Science* 1998; 68:1237-1244.

- DOI: 0021-8995/98/081237-08
51. X. Shi, J. Jin, S. Chen, J. Zhang. Multiple melting and partial miscibility of ethylene-vinyl acetate copolymer/low density polyethylene blends. *Journal of Applied Polymer Science* 2009; 113:2868-2871.  
DOI: 10.1002/app.30271
  52. J. Peón, J.F. Vega, M. Aroca, J. Martínez-Salazar. Rheological behaviour of LDPE/EVA-c blends. On the effect of vinyl acetate comonomer in EVA copolymers. *Polymer* 2001; 42:8093-8101.  
DOI: S0032-3861(01)00313-5
  53. Y. Bai, J. Qian, A. Quanfu, Z. Zhu, P. Zhang. Pervaporation characteristics of ethylene vinyl acetate copolymer membranes with different composition for recovery of ethyl acetate from aqueous solution. *Journal of Membrane Science* 2007; 305:152-159.  
DOI: 10.1016/j.memsci.2007.07.042
  54. M.A.R. Moraes, A.C.F. Moreira, R.V. Barbosa, B.G. Soares. Graft copolymer from modified ethylene-vinyl acetate (EVA) copolymers. Poly (EVA-g-methyl methacrylate) from mercapto-modified EVA. *Macromolecules* 1996; 29:416-422.  
DOI: 0024-9297/96/2229-0416
  55. G.C. Stael, M.I.B. Tavares, J.R.M. d'Almeida. Impact behaviour of sugarcane bagasse waste-EVA composites. *Polymer Testing* 2001; 20:869-872.  
DOI: S0142-9418(01)00014-9
  56. M.E. Malunka, A.S. Luyt, H. Krump. Preparation and characterization of EVA-sisal fibre composites. *Journal of Applied Polymer Science* 2006; 100:1607-1617.  
DOI: 10.1002/app.23650
  57. D.G. Dikobe, A.S. Luyt. Effect of poly (ethylene-co-glycidyl methacrylate) compatibilizer content on the morphology and physical properties of ethylene vinyl acetate-wood fibre composites. *Journal of Applied Polymer Science* 2007; 104:3206-3213.  
DOI: 10.1002/app.26080
  58. A.K. Rana, A. Mandal, B.C. Mitra, R. Jacobson, R. Rowell, A.N. Banerjee. Short jute fibre-reinforced polypropylene composites: Effect of compatibilizer. *Journal of Applied Polymer Science* 1998; 69:329-338.  
DOI: 0021-8995/98/020329-10

59. J.R. Araújo, W.R. Waldman, M.A. De Paoli. Thermal properties of high density polyethylene composites with natural fibres: Coupling agent effect. *Polymer Degradation and Stability* 2008; 93:1770-1775.  
DOI: 10.1016/j.polymdegradstab.2008.07.021
60. M. Khalid, A. Salmiaton, C.T. Ratnam, C.A. Luqman. Effect of trimethylolpropane triacrylate (TMPTA) on the mechanical properties of palm fibre empty fruit bunch and cellulose fibre biocomposite. *Journal of Engineering Science and Technology* 2008; 3(2):153-162.
61. M.F. Rosa, B.-S. Chiou, E.S. Medeiros, D.F. Wood, T.G. Williams, L.H.C. Mattoso, W.J. Orts, S.H. Imam. Effect of fibre treatments on tensile and thermal properties of starch/ethylene vinyl alcohol copolymers/coir biocomposites. *Bioresource Technology* 2009; 100:5196-5202.
62. P.V. Joseph, K. Joseph, S. Thomas. Effect of processing variables on the mechanical properties of sisal fibre-reinforced polypropylene composites. *Composites Science and Technology* 1999; 59:1625-1640.  
DOI: S0266-3538(99)00024-X
63. P.J. Herrera-Franco, A. Valadez-González. Mechanical properties of continuous natural fibre-reinforced polymer composites. *Composites Part A* 2004; 35:339-345.  
DOI: 10.1016/j.compositesa.2003.09.012
64. J. Biagiotti, D. Puglia, L. Torre, J.M. Kenny. A systematic investigation on the influence of the chemical treatment of natural fibres on the properties of their polymer matrix composites. *Polymer Composites* 2004; 25(5):470-479.  
DOI: 10.1002/pc.20040
65. X.L. Xie, K.L. Fung, R.K.Y. Li, S.C. Tjong, Y.-W. Mai. Structural and mechanical behaviour of polypropylene/maleated styrene-(ethylene-co-butylene)-styrene/sisal fibre composites prepared by injection molding. *Journal of Polymer Science, Part B: Polymer Physics* 2002; 40:1214-1222.
66. M. Khalid, C.T. Ratnam, T.G. Chuah, S. Ali, T.S.Y. Choong. Comparative study of polypropylene composites reinforced with oil palm empty fruit bunch fibre and oil palm derived cellulose. *Materials and Design* 2008; 29:173-178.  
DOI: 10.1016/j.matdes.2006.11.002
67. X.P. Zhou, R.K.Y. Li, X.L. Xie, S.C. Tjong. Reinforcement of polypropylene using sisal fibres grafted with poly (methyl methacrylate). *Journal of Applied Polymer Science* 2003; 88:1055-1064.

68. A. Keller, D. Bruggmann, A. Neff, B. Müller, E. Wintermantel. Degradation kinetics of biodegradable fibre composites. *Journal of Polymers and the Environment* 2000; 8(2):91-96.
69. I. Krupa, V. Cecen, R. Tlili, A. Boudenne, L. Ibos. Thermophysical properties of ethylene-vinyl acetate copolymer (EVA) filled with wollastonite fibres coated by silver. *European Polymer Journal* 2008; 44:3817-3826.
70. T.-T.-L. Doan, H. Brodowsky, E. Mäder. Jute fibre/polypropylene composites II. Thermal, hydrothermal and dynamic mechanical behaviour. *Composites Science and Technology* 2007; 67:2707-2714.  
DOI: 10.1016/j.compscitech.2007.02.011
71. I. Baroulaki, J.A. Mergos, G. Pappa, P.A. Tarantili, D. Economides, K. Magoulas, C.T. Dervos. Performance of polyolefin composites containing recycled paper fibres. *Polymers for Advanced Technologies* 2006; 17:954-966.  
DOI: 10.1002/pat.827
72. J.Z. Lu, Q. Wu, I.I. Negulescu. Wood-fibre/high-density polyethylene composites: coupling agent performance. *Journal of Applied Polymer Science* 2005; 96:93-102.  
DOI: 10.1002/app.21410
73. F. Mengeloglu, A. Kabakci. Determination of thermal properties and morphology of eucalyptus wood residue filled high density polyethylene composites. *International Journal of Molecular Sciences* 2008; 9:107-119.
74. J. George, M.S. Sreekala, S. Thomas. A review on interface modification and characterization of natural fibre reinforced plastic composites. *Polymer Engineering and Science* 2001; 41(9):1471-1485.
75. D. Pasquini, E.M. Teixeira, A.A.S. Curvelo, M.N. Belgacem, A. Dufresne. Surface esterification of cellulose fibres: Processing and characterisation of low density polyethylene/cellulose fibres composites. *Composites Science and Technology* 2008; 68:193-201.  
DOI: 10.1016/j.compscitech.2007.05.009
76. N.E. Marcovich, M.A. Villar. Thermal and mechanical characterization of linear low-density polyethylene/wood flour composites. *Journal of Applied Polymer Science* 2003; 90:2775-2784.
77. B. Liao, Y. Huang, G. Cong. Influence of modified wood fibres on the mechanical properties of wood fibre-reinforced polyethylene. *Journal of Applied Polymer Science* 1997; 66:1561-1568.

- DOI: 0021-8995/7/081561-08
78. A. Choudhury, S. Kumar, B. Adhikari. Recycled milk pouch and virgin low-density polyethylene/linear low-density polyethylene based coir fibre composites. *Journal of Applied Polymer Science* 2007; 106:775-785.  
DOI: 10.1002/app.26522
  79. D.G. Dikobe, A.S. Luyt. Effect of filler content and size on the properties of ethylene vinyl acetate copolymer-wood fibre composites. *Journal of Applied Polymer Science* 2007; 103:3645-3654.  
DOI: 10.1002/app.25513
  80. H.D. Rozman, K.W. Tan, R.N. Kumar, A. Abubakar, Z.A. Mohd. Ishak, H. Ismail. The effect of lignin as a compatibilizer on the physical properties of coconut fibre-polypropylene composites. *European Polymer Journal* 2000; 36:1483-1494.  
DOI: S0014-3057(99)00200-1
  81. H.D. Rozman, M.J. Saad, Z.A. Mohd. Ishak. Modification of oil palm empty fruit bunches with maleic anhydride: The effect on the tensile and dimensional stability properties of empty fruit bunch/polypropylene composites. *Journal of Applied Polymer Science* 2003; 87:827-835.
  82. M.J. John, R.D. Anandjiwala. Recent developments in chemical modification and characterization of natural fibre-reinforced composites. *Polymer Composites* 2008; 29:187-207.  
DOI: 10.1002/pc.20461
  83. H.D. Rozman, B.K. Kon, A. Abusamah, R.N. Kumar, Z.A. Mohd. Ishak. Rubberwood high-density polyethylene composites: Effect of filler size and coupling agents on mechanical properties. *Journal of Applied Polymer Science* 1998; 69:1993-2004.  
DOI: 0021-8995/98/101993-12
  84. F. Mengeloglu, K. Karakus. Thermal degradation, mechanical properties and morphology of wheat straw flour filled recycled thermoplastic composites. *Sensors* 2008; 8:500-519.
  85. H.-S. Kim, S. Kim, H.-J. Kim, H.-S. Yang. Thermal properties of bio-flour filled polyolefin composites with different compatibilizing agent type and content. *Thermochimica Acta* 2006; 451:181-188.  
DOI: 10.1016/j.tca.2006.09.013

86. R.R.N. Sailaja. Mechanical and thermal properties of bleached kraft pulp-LDPE composites: Effect of epoxy functionalized compatibilizer. *Composites Science and Technology* 2006; 66:2039-2048.  
DOI: 10.1016/j.compscitech.2006.01.029
87. B. Tajeddin, R.A. Rahman, L.C. Abdulah, N.A. Ibrahim, Y.A. Yusof. Thermal properties of low density polyethylene filled kenaf cellulose composites. *European Journal of Scientific Research* 2009; 32(2):223-230.  
DOI: ISSN 1450-216X
88. B. Ramaraj, K.R. Yoon. Thermal and physicomechanical properties of ethylene-vinyl acetate copolymer and layered double hydroxide composites. *Journal of Applied Polymer Science* 2008; 108:4090-4095.  
DOI: 10.1002/app.28026
89. S.K. Nayak, S. Mohanty, S.K. Samal. Influence of short bamboo/glass fibre on the thermal, dynamic mechanical and rheological properties of polypropylene hybrid composites. *Materials Science and Engineering A* 2009; 523:32-38.  
DOI: 10.1016/j.msea.2009.06.020
90. D.F. Caulfield, D. Feng, S. Prabawa, R.A. Young, A.R. Sanadi. Interphase effects on the mechanical and physical aspects of natural fibre composites. *Die Angewandte Makromolekulare Chemie* 1999; 272:57-64.  
DOI: 0003-3146/99/0112-0057
91. N.C. Das, T.K. Chaki, D. Khastgir. Effect of filler treatment and crosslinking on mechanical and dynamic mechanical properties and electrical conductivity of carbon black-filled ethylene vinyl acetate copolymer composites. *Journal of Applied Polymer Science* 2003; 90:2073-2082.
92. M. Behzad, M. Tajvidi, G. Ehrahimi, R.H. Falk. Dynamic mechanical analysis of compatibilizer effect on the mechanical properties of wood flour-high-density polyethylene composites. *IJE Transactions B: Applications* 2004; 17(1):95-104.
93. D. Bikiaris, P. Matzinos, A. Larena, V. Flaris, C. Panayiotou. Use of silane agents and poly (propylene-g-maleic anhydride) copolymer as adhesion promoters in glass fibre/polypropylene composites. *Journal of Applied Polymer Science* 2001; 81:701-709.
94. M. Abdelmouleh, S. Boufi, M.N. Belgacem, A. Dufresne. Short natural fibre-reinforced polyethylene and natural rubber composites: Effect of silane coupling agents and fibres loading. *Composites Science and Technology* 2007; 67:1627-1639.

DOI: 10.1016/j.compscitech.2006.07.003

95. M.M. Haque, M. Pracella. Reactive compatibilization of composites of ethylene-vinyl acetate copolymers with cellulose fibres. *Composites Part A* (In press).

DOI: 10.1016/j.compositesa.2010.07.001

96. J.-P. Kim, T.-H. Yoon, S.-P. Mun, J.-M. Rhee, J.-S. Lee. Wood-polyethylene composites using ethylene vinyl alcohol copolymer as adhesion promoter. *Bioresource Technology* 2006; 97:494-499.

DOI: 10.1016/j.biortech.2005.02.048



## CHAPTER 3

### EXPERIMENTAL

#### 3.1 Materials

##### 3.1.1 Ethylene vinyl acetate (EVA)

EVA-460 was manufactured and supplied in granule form by DuPont Packaging & Industrial Polymers. EVA-460 contains 18% by weight of VA with a BHT antioxidant thermal stabilizer. It has an MFI (190 °C / 2.16 kg) of 2.5 g/10 min (ASTM D1238-ISO 1133),  $T_m$  of 88 °C, vicat softening point of 64 °C, and density of 0.941 g cm<sup>-3</sup>.

EVA-260 was manufactured and supplied in granule form by DuPont Packaging & Industrial Polymers. EVA-260 contains 28% by weight VA with a BHT antioxidant thermal stabilizer. It has an MFI (190 °C / 2.16 kg) of 6.0 g/10 min (ASTM D1238-ISO 1133),  $T_m$  of 75 °C, vicat softening point of 46 °C, cloud point in paraffin wax of 66 °C, softening point ring and ball of 154 °C, brittleness temperature of -100 °C and density of 0.955 g cm<sup>-3</sup>.

##### 3.1.2 Empty fruit bunch (EFB) fibre

The EFB fibre was obtained from palm oil mills in Malaysia. It had a particle size of less than 150 µm and a bulk density in the range of 0.75 to 0.90 g cm<sup>-3</sup>.

#### 3.2 Methods

##### 3.2.1 Preliminary work on EFB fibre

The raw fruit bunch was taken directly from a palm oil mill, then pre-treated (pressed, shredded), dried, and converted into the EFB fibre by a processing technique called pyrolysis. In the pyrolysis unit, sufficient heat was generated to dry the wet EFB to less than 10 wt% by weight of water [1].

### 3.2.2 Preparation of composites

The EFB fibres were sieved through a 150  $\mu\text{m}$  pore size sieve and put into an oven at 105  $^{\circ}\text{C}$  overnight for moisture reduction. The materials were prepared by a melt mixing process using a Brabender Plastograph internal mixer. The mixing speed was 30 rpm at a temperature of 120  $^{\circ}\text{C}$  for 10 min. The compositions of the investigated samples are listed in Table 3.1. The samples were melt-pressed at 120  $^{\circ}\text{C}$  and 50 bars for 5 min into 100 mm x 100 mm x 2 mm square sheets by using a hot hydraulic press. These conditions were set in order to ensure the film production efficiency and the avoidance of the bubbles on the film. All the test samples were then cut from the sheets for different analyses.

**Table 3.1 List of the samples and compositions used in the present study**

<b>EVA-460/EFB (w/w)</b>	<b>EVA-260/EFB (w/w)</b>
100/0	100/0
90/10	90/10
80/20	80/20
70/30	70/30

### 3.3 Characterization and analysis

#### 3.3.1 Scanning electron microscopy (SEM)

SEM is a well-known imaging technique, making use of the emission of electrons from a surface when irradiated by a scanning electron beam. In SEM the focused electron beam is scanned over the area of interest of the specimen surface at high speed. The scan rate for the electron beam can be increased so that a virtual three dimensional (3-D) image of the specimen is observed. When the primary electrons hit the sample, the interaction of the beam electrons with the sample atoms generates a variety of signals such as secondary electrons (SE), backscattered electrons (BSE) and x-rays used for making an image of the sample. The image can be captured by standard photography. SEM images have great depth of information giving out a characteristic 3-D appearance useful for understanding the surface structure of a sample [2].

SEM analyses were carried out in a Shimadzu SSX-550 Superscan scanning electron microscope (SEM) (Tokyo, Japan). The surfaces of the samples were coated with gold by a BioRAD Sputter Coater for 135 seconds at 120  $\mu\text{m}$  probe size, the probe current was 0.02 nA, the lateral resolution 2.0  $\mu\text{m}$  and the AC voltage 5.0 keV. The images were then captured by standard photography.

### 3.3.2 Differential scanning calorimetry (DSC)

DSC is a thermoanalytical technique in which the difference in the amount of heat required to increase the temperature of a sample and reference are measured as a function of temperature or time. DSC is used to study the thermal or phase transitions of a polymer like the melting temperature, crystallization temperature ( $T_c$ ), glass transition temperature ( $T_g$ ), and exothermic or endothermic decompositions ( $T_d$ ). It is widely used in industrial settings as a quality control instrument due to its applicability in evaluating sample purity and for studying polymer curing. The most common application of DSC is to study the melting process which, in principle, contains information on both the quality (temperature) and the quantity (peak area) of crystallinity in a polymer [3-5].

The sample analyses were carried out under nitrogen flow (20 ml min<sup>-1</sup>) using a Perkin Elmer Pyris-1 differential scanning calorimeter (Waltham, Massachusetts, U.S.A). The instrument was computer controlled and calculations were performed using Pyris software. The instrument was calibrated using the onset temperatures of melting of indium and zinc standards as well as the melting enthalpy of indium. The sample weights were in the range of 5-10 mg, and they were heated from 25 to 180 °C at a heating rate of 10 °C min<sup>-1</sup>. The cooling and second heating were also performed under the same conditions. For all the samples, the onset and peak temperatures of melting and crystallization, as well as the melting and crystallization enthalpies were determined from the second scan. The degree of crystallinity was calculated using the total enthalpy method, according to equation 3.1.

$$\chi_c = \frac{\Delta H_m}{\Delta H_m^0} \times 100\% \quad (\text{Eq. 3.1})$$

where  $\chi_c$  is the degree of crystallinity,  $\Delta H_m$  is the specific enthalpy of melting, and  $\Delta H_m^0$  is the specific enthalpy of melting for 100% crystalline PE. A value of  $288 \text{ J g}^{-1}$  was used in the calculations [6].

### **3.3.3 Thermogravimetric analysis (TGA)**

By definition, thermogravimetric analysis is a technique in which the mass of a substance is measured as a function of time or temperature while the substance is subjected to a controlled temperature program. It provides a quantitative measurement of any mass change in the polymer or material associated with a transition or thermal degradation. It can directly record the change in mass due to dehydration, decomposition, or oxidation of a polymer with time or temperature. It provides a rapid means to distinguish one polymer from another on the basis of the temperature range, extent, rate, and activation energy of decomposition. It is often used to characterize degradation reactions and to quantify thermal stability of materials under a variety of conditions. TGA is also useful for compositional analysis of multi-component materials and used to examine the kinetics of the physio-chemical processes occurring in the sample [7,8].

The analyses were done under flowing nitrogen atmosphere at a constant heating rate of  $20 \text{ ml min}^{-1}$  using a Perkin Elmer TGA 7 thermogravimetric analyser (Waltham, Massachusetts, U.S.A). The sample is placed in a furnace while being suspended from one arm of a precision balance. The samples, weighing 5-10 mg each, were then heated from 30 to  $600 \text{ }^\circ\text{C}$  at a heating rate of  $10 \text{ }^\circ\text{C min}^{-1}$ . The instrument was computer controlled and calculations were done using Pyris software. The instrument was calibrated using the Curie temperatures of five different metal standards.

### **3.3.4 Dynamic mechanical analysis (DMA)**

DMA is a thermal analysis technique that measures the properties of materials as they are deformed under periodic stress. The DMA determines changes in sample properties resulting from changes in five respective experimental variables: temperature, time, frequency, force, and strain. DMA measures also the stiffness and damping properties of a material. The stiffness depends on the mechanical properties of the material and its dimensions. The storage

modulus  $E'$  (elastic response) and loss modulus  $E''$  (viscous response) of polymers are measured by DMA as a function of temperature or time. DMA is the most sensitive of all thermoanalytical techniques for monitoring relaxation events, such as glass transitions ( $T_g$ ) and other relaxation transitions [9].

In DMA the sample is clamped between the ends of the two parallel arms. The distance between the arms is adjustable by means of a precision mechanical slide to accommodate a wide range of sample lengths from less than 1 mm up to 65 mm. An electromechanical motor attached to one arm drives the arm/sample system to a selected strain or amplitude. As the arm/sample system is displaced, the sample undergoes a flexural deformation. The sample is positioned in a temperature-controlled chamber. This heating system is precise and gives accurate control of the sample temperature. The viscoelastic properties of the composites were studied using the Perkin Elmer Diamond DMA (Waltham, Massachusetts, U.S.A). Table 3.2 summarizes the analysis conditions used for the different types of samples.

**Table 3.2 Summary of DMA analysis conditions**

<b>EVA-460</b>	
<b>Parameters</b>	<b>Typical set values</b>
Frequency	1 Hz
Amplitude	20 $\mu\text{m}$
Temperature range	-90 to 90 $^{\circ}\text{C}$
Heating rate	5 $^{\circ}\text{C min}^{-1}$
Preload force	800 mN
Sample length	20 mm
Sample width	11-12 mm
Sample thickness	2 mm
<b>EVA-260</b>	
<b>Parameters</b>	<b>Typical set values</b>
Frequency	1 Hz
Amplitude	20 $\mu\text{m}$
Temperature range	-90 to 75 $^{\circ}\text{C}$
Heating rate	5 $^{\circ}\text{C min}^{-1}$
Preload force	800 mN
Sample length	20 mm
Sample width	11-12 mm
Sample thickness	2 mm

### 3.3.5 Tensile testing

Tensile testing is the mechanical or physical testing of polymer materials carried out under an extension force. The results of tensile tests are used in selecting appropriate materials for engineering applications. The tests are also used to assess the ageing or chemical resistance of materials. They are, however, of limited use in predicting material performance due to limited information provided by the tests. Tensile properties are frequently useful indicators to ensure quality control of material specifications, and to predict the behaviour of a material under forms of loading other than uniaxial tension [10].

The mechanical properties were investigated using a Hounsfield H5KS tensile tester at a cross-head speed of  $10 \text{ mm min}^{-1}$ . The tensile modulus, as well as stress and elongation at break of the samples were calculated from the stress-strain curves. At least five specimens were tested for each sample and the mean values and standard deviations are reported. The dimensions of the dumbbell shaped samples are shown in Figure 3.1, and the analysis conditions are summarized in Table 3.3.

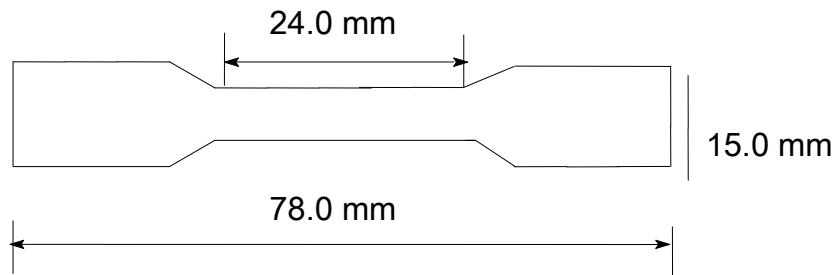


**Figure 3.1** Dumbbell-shaped specimen used for tensile testing (sample thickness 2 mm)

**Table 3.3 Tensile testing analysis conditions**

Parameters	Set values
Stress range / Mpa	100.0
Extension range / %	50.00
Gauge length / mm	24.00
Speed / mm min <sup>-1</sup>	10.00
Approach speed / mm min <sup>-1</sup>	10.00
Preload force / N	0.00

### 3.3.6 Fourier transform infrared (FTIR) spectroscopy

FTIR spectroscopy provides specific information about chemical bonding and molecular structures, making it useful for analysing organic materials and certain inorganic materials. FTIR is routinely used for forensic analysis as an attempt to identify foreign materials in food or beverage products by matching the spectra of the material in question with the spectra of known compounds. It can also be used to assess quantitatively some fundamental components of an unknown or unidentifiable mixture. FTIR spectroscopy involves collecting absorption information and analysing it in the form of a spectrum – the frequencies at which there are absorptions of IR radiation (“peaks” or “signals”) can be correlated directly to bonds within the compound in question [11,12].

FTIR spectroscopy was performed using a Perkin Elmer precisely multiscope (Waltham, Massachusetts, U.S.A) connected to a Perkin Elmer Spectrum 100 FTIR spectrophotometer. The samples were scanned 32 times using over a 400 to 4000 cm<sup>-1</sup> wavenumber range at a resolution of 4 cm<sup>-1</sup>. The FTIR spectra were eventually recorded in the transmittance mode.

### 3.4 References

1. R.M. Soom, W.H.W. Hassan, A.B. Gapor Md Top, K. Hassan. Thermal properties of oil palm fibre, cellulose and its derivatives. *Journal of Oil Palm Research* 2006; 18:272-277.
2. <http://knowledgecontext.org/COSMOS/Surface and Materials Analysis Techniques>.

3. C. Schick. Differential scanning calorimetry (DSC) of semicrystalline polymers. *Analytical and Bioanalytical Chemistry* 2009; 395:1589-1611.
4. E. Gmelin, St.M. Sarge. Calibration of differential scanning calorimeters. *Pure and Applied Chemistry* 1995; 67:1789-1800.
5. R.L. Danley. New heat flux DSC measurement technique. *Thermochimica Acta* 2003; 395:201-208.
6. H.A. Khonakdar, U. Wagenknecht, S.H. Jafari, R. Hässler, H. Eslami. Dynamic mechanical properties and morphology of polyethylene/ethylene vinyl acetate copolymer blends. *Advances in Polymer Technology* 2004; 23:307-315.
7. M. Fan, R.C. Brown. Comparison of the loss-on-ignition and thermogravimetric analysis techniques in measuring unburned carbon in coal fly ash. *Energy and Fuels* 2001; 15:1414-1417.
8. R.E. Zacharia, S.L. Simon. Dynamic and isothermal thermogravimetric analysis of a polycyanurate thermosetting system. *Polymer Engineering and Science* 1998; 38:566-572.
9. <http://www.perkinelmer.com>
10. W.F. Hosford. Overview of tensile testing. *Tensile Testing*, P. Han, Ed., ASM International (1992) p.1-24.
11. E. David-Vaudey, A. Burghardt, K. Keshari, A. Brouchet, M. Ries, S. Majumdar. Fourier transform infrared imaging of focal lesions in human osteoarthritic cartilage. *European Cells and Materials* 2005; 10:51-60.
12. J.M. Chalmers, N.J. Everall, K. Hewitson, M.A. Chesters, M. Pearson, A. Grady, B. Ruzicka. Fourier transform infrared microscopy: some advances in techniques for characterisation and structure-property elucidations of industrial material. *Analyst* 1998; 123:579-586.



## CHAPTER 4

### RESULTS AND DISCUSSION

#### 4.1 Scanning electron microscopy (SEM)

The SEM micrographs of the different EVA/EFB fibre composites are presented in Figures 4.1 to 4.2. Figure 4.1 shows the SEM micrographs of the 90/10 and 70/30 w/w EVA18/EFB composites. The pictures in Figure 4.1(a) and Figure 4.1(c) show some fewer fibre pull-outs creating holes with smooth walls in the EVA matrix. Generally there seems to be quite intimate contact between the EVA18 and the EFB, although the high-magnification picture in Figure 4.1(b) does show the presence of a very small void around the fibre. The very negligible void indicates better wettability of the fibre and improved interfacial adhesion [1-6]. This can be attributed to an increase in the vinyl acetate (VA) content, which allows more effective interaction between the -OH groups on EFB and the polar functional groups on the polymer [7]. It seems from Figures 4.1(a), 4.1(c) and 4.1(d) as if a layer of EVA may cover the fibre surfaces (marked A, B and C in the figures), suggesting good interaction. This is because of the interaction of the VA group on the polymer interacting with the OH groups on the fibre [1,2,10]. This was also reported by various authors [5,6,8]. Yusoff *et al.* [5] studied the mechanical properties of short random oil palm fibre reinforced epoxy composites, while Abdul-Khali *et al.* [6] worked on the effects of mechanical and physical properties of oil palm fibre (EFB) reinforced polyester composites. Arib *et al.* [8] investigated the mechanical properties of pineapple leaf fibre reinforced polypropylene composites. They found that there was a void or small gap formed between the matrix and fibre due to insufficient wetting of the fibre by the polymer. This is in agreement with other published research work on natural fibre reinforced polymer composites [7,9-11]. Figures 4.1(c) and (d) show small fibre agglomerations and contact between different fibres in the polymer matrix (marked A and B in the figures). There is also an evidence of fibre disorientation and differences in fibre sizes in the composites, which may affect the efficiency of stress transfer [11,13].

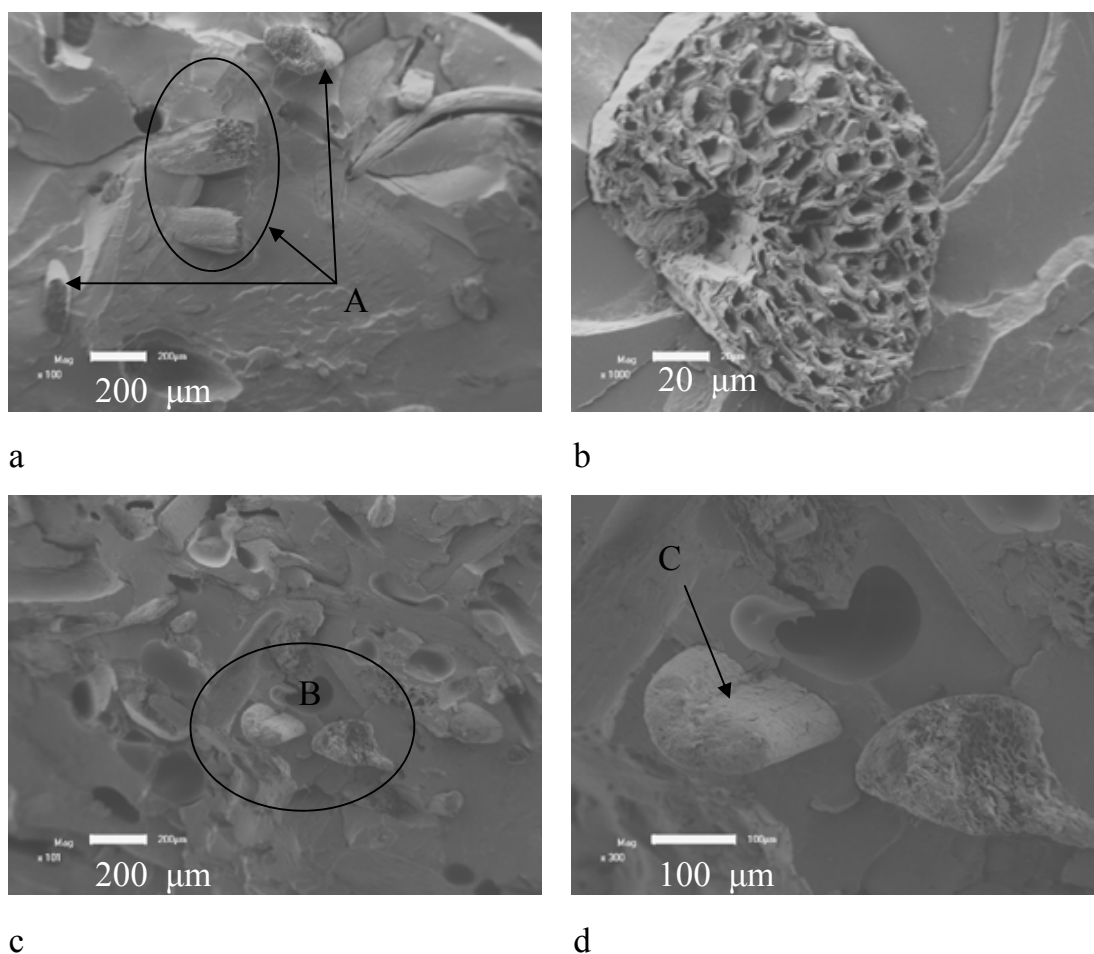


**Figure 4.1 SEM micrographs of 90/10 w/w EVA18/EFB ((a) 100x magnification & (b) 1000x magnification), and 70/30 w/w EVA18/EFB ((c) 100x magnification & (d) 300x magnification) composites**

The SEM micrographs of the 90/10 and 70/30 w/w EVA28/EFB composites are presented in Figure 4.2. It is clear from the pictures in this figure that (i) there are little or no voids around the fibres, (ii) there is almost no fibre pull-out resulting from the fracturing of the composites, and (iii) there are fibre bending, twisting and fracturing on the composites' fracture surfaces. There are also indications of EVA28 adhering to the EFB surfaces. All these observations indicate that the compatibility between these components is improved, which is mainly due to an increase in the number of VA groups that interact with the -OH groups on the EFB fibre surface [1,6,13,14].

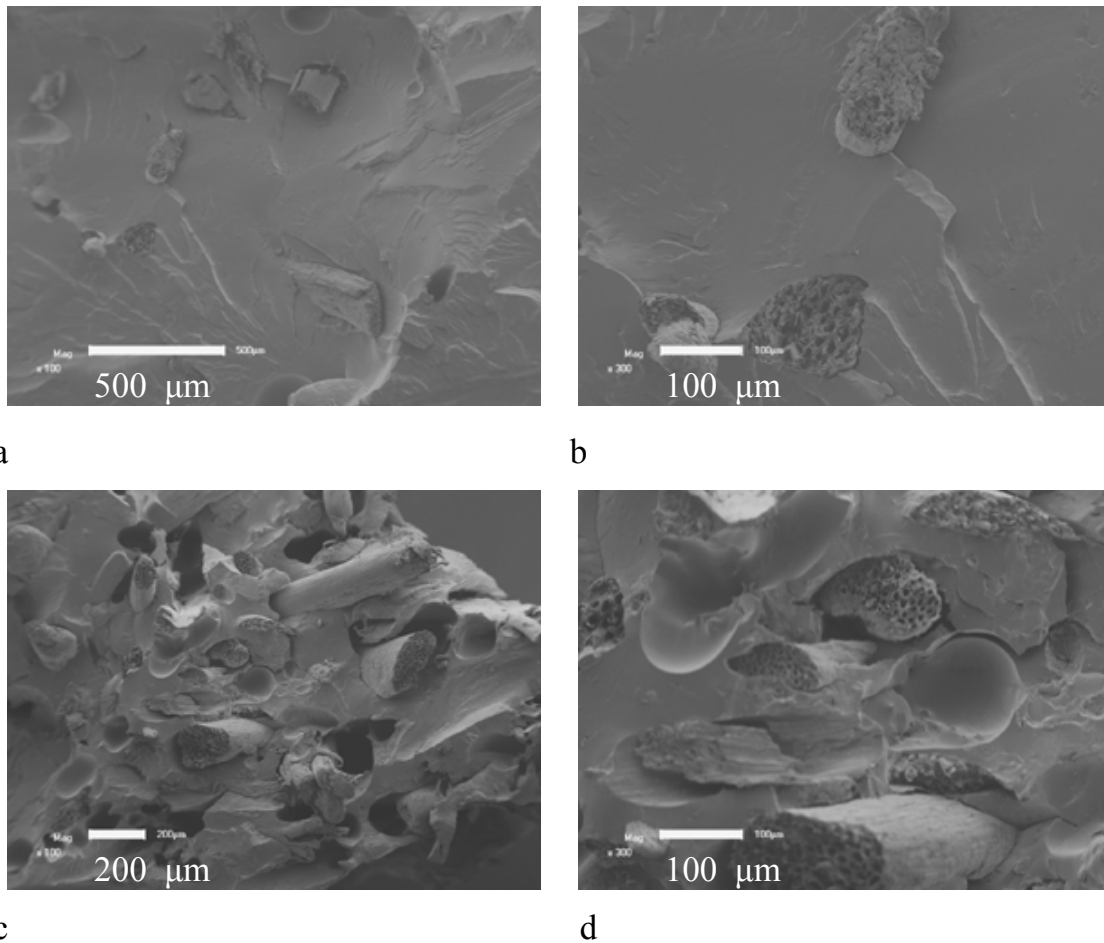


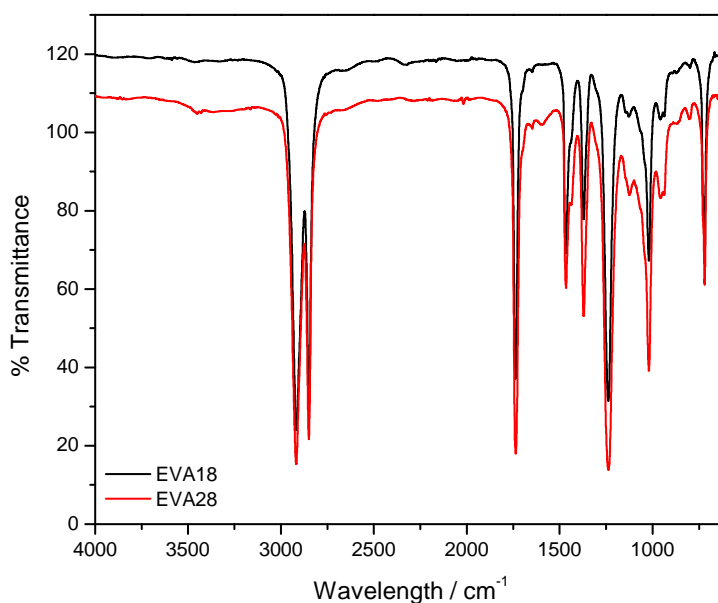
**Figure 4.2 SEM micrographs of 90/10 w/w EVA28/EFB ((a) 100x magnification & (b) 300x magnification), and 70/30 w/w EVA28/EFB ((c) 100x magnification & (d) 300x magnification) composites**

#### **4.2 Attenuated total reflectance Fourier-transform infrared spectroscopy (ATR-FTIR)**

Figures 4.3 to 4.5 show the FTIR spectra of the EVA copolymers with different VA contents, the EFB fibre and the EVA/EFB composites. The absorption bands for these samples are summarized in Table 4.1. In Figure 4.3, the spectra of the pure EVA copolymers present absorption peaks around 2850 and 2920  $\text{cm}^{-1}$  that correspond to the C–H asymmetric stretching of the EVA copolymers. The characteristic absorption peaks of the VA groups are as follows: 1736  $\text{cm}^{-1}$  attributed to the stretching vibration of the  $\text{–C=O}$  band; 1240  $\text{cm}^{-1}$

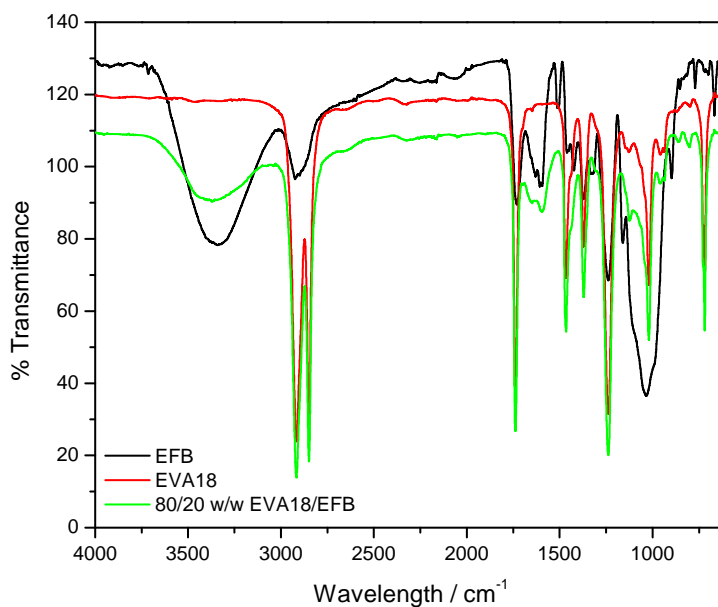
attributed to the asymmetrical stretching vibration of the C–O band;  $1030\text{ cm}^{-1}$  attributed to the symmetric stretching vibration of the C–O–C band;  $718\text{ cm}^{-1}$  attributed to the inner rocking vibration of methylene [15]. The observed absorption peaks around  $1439\text{ cm}^{-1}$  are largely attributed to the contributions from both VA and ethylene ( $-\text{CH}_2$ ) units [15-17]. The intensities of the absorption peaks at 718, 1030, 1240, 1439, 2850 and  $2920\text{ cm}^{-1}$  seem to increase with an increase in the VA content, which is to be expected. The spectra of pure EVA copolymers show a peak at around  $1372\text{ cm}^{-1}$ , which could be associated with the acetoxy groups of the EVA matrix [18].

Figure 4.4 represents the FTIR spectra of the pure EVA18, the EFB fibre and the EVA18/EFB composites. The spectrum of the EFB fibre shows a broad characteristic peak around  $3430\text{--}3300\text{ cm}^{-1}$ , which indicates the presence of O–H stretching. The bands at 2920, 2850 and  $1496\text{ cm}^{-1}$  due to C–H stretching of methyl or methylene groups are also observed in the spectrum of the EFB fibre. The EVA18/EFB composite spectrum shows all the characteristic peaks for both pure EVA18 and EFB, and a slight shift in the peaks is observed. The peak at  $1592\text{ cm}^{-1}$  is due to a C=C stretching [19], and indicates that EFB contains fatty acids from lignin. The C=C peak at  $1592\text{ cm}^{-1}$  in the 80/20 w/w EVA18/EFB composite is much less intense than that of EFB. The most probable reason for this is the smaller amount of fibre on the composite surface. There is a slight shift in the carbonyl peak, the C=O stretching vibration at  $1727\text{ cm}^{-1}$  to  $1736\text{ cm}^{-1}$  in the EVA18/EFB composites. This may indicate an interaction between the carbonyl group of lignin and the methine ( $-\text{CH}$ ) hydrogen of the EVA [20]. A slight increase in the intensity of the carbonyl peak at  $1736\text{ cm}^{-1}$  is observed, which may be the result of additional carbonyl groups contributed by the EFB fibre. It is expected that the interaction between the VA carbonyl group and the EFB hydroxyl group may influence the position and intensity of the carbonyl peak in the composite spectrum. In this case there is an observable increase in the intensity of this peak, which is contrary to what one would expect, and there does not seem to be any change in the peak position. It seems as if it is not possible to conclusively confirm interactions between the polymer and the fibre from the FTIR results.



**Figure 4.3 Comparison of the FTIR spectra of the pure EVA copolymers containing different VA contents**

Some studies were carried out by various researchers such as Mwaikambo and Ansell [19], Dikobe and Luyt [21] and Pracella *et al.* [22] which explained the changes in the  $\text{-C=O}$  peak intensity. Mwaikambo and Ansell [19] found a reduction in the peak intensity at around  $1654\text{ cm}^{-1}$  in alkali treated fibres, indicating partial reaction between the  $\text{-C=O}$  groups of hemicellulose and the  $\text{-OH}$  group in NaOH. Their study was on the chemical modification of hemp, sisal, jute, and kapok fibres by alkalization. Dikobe and Luyt [21] investigated the morphology and properties of polypropylene/ethylene vinyl acetate copolymer/wood powder blend composites. They found that the  $\text{-C=O}$  peak at  $1750\text{ cm}^{-1}$  in the blend composite was much less intense than that of pure EVA and the PP/EVA blend, due to the interaction of the  $\text{-C=O}$  group in EVA with the  $\text{-OH}$  group in wood powder (WP). In contrast to these studies, Pracella *et al.* [22], who studied the compatibilization and properties of EVA copolymers containing surface-functionalized cellulose microfibrils, found an increase in the intensity of the carbonyl peak at  $1718\text{ cm}^{-1}$  and explained it as being due to the formation of hydrogen bonding between the epoxy moiety in glycidyl methacrylate (GMA) and the  $\text{-OH}$  group of cellulose. Although they investigated a different system, the FTIR results of Pracella *et al.* [22] seem to be in line with the results reported in this thesis.



**Figure 4.4 FTIR spectra of EFB, EVA18 and an EVA18/EFB composite**

Figure 4.5 shows the FTIR spectra of the neat EVA copolymer, the EFB fibre and an 80/20 w/w EVA/EFB fibre composite for EVA28. The spectrum for the EVA28/EFB fibre composite shows a broad characteristic peak around  $3430\text{--}3300\text{ cm}^{-1}$  which indicates the presence of  $\text{-OH}$  stretching. The absorption peak at  $1592\text{ cm}^{-1}$  is less intense for the EVA28/EFB composite than for the EVA18/EFB composite (Figures 4.4 and 4.5). This absorption is caused by the carboxylic groups of the fatty acids present in the EFB fibre, and in particular from the lignin constituent and, as discussed above, the most probable reason is the smaller amount of fibre on the sample surface.

**Table 4.1** Some important peaks in the FTIR spectra of the EVA copolymers, EFB and the EVA/EFB composites

Wavenumber / $\text{cm}^{-1}$	Assigned vibrations	Visible in
718	Inner rocking vibration of methylene groups	All samples
1030	C-O-C vibration	All samples
1240	-C-O- stretching	EFB
1372	Characteristic absorptions of acetoxy groups	EVA
1439	C-H bending of $\text{CH}_3$ groups	All samples
1592	C=C stretching of fatty acids	EFB
1736	C=O stretching vibration from free carboxylic acid and from esters	EVA
2850	C-H stretching	All samples
2920	$\text{CH}_2$ stretching	All samples
3430-3300	-OH stretching	EFB + EVA/EFB

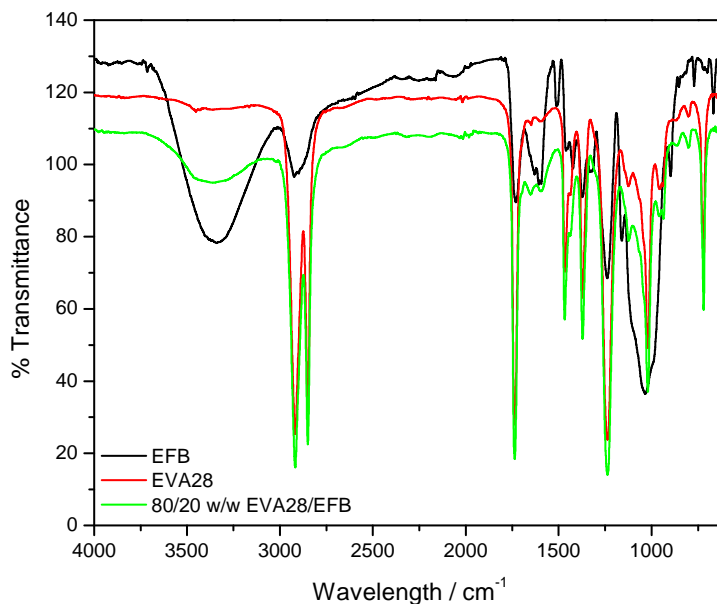


**Figure 4.5** FTIR spectra of EFB, EVA28 and an EVA28/EFB composite

### 4.3 Differential scanning calorimetry (DSC)

The DSC results of the pure EVA copolymers and the EVA/EFB fibre composites are presented in Figures 4.6 to 4.11. The peak temperatures of melting and crystallization, as well as the melting and crystallization enthalpies of these samples are summarized in Tables 4.2 and 4.3. The heating curves in Figure 4.6 show endotherms with peak temperatures of melting at 87 and 73 °C for EVA18 and EVA28 respectively. The melting temperature of EVA decreases significantly with an increase in VA content. This is due to the acetate branch points which reduce the packing and folding of the chains and inhibit the crystallization of the EVA backbone [23], giving rise to reduced crystallinity. It is evident from Figure 4.6 that the melting peak of EVA18, which has the lowest VA concentration, is more resolved which indicates more crystal perfection [24]. The EVA28 sample has a melting peak that is less resolved due to more defects induced by the higher VA content.

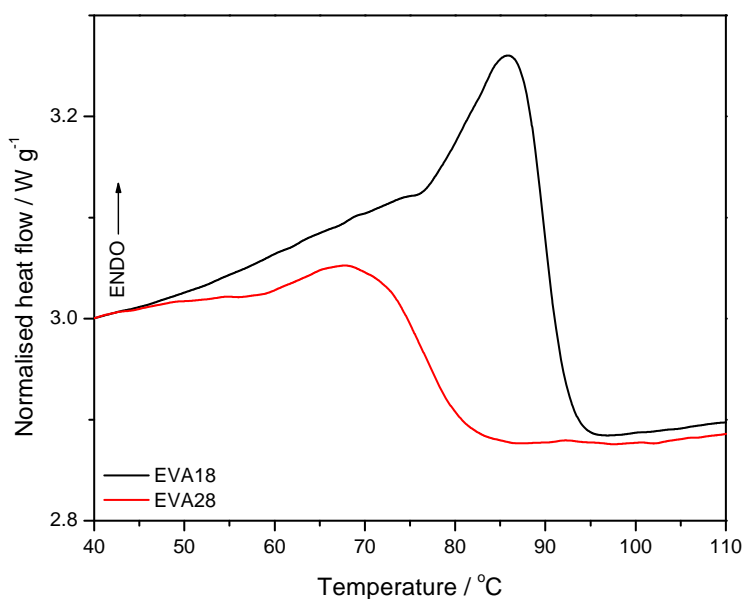


**Figure 4.6** DSC heating curves for the EVA18 and EVA28 copolymers

EVA18 has a melting enthalpy of 20 J g<sup>-1</sup>, while EVA28 has a much lower melting enthalpy of 5 J g<sup>-1</sup> (Table 4.2). The results in the table were obtained from the second heating scan to eliminate the effect of thermal history. This confirms the lower crystallinity of EVA28, as discussed above.



**Table 4.2 DSC heating results for all the investigated samples**

EVA/EFB (w/w)	T <sub>o,m</sub> / °C	T <sub>p,m</sub> / °C	ΔH <sub>m</sub> <sup>obs</sup> / J g <sup>-1</sup>	ΔH <sub>m</sub> <sup>calc</sup> / J g <sup>-1</sup>	χ <sub>c</sub> / %
<b>EVA18/EFB</b>					
100/0	76.1 ± 0.5	87.4 ± 0.3	20.0 ± 0.9	20.0	6.9
90/10	75.0 ± 0.9	86.4 ± 0.3	16.1 ± 0.4	18.0	6.2
80/20	73.5 ± 0.9	86.3 ± 0.5	15.2 ± 0.6	16.0	6.6
70/30	73.1 ± 0.9	85.6 ± 0.2	14.6 ± 0.7	14.0	7.2
<b>EVA28/EFB</b>					
100/0	60.6 ± 0.1	73.4 ± 0.3	4.7 ± 0.6	4.7	1.6
90/10	61.0 ± 0.5	73.4 ± 0.4	4.2 ± 0.8	4.2	1.6
80/20	61.3 ± 0.2	72.6 ± 0.7	3.8 ± 0.1	3.8	1.6
70/30	60.0 ± 0.6	72.2 ± 0.4	3.4 ± 0.2	3.3	1.7

T<sub>o,m</sub> is the onset temperature of melting; T<sub>p,m</sub> is the peak temperature of melting; ΔH<sub>m</sub><sup>obs</sup> is the observed melting enthalpy; ΔH<sub>m</sub><sup>calc</sup> is the calculated melting enthalpy; χ<sub>c</sub> is the percentage crystallinity

The calculated melting enthalpy and crystallinity values in Tables 4.2 and 4.3 were determined according to Equations 4.1 and 4.2.

$$\Delta H_m^{calc} = \Delta H_{m,EVA} w_{EVA} \quad (4.1)$$

where ΔH<sub>m,EVA</sub> is the experimentally observed melting enthalpy for the pure EVA, and ΔH<sub>m</sub><sup>calc</sup> is the calculated enthalpy of the EVA in the composite taking into account the weight fraction w<sub>EVA</sub> in the composite.

$$\chi_c = (\Delta H_m^{obs} \div (\Delta H_m^o \times w_{EVA})) \times 100\% \quad (4.2)$$

where χ<sub>c</sub> is the percentage crystallinity, ΔH<sub>m</sub><sup>obs</sup> is the specific enthalpy of melting, and ΔH<sub>m</sub><sup>o</sup> is the specific enthalpy of melting for 100% crystalline PE. A value of 288 J g<sup>-1</sup> was used in the calculations [25].

Figure 4.7 shows the DSC cooling curves of EVA18 and EVA28. The DSC curves show a single crystallization peak for both copolymers. The difference between the crystallization peaks of EVA18 and EVA28 is considerable, indicating that the VA content also influenced the crystallization behaviour of the polymers. EVA28 shows a single crystallization peak

which is less intense than that of EVA18, and which appears at a lower temperature. This suggests that the vinyl acetate groups reduce the stereoregularity of the polyethylene backbone and restricts its crystallization [25,26].

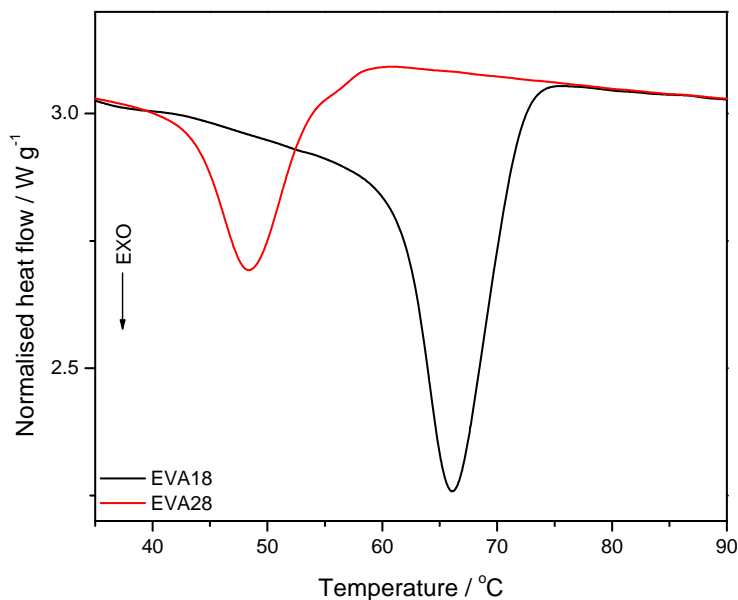


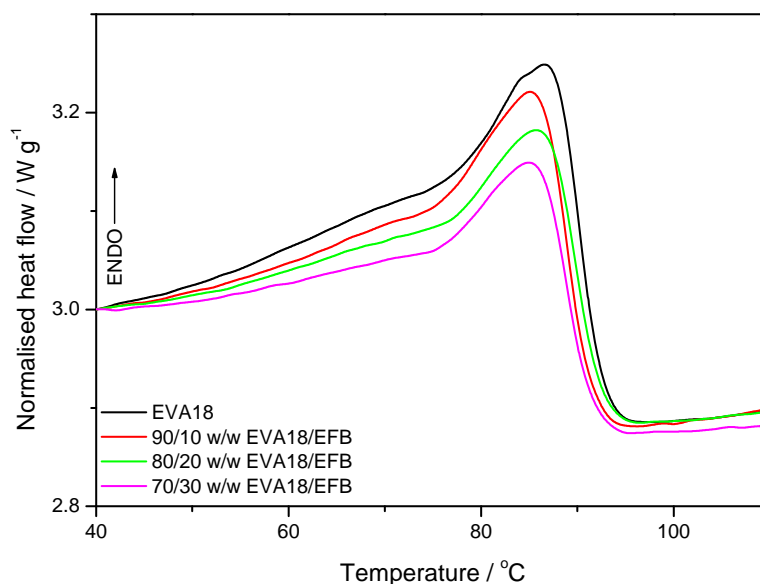
**Figure 4.7 DSC cooling curves for EVA18 copolymer and EVA28 copolymer**

The DSC heating curves of EVA18 and the EVA18/EFB composites are shown in Figure 4.8. All the curves show only one endothermic peak. The peak temperatures of melting show little change with increasing fibre content in the composites, and could be regarded as being the same within experimental error (Table 4.2). This implies that the crystallite sizes were not observably influenced by the presence of EFB fibres, or by increasing EFB fibre content. The observed melting enthalpy values are slightly different than the calculated enthalpies for the different composites. However, the observed crystallization enthalpies are observably higher than the calculated crystallization enthalpies, and the difference increases with increasing fibre content. This is indicative of a higher extent of crystallization in the presence of EFB fibres. EFB fibre particles may influence polymer crystallization in two ways: (i) they may act as nucleation sites, which may increase the total crystallinity, or (ii) they may also immobilise the polymer chains, giving rise to a reduced degree of crystallization. Mostly both these opposing effects are present, and it can be assumed that the effects in this case balance each other, therefore the small differences between the crystallinities of the different samples.

**Table 4.3 DSC cooling results for all the investigated samples**

EVA/EFB (w/w)	$T_{o,c} / ^\circ\text{C}$	$T_{p,c} / ^\circ\text{C}$	$\Delta H_c^{obs} / \text{J g}^{-1}$	$\Delta H_c^{calc} / \text{J g}^{-1}$
<b>EVA18/EFB</b>				
100/0	$71.6 \pm 0.1$	$66.1 \pm 0.1$	$-30.4 \pm 0.2$	-30.4
90/10	$71.7 \pm 0.1$	$66.2 \pm 0.1$	$-31.3 \pm 0.4$	-27.4
80/20	$71.3 \pm 0.2$	$65.8 \pm 0.6$	$-27.3 \pm 0.5$	-24.3
70/30	$71.0 \pm 0.7$	$65.8 \pm 0.1$	$-26.3 \pm 0.5$	-21.3
<b>EVA28/EFB</b>				
100/0	$54.3 \pm 0.1$	$48.7 \pm 0.1$	$-16.3 \pm 0.3$	-16.3
90/10	$54.1 \pm 0.1$	$48.9 \pm 0.1$	$-15.6 \pm 0.3$	-14.7
80/20	$54.2 \pm 0.5$	$48.3 \pm 0.1$	$-12.9 \pm 0.7$	-13.0
70/30	$54.3 \pm 0.2$	$48.1 \pm 0.1$	$-12.4 \pm 0.1$	-11.4

$T_{o,c}$  is the onset crystallization temperature;  $T_{p,c}$  is the peak temperature of crystallization;  $\Delta H_c^{obs}$  is the observed crystallization enthalpy;  $\Delta H_c^{calc}$  is the calculated crystallization enthalpy.

**Figure 4.8 DSC heating curves for EVA18 and the EVA18/EFB composites**

The DSC cooling curves show only a single exothermic crystallization peak (Figure 4.9) for all the composites. The crystallization results for all the investigated samples are summarized in Table 4.3. It is evident that the presence of EFB fibre causes no difference in the crystallization peak temperatures, while the experimental crystallization enthalpies are observably higher than the calculated ones. The reason for this is not clear, since there was a

good correlation between the observed and calculated melting enthalpies of EVA18 and its different composites.

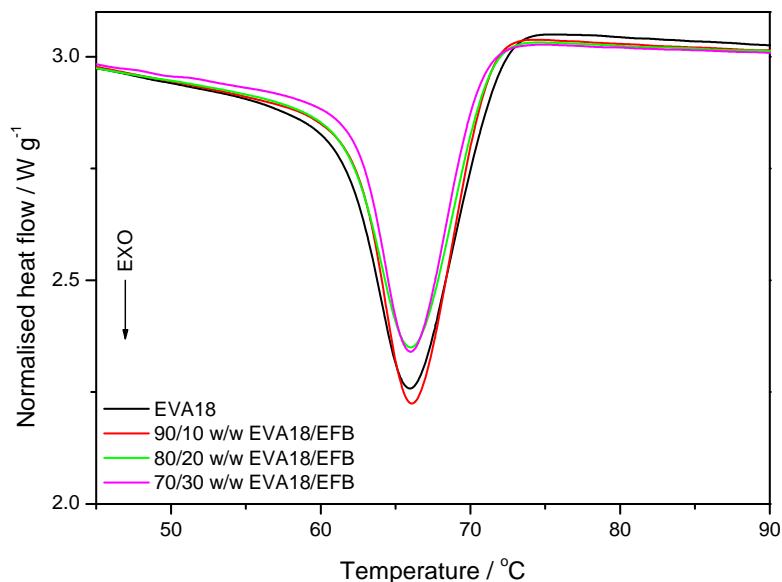


**Figure 4.9** DSC cooling curves for EVA18 and the EVA18/EFB composites

Figure 4.10 shows the DSC heating curves of EVA28 and the EVA28/EFB composites. These curves show one endothermic peak for EVA28 and the EVA28/EFB composites. The broad melting temperature range indicates that EVA28 has a broad crystal size distribution. This can be explained as being the result of a large number non-crystallisable segments and intra-molecular defects, known as VA defects [24,26]. The presence of EFB fibre had little influence on the melting temperatures, and the observed melting enthalpies are almost the same as the calculated melting enthalpies for all the samples, indicating no change in crystallinity when EVA28 was heated and cooled in the presence of EFB fibres (Table 4.2). The crystallinity of EVA28 seems to be the same for almost all the samples. The reason is the same as discussed above for the EVA18 composites.

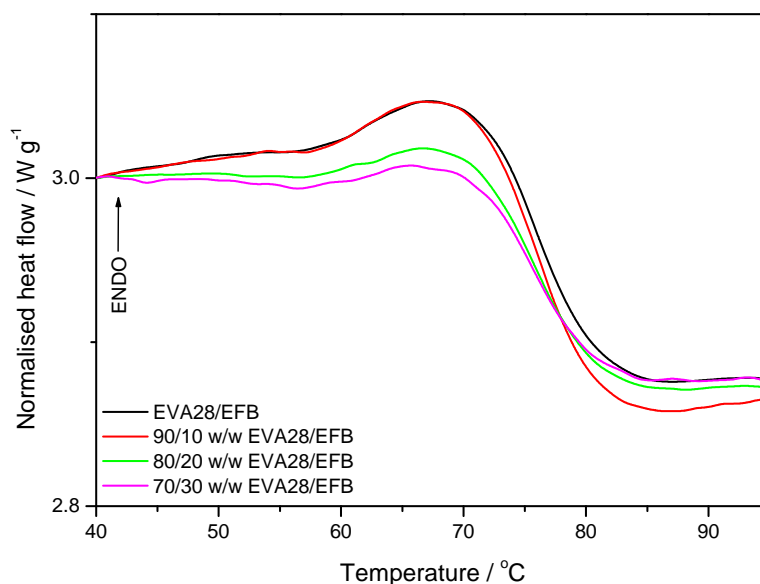


**Figure 4.10 DSC heating curves for EVA28 and the EVA28/EFB composites**

The DSC cooling curves of EVA28 and the EVA28/EFB composites are shown in Figure 4.11. The results are summarized in Table 4.3. The trends observed from the cooling curves are the same as those observed from the heating curves, and they can be explained in a similar manner.

The results from this section are in accordance with the work done on natural fibre reinforced polymer composites by various authors such as Pracella *et al.* [18], Luyt *et al.* [27], Mishra *et al.* [28] and Arzac *et al.* [29]. Pracella *et al.* [18] investigated the reactive compatibilization of composites of ethylene vinyl acetate copolymers with cellulose fibres. They found that the enthalpy of crystallization with respect to the polymer fraction significantly decreased for the fibre containing composites. This was explained in terms of the immobilization effect of the polymer chains by the cellulose fibre, as the interaction between the fibre and EVA-MA was strong which in essence reduced the extent of crystallization. Luyt *et al.* [27] focused on the preparation and characterization of EVA/sisal fibre composites. They found that the melting peaks shifted to lower temperatures with the incorporation of sisal fibre, indicating the formation of thinner crystal lamellae, and that the melting enthalpies decreased, indicating lower crystallinity. Mishra *et al.* [28] studied the influence of TiO<sub>2</sub>-modification on the

mechanical and thermal properties of sugarcane bagasse-EVA composites. They concluded that there was no significant decrease in the crystallization temperature ( $T_c$ ), and no significant difference between the melting temperatures with an increase in the sugarcane bagasse (SCB) content, except after 20% SCB loading. This was explained as the total disruption of the polymer chains by the high SCB content so that the EVA with 9% VA could not easily orientate itself. Arsac *et al.* [29] determined the primary relaxation temperatures and melting points of ethylene vinyl acetate copolymers with different VA contents. They found that the EVA copolymers showed two endothermic peaks and the melting temperatures decreased with an increase in the VA content. The reason for the two peaks was not clearly explained by the authors. The decrease in the melting temperatures with an increase in VA content was due to an increasing percentage of amorphous phase which reduced the crystallinity. This lower crystallinity was reflected in lower melting and crystallization temperatures along with lower melting enthalpies. These findings are in agreement with some observations in this section such as a decrease in crystallization enthalpies for the EVA18 composites.

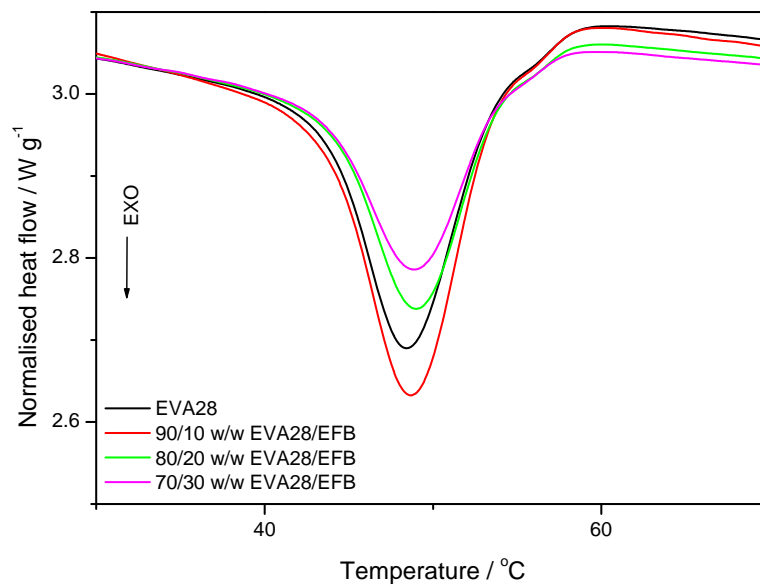


**Figure 4.11 DSC cooling curves for EVA28 and the EVA28/EFB composites**

In summary it may be said that the presence of EFB fibre had very little influence on the melting and crystallization behaviour of both EVA18 and EVA28. If EVA28 more strongly

interacted with the fibre than EVA18, it cannot be seen in the influence of the fibre on the melting and crystallization behaviour of these two copolymers.

#### 4.4 Thermogravimetric analysis (TGA)

The TGA results of the EVA copolymers, EFB and the EVA/EFB composites are shown in Figures 4.12 to 4.14. The thermal stabilities of all the samples, summarized in terms of the temperatures at 10 and 70% mass loss, as well as the mass % residue at 600 °C, are shown in Table 4.4.

The TGA curves of the two EVA copolymers with different VA contents are shown in Figure 4.12. Both EVA18 and EVA28 show two degradation steps. The first step, which starts in the temperature range of 350-370 °C, is attributed to the removal of the acetate groups. The second step around 443-470 °C is due to the degradation of the PE backbone of the copolymer [30-32]. EVA18 is more thermally stable than EVA28 because of the larger amount of VA in EVA28 which increases the amorphous phase in the semi-crystalline material. This is also clear from the  $T_{10\%}$  and  $T_{70\%}$  values for these two copolymers in Table 4.4. None of these copolymers show any residue at 600 °C.

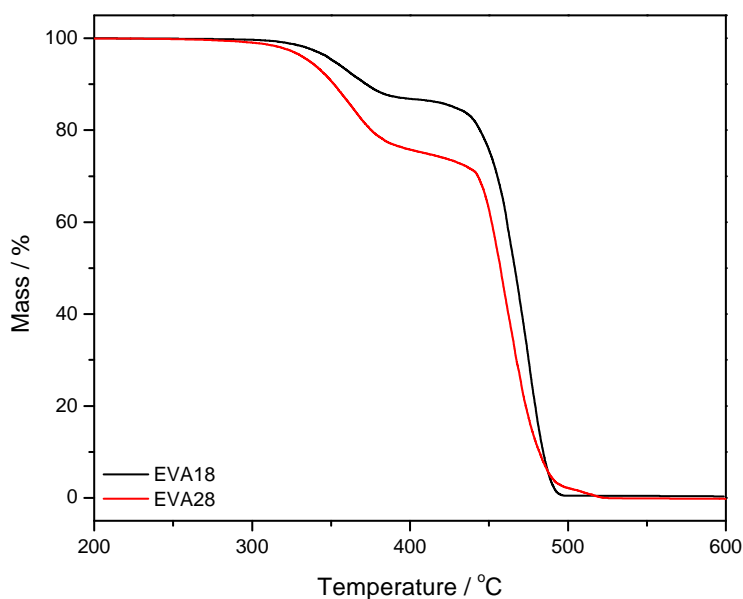


**Figure 4.12** TGA curves for the different EVA copolymers

**Table 4.4 TGA results for all the investigated samples**

<b>EVA18/EFB</b>			
<b>EVA18/EFB (w/w)</b>	<b>T<sub>10%</sub> / °C</b>	<b>T<sub>70%</sub> / °C</b>	<b>Weight % residue</b>
0/100	282.2	336.2	10.0
100/0	371.9	457.0	-
90/10	353.2	455.4	2.4
80/20	328.4	405.5	4.7
70/30	312.2	366.0	7.5
<b>EVA28/EFB</b>			
<b>EVA28/EFB (w/w)</b>	<b>T<sub>10%</sub> / °C</b>	<b>T<sub>70%</sub> / °C</b>	<b>Weight % residue</b>
0/100	282.2	336.2	10.0
100/0	353.8	442.5	-
90/10	341.8	436.9	2.3
80/20	327.0	408.9	4.8
70/30	310.9	367.3	8.0

T<sub>10%</sub> and T<sub>70%</sub> are degradation temperatures at 10% and 70% mass loss respectively

The TGA results of EVA18, EFB and the EVA18/EFB composites are shown in Figure 4.13. It can be seen that the decomposition of EFB is characterized by four steps. The first step is related to the evaporation of water which occurs below 100 °C. The second step starts at about 250 °C and corresponds to the depolymerisation of hemicellulose, while the third step at about 350 °C is due to the random cleavage of the glycosidic linkage of cellulose. The fourth step is a slow mass loss between 400 and 600 °C and is associated with the degradation of lignin [4,33-35]. The EVA18/EFB composites also show four degradation steps. The first step corresponds to the evaporation of water, the second is an overlap of the removal of the acetate groups and the constituents of the EFB degradation in this temperature region, while the third step is due to the degradation of the PE backbone in EVA18. The fourth degradation step in the EVA18 composites at temperatures beyond 500 °C is the same as the fourth step of EFB degradation. The presence of EFB generally decreases the thermal stability of the neat EVA samples. The first decomposition step, which is a combination of the deacetylation of EVA and fibre decomposition, moves to lower temperatures with increasing fibre content, but still occurs at higher temperatures than the decomposition of pure fibre. The fibre decomposition seems to be retarded when mixed with EVA due to the higher thermal stability of the polymer. The slope of the decomposition step (which is equivalent to the rate of decomposition) between 450 and 500 °C decreases with increasing



fibre content. This is probably due to the presence of fibre char residue which seems to inhibit the EVA main chain degradation, or the diffusion of volatile degradation products out of the degrading sample.

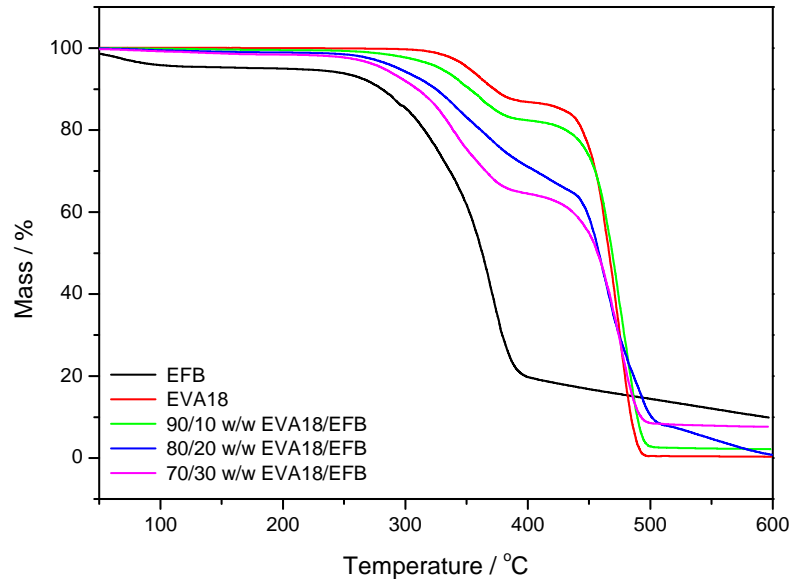


**Figure 4.13** TGA curves for EFB, EVA18, and the EVA18/EFB composites

Dikobe and Luyt [32], in their investigation of the effect of filler content and size on the properties of ethylene vinyl acetate copolymer-wood fibre composites, reported that the onset temperatures of degradation of the first degradation step of the composites decreased with increasing WF content. The reason given for this was that at low WF loadings, the heat was primarily conducted by the EVA copolymer, and thus the VA scission started before degradation of cellulose. At higher WF loadings the heat energy reached WF particles to start degrading before EVA. These results are in line with those obtained in this thesis, and the explanations may be valid for our current findings. Li *et al.* [34] investigated the mechanical properties, flame retardancy and thermal degradation of LLDPE/wood fibre composites. They found that the LLDPE shows a higher thermal stability than the composites. This was explained in terms of carbon free radicals produced by the wood decomposition that attack hydrogens on the LLDPE chains to form long-chain free radicals that further degrade into volatiles. Their investigated system and observations seem to be similar to ours. Sailaja *et al.* [36] studied the mechanical and thermal properties of bleached kraft pulp/LDPE composites. They found that there was no significant difference in the thermal degradation behaviour for

uncompatibilized and compatibilized composites with 20% wood pulp grafted with PMMA. However, on increasing the loading to 40%, the compatibilized composites were more thermally stable than the uncompatibilized ones. The authors did not explain this behaviour.

Figure 4.14 shows the TGA curves of EVA28, EFB and the EVA28/EFB composites. The curves show the same degradation steps as were observed and explained for EVA18. There is not much of a difference in the decomposition rate of the last step between EVA28 and its composites, while in the case of EVA18 there was a clear decrease in the decomposition rate with increasing EFB content. The reason for this is not immediately apparent, but it could be related to polymer-fibre interactions that influenced either the mobility of free radicals formed during degradation, or the rate of diffusion of volatile degradation products out of the degrading sample.

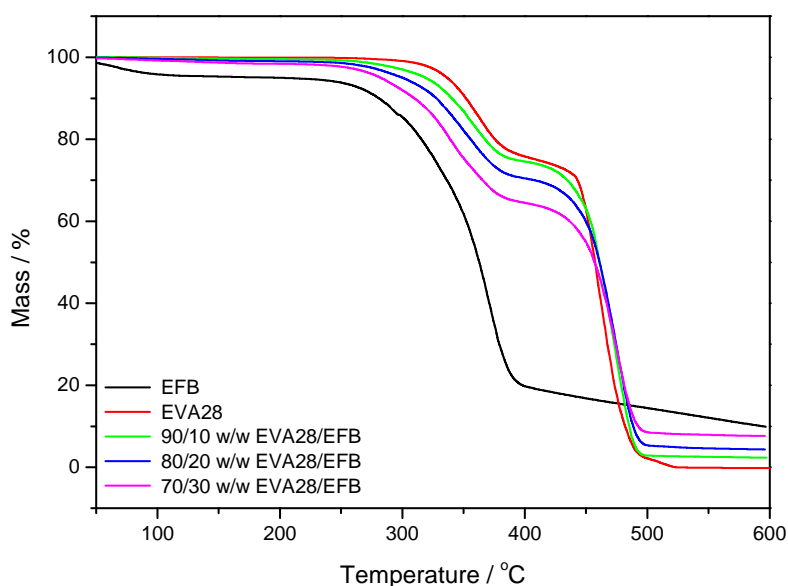


**Figure 4.14** TGA curves for EFB, EVA28, and the EVA28/EFB composites

#### 4.5 Dynamic mechanical analysis (DMA)

The DMA results of the pure EVA copolymers and their composites are presented in Figures 4.15 to 4.23. Figure 4.15 shows the storage modulus as a function of temperature for the pure EVA18 and EVA28 copolymers. The value of the storage modulus ( $E'$ ) signifies the stiffness

of the material. It can be seen that the storage modulus for both EVA18 and EVA28 samples decrease with an increase in the temperature. EVA18 shows higher storage modulus values than EVA28. This can be related to the vinyl acetate (VA) content, which is lower in the case of EVA18. The increase in the VA content increases the amorphous phase and reduces the storage modulus as well as the crystallinity (as observed in the DSC results). These curves show three distinct regions i.e. a glassy region (high storage modulus, where the segmental mobility is restricted), a transition zone (a substantial decrease in the  $E'$  values), and a rubbery flow region [25,37,38].

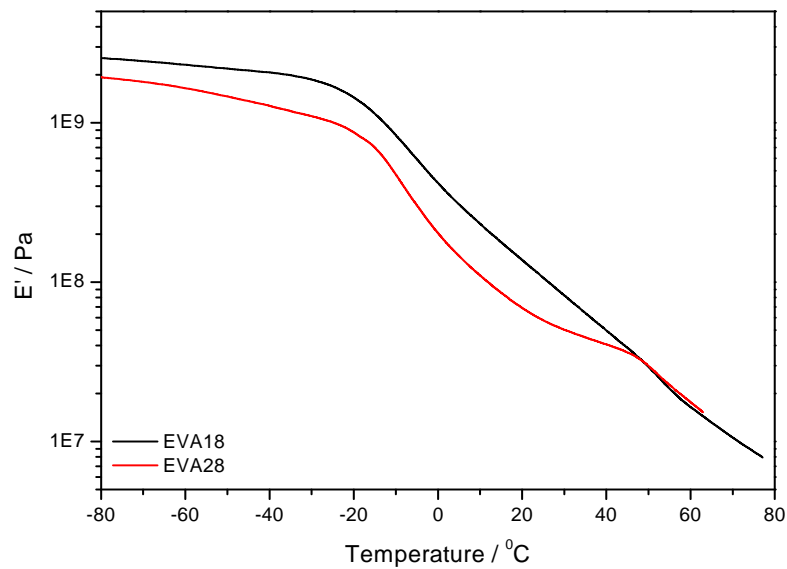


**Figure 4.15 Comparison of the storage modulus as a function of temperature for the pure EVA18 and EVA28 copolymers**

Figure 4.16 shows the variation of the loss modulus  $E''$  of EVA18 and EVA28 with temperature. The two EVA copolymers show a  $\beta$ -relaxation peak at around  $-15\text{ }^\circ\text{C}$ , which is attributed to the glass transition of EVA [39,40]. EVA28 shows a second relaxation around  $50\text{ }^\circ\text{C}$  in both the  $E'$  and  $E''$  curves, which probably has no significance in view of the discussion of the  $\tan \delta$  curves below.

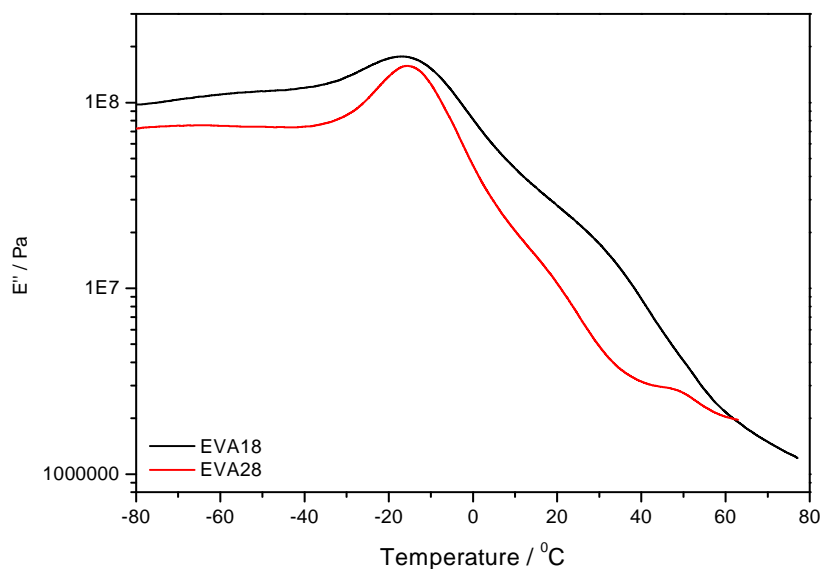


**Figure 4.16 Comparison of the loss modulus as a function of temperature for the pure EVA18 and EVA28 copolymers**

Figure 4.17 represents the variation of  $\tan \delta$  with temperature for EVA18 and EVA28. A summary of the transition peak temperatures for all the investigated samples is shown in Table 4.5. EVA18 shows two distinct relaxations, a  $\beta$ -relaxation at  $-4.2$  °C and an  $\alpha$ -relaxation at  $28.0$  °C. The  $\beta$ -relaxation is attributed to the motion of chain segments of three or four methylene ( $-\text{CH}_2$ ) groups in the amorphous phase [41,42], and is known as the glass transition ( $T_g$ ). Below  $T_g$  the molecular chain segments are frozen in, the damping is low and little energy is stored for elastic deformations. In the rubbery region, the damping is high compared to the glassy state, because the molecular segments are free to move causing a decrease in stiffness, and excess energy is dissipated as heat. The  $\alpha$ -relaxation is related to the motion of amorphous regions within the crystalline phase, which is probably the re-orientation of defect regions between crystals [39]. The  $\alpha$ -transition can also reflect the relaxation of flexible chains of the vinyl acetate (VA) groups present in the EVA copolymer chains. It can be seen from this figure that EVA28 has one well resolved transition peak at about  $-8$  °C, which is the result of the glass transition in the polymer. The chain flexibility results in a lower  $T_g$  because the energy for conformational changes is lower. The EVA28 seems to have more branching with more chain ends, resulting into more free volume which reduces the  $T_g$ . The peak shoulder at approximately  $15$  °C is due to the  $\alpha$ -relaxation. There is

a shift in the  $T_g$  to lower temperatures (Table 4.5) with an increase in the VA content. This is explained in terms of the enhanced chain mobility of EVA due to the plasticizing effect of the flexible VA phase. The lower resolution and lower transition temperature of the  $\alpha$ -peak in the EVA28 curve is related to the lower crystallinity of EVA28, since this relaxation is related to the amorphous material between the crystalline lamellae in a semicrystalline polymer.

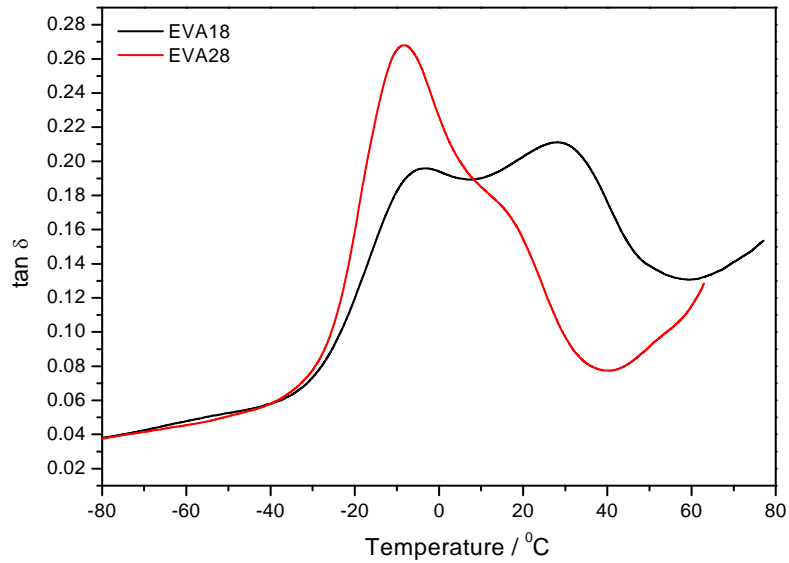
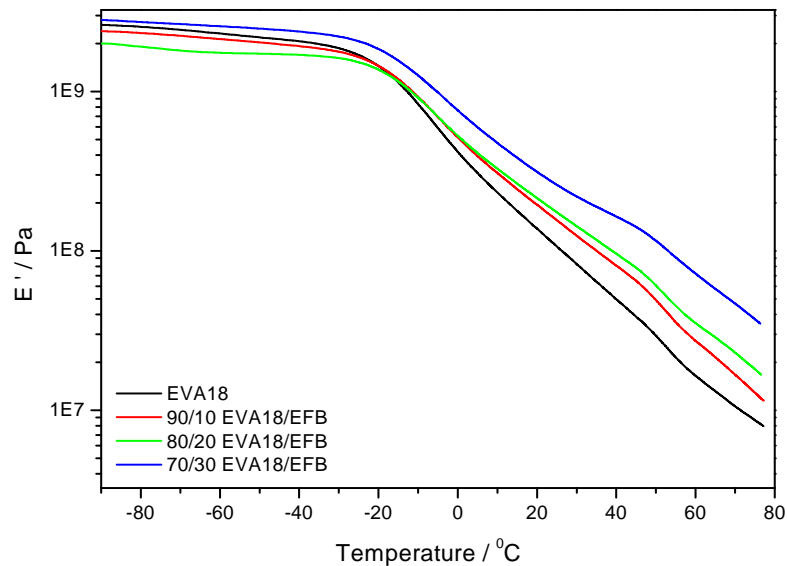


**Figure 4.17 Comparison of  $\tan \delta$  as a function of temperature for pure EVA18 and EVA28 copolymers**

**Table 4.5 Relaxation temperatures for the EVA copolymers and the EVA/EFB composites as determined from the  $\tan \delta$  curves**

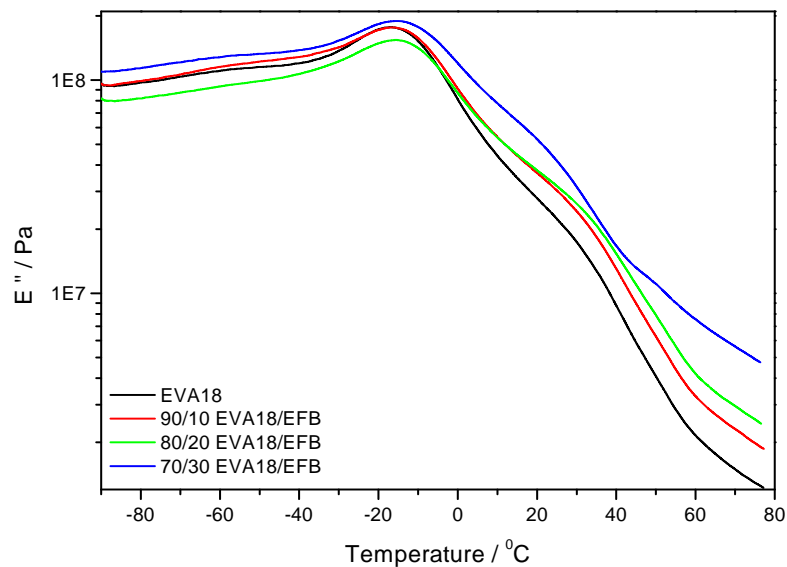
EVA/EFB (w/w)	EVA18/EFB		EVA28/EFB	
	$\beta$ -relaxation	$\alpha$ -relaxation	$\beta$ -relaxation	$\alpha$ -relaxation
100/0	-4.2	27.6	-8.3	15.4
90/10	-3.8	27.5	-7.3	16.2
80/20	-3.0	28.8	-6.5	16.4
70/30	-1.2	21.4	-5.3	17.6

Figure 4.18 shows the storage modulus ( $E'$ ) as a function of temperature for EVA18 and the EVA18/EFB composites. The storage modulus values below  $-20\text{ }^{\circ}\text{C}$  are different for the different samples, and there is no trend with respect to the presence and amount of fibre in EVA18. Above the  $T_g$  the  $E'$  values increase with increasing fibre content, but decrease with increasing temperature. This is probably due to the presence of stiff fibres, as well as some interaction between the fibre and the VA groups which reduce the mobility of the EVA chains. Kim *et al.* [43] investigated the thermal properties of bio-flour filled polyolefin composites with different compatibilizing agent type and content. They observed a slight increase in  $E'$  values compared to the non-treated composites with increasing the MAPP content. This enhanced stiffness of the composites was primarily attributed to the improved compatibility between the rice husk flour (RHF) and the PP matrix. The  $E'$  values significantly increased at the temperatures above  $T_g$  with the incorporation of RHF in PP. The authors explained this as being due to the improved compatibility between the RHF and PP in the presence of MAPP. This restricted the chain mobility of the neat polymer and improved stress transfer between the polymer and the fibre. This is most probably the reason why we also see an increasing storage modulus with fibres present in the EVA18 matrix.



**Figure 4.18 Storage modulus as a function of temperature for pure EVA18 and the EVA18/EFB composites**

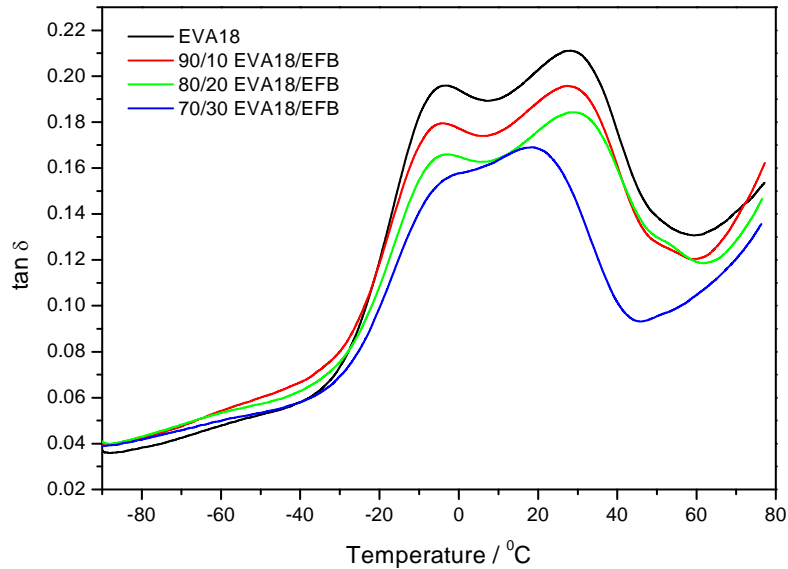
The loss modulus curves in Figure 4.19 show the same trend as the storage modulus curves in Figure 4.18. The EVA18 and its composites show relaxation peaks between -5 and 0 °C, which are attributed to the  $\beta$ -relaxation or glass transition of the EVA. There are differences between the peak temperatures of this transition for pure EVA28 and the composites, but since these differences are more clear in the  $\tan \delta$  curves, they will be discussed and explained below. There is a significant decrease in the loss modulus above  $T_g$  with an increase in temperature. This is attributed to the increased mobility of the polymer chain, as discussed earlier.



**Figure 4.19 Loss modulus as a function of the temperature for pure EVA18 and the EVA18/EFB composites**

Figure 4.20 shows the variation of  $\tan \delta$  with temperature for EVA18 and the EVA18/EFB composites. The  $T_g$  of EVA18 is -4 °C, and it observably increases with an increase in EFB content (Table 4.5). This increase is due to the restricted chain mobility as a result of the interaction between the VA groups and the EFB fibre. There is a decrease in the total damping during the transitions with an increase in the EFB fibre content. This is due to the improved interfacial bonding of the EVA18/EFB composites which may be characterized by lower energy dissipation [43,44]. It was reported in the literature that the higher the damping at the interfaces, the poorer the interfacial adhesion [44]. The temperature of the  $\alpha$ -peak, which is related to relaxations of the interlamellar amorphous polymer chains, is observably

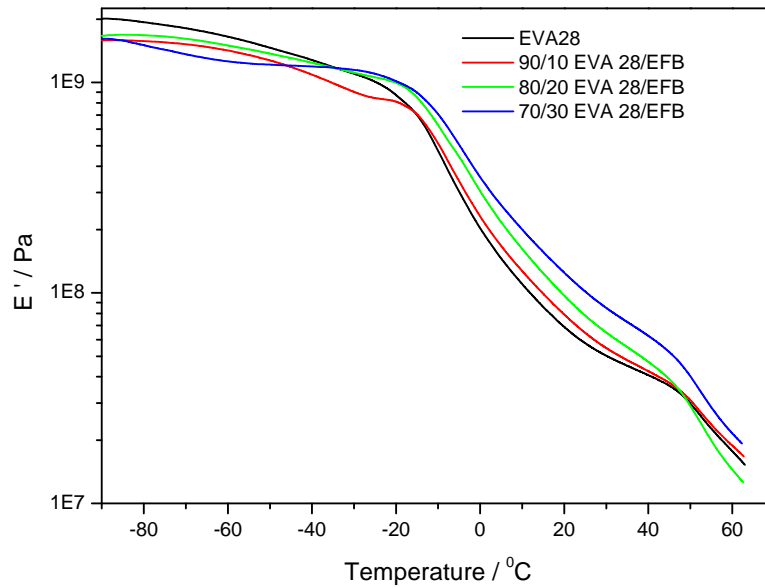
lower for the 30% fibre containing sample. This indicates that the crystallization of EVA on the fibre surfaces might have had an influence on the morphology and mobility of the interlamellar amorphous fraction of the polymer.



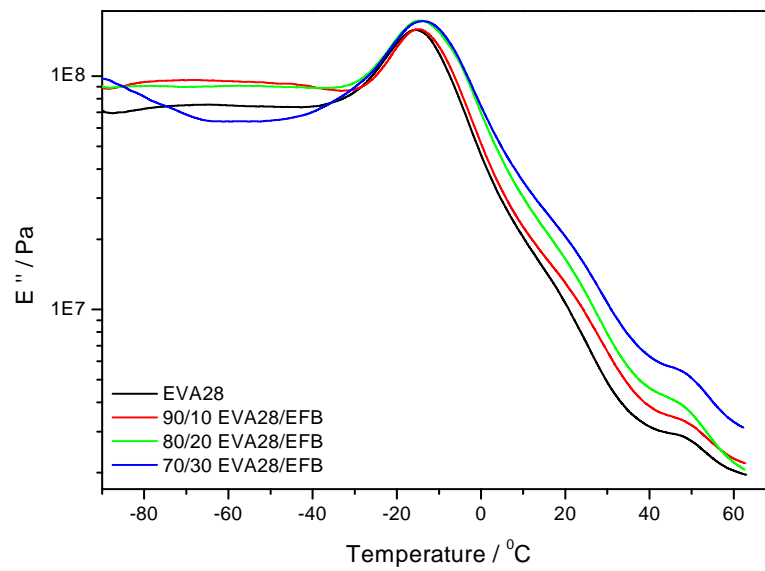
**Figure 4.20 Dissipation factor as a function of the temperature for pure EVA18 and the EVA18/EFB composites**

Figure 4.21 shows the storage modulus as a function of temperature for pure EVA28 and the EVA28/EFB composites. There are differences in storage modulus between EVA28 and its composites at temperatures below  $T_g$ , but the differences are small and there is no clear trend as function of EFB content. However, there is a general increase in the storage modulus as a function of EFB content at temperatures above  $T_g$ . This could be explained in a similar way as was explained for the EVA18 samples. Similar observations were reported by Behzad *et al.* [45] in their DMA investigation of a compatibilizer effect on the mechanical properties of high density polyethylene/wood flour composites. They observed that for the 25% wood flour (WF) containing samples, with and without compatibilizer, there was no significant change in the  $E'$  values, while for the 50% WF containing samples the  $E'$  values were higher for the compatibilized system due to an improved compatibility between the matrix and the WF phase. This observation and explanation support our own results, which also show higher storage modulus values as a result of some interfacial interaction between EVA and EFB fibre.





**Figure 4.21** Storage modulus as a function of the temperature for pure EVA28 and EVA28/EFB composites



**Figure 4.22** Loss modulus as a function of the temperature for pure EVA28 and EVA28/EFB composites

Figure 4.22 shows that there is a slight increase in the temperatures of the peak maxima of the  $\beta$ -relaxation in the loss modulus curves upon addition of EFB fibre. This slight increase is due to the reduced chain mobility of the polymer as a result of the interaction with the EFB fibre. There is a significant decrease in the loss modulus with an increase in temperature up to 40 °C, which has already been explained.

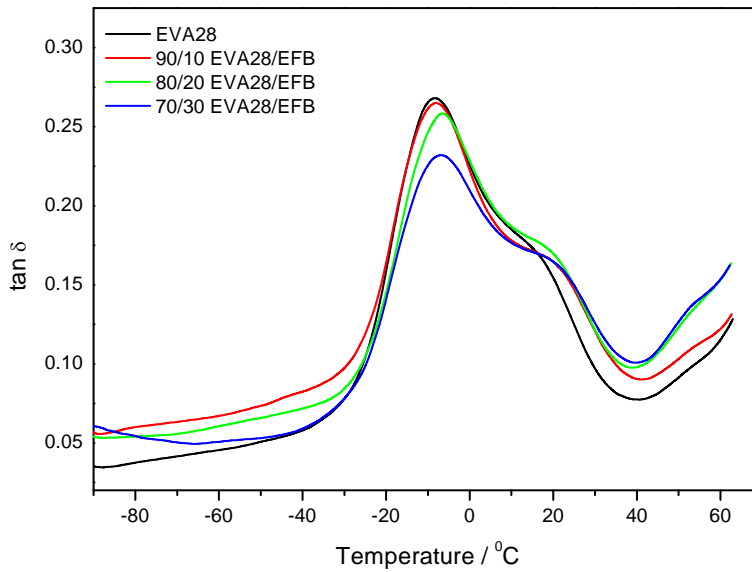


**Figure 4.23**  $\tan \delta$  as a function of the temperature for pure EVA28 and EVA28/EFB composites

The variation of  $\tan \delta$  with temperature for EVA28 and the EVA28/EFB composites are shown in Figure 4.23. The glass transition temperature ( $T_g$ ) of EVA28 is around -8.0 °C, which corresponds to the  $\beta$ -relaxation of the material. The  $T_g$  generally increases with increasing fibre content in the composites. This could be explained in a similar way as for the EVA18 samples above. However, the intensity of the  $\beta$ -relaxation peak decreases with increasing EFB content, which indicates that the energy dissipation of the system decreases due to the incorporation of EFB in the polymer matrix [37,47]. The reason for this has also been explained above. The  $\alpha$ -relaxation is observed as a shoulder around 20-24 °C, and is associated with crystalline fraction of the polymer. The  $\alpha$ -relaxation peak in the EVA28 and its composite curves is less intense than the  $\beta$ -relaxation peak, compared to the curves for EVA18 and its composites. This is due to the lower crystallinity of EVA28. At about 50 °C

there seems to be a third relaxation, which may be related to the  $\alpha'$ -relaxation. This has been explained as being the result of the slippage between crystallites during heating of the sample [47].

#### **4.6 Tensile testing**

The mechanical properties such as stress at break, strain at break and Young's modulus of the pure EVA copolymers containing 18 and 28% VA, and their composites, were determined from the stress-strain curves in Figures A.1 to A.8 in the appendix. The tensile properties are summarized in Table 4.6. For the pure polymers, the EVA with lower vinyl acetate content has a higher crystallinity and better mechanical properties such as stress at break and Young's modulus, but lower elongation at break. The main reason for the better tensile modulus and tensile strength at break values for EVA18 is its significantly higher crystallinity. EVA28 has a larger elongation at break value than EVA18 because of its larger amorphous fraction which increases the extent of chain flexibility, as a result of which the polymer chains can slip more easily and be oriented in the direction of the applied stress. Both these polymers show strain hardening, but this effect is more predominant in the case of EVA18. Since the rearrangement of the crystalline part of a semicrystalline polymer through a tilt, slip and twist process during drawing [48] is one of the main contributors to strain hardening, EVA18 is expected to show a larger extent of strain hardening because of its higher crystallinity. EVA18 has a better toughness than EVA28 and thus absorb much more energy before breakage. Both EVA copolymers do not display a clear yield point and also no neck formation during stretching.

The stress-strain curves in Figures A.1 to A.8 in the appendix show ductility which seems to decrease with an increase in EFB. The curves of EVA18 show more pronounced strain hardening than those of EVA28. The reason for this has already been explained in the above paragraph. The incorporation of the EFB fibres observably reduced the strain hardening of the materials. This suggests that the interaction between the fibre and the polymer inhibited the orientation of the chains in the amorphous parts of the polymer, and the reorientation of the chains in the crystalline parts.

**Table 4.6 Summary of mechanical properties for all the samples**

<b>EVA18/EFB</b>			
<b>EVA18/EFB (w/w)</b>	<b><math>\sigma_b</math> / MPa</b>	<b><math>\epsilon_b</math> / %</b>	<b>E / MPa</b>
100/0	17.5 ± 0.1	512 ± 2	59.9 ± 7.3
90/10	9.0 ± 0.4	218 ± 8	63.2 ± 2.6
80/20	6.6 ± 0.8	146 ± 2	64.0 ± 1.4
70/30	4.3 ± 0.2	104 ± 2	66.2 ± 1.4
<b>EVA28/EFB</b>			
<b>EVA 28%/EFB (w/w)</b>	<b><math>\sigma_b</math> / MPa</b>	<b><math>\epsilon_b</math> / %</b>	<b>E / MPa</b>
100/0	14.6 ± 1.3	692 ± 6	20.2 ± 4.6
90/10	8.5 ± 0.1	321 ± 7	28.6 ± 10.3
80/20	5.7 ± 0.1	258 ± 4	33.3 ± 8.7
70/30	4.0 ± 0.2	193 ± 5	47.8 ± 5.8

$\sigma_b$  is the stress at break;  $\epsilon_b$  is the elongation at break; and E is Young's modulus

Figure 4.24 shows the stress at break for EVA18 and EVA28, and their composites, as a function of EFB fibre content. It can be seen that the incorporation of EFB fibre significantly decreased the tensile stress at break of both polymers. This could be associated with the fact that the dispersion and the length of the EFB fibre were not optimal in order to give good properties. Short fibres normally reduce the tensile strength at break, because they act as stress concentration points where cracks and crazes start to develop. The more short fibres there are, the higher is the possibility of crack propagation at lower stresses, giving rise to reduced tensile strengths at break. Another possible reason is the insufficient adhesion between the EFB fibre and the EVA copolymers, as observed from SEM. The presence and amount of fibre had a similar effect on the stress at break of EVA18 and EVA28, despite the differences in the VA content of the two polymers. The reason for this is not immediately apparent, but it is possible that the difference in the strength of the interactions between EVA18 and EFB, and EVA28 and EFB, is not significant enough to allow improved stress transfer between EVA28 and EFB.

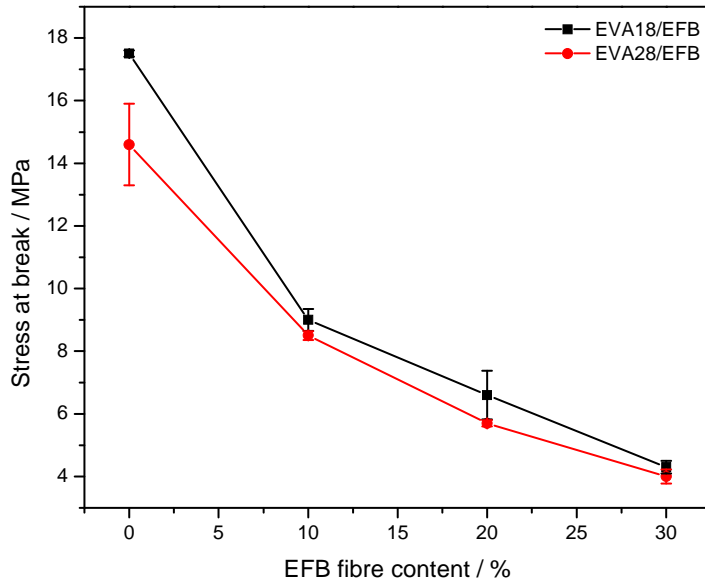


**Figure 4.24** Stress at break of EVA18/EFB and EVA28/EFB as a function of EFB fibre content

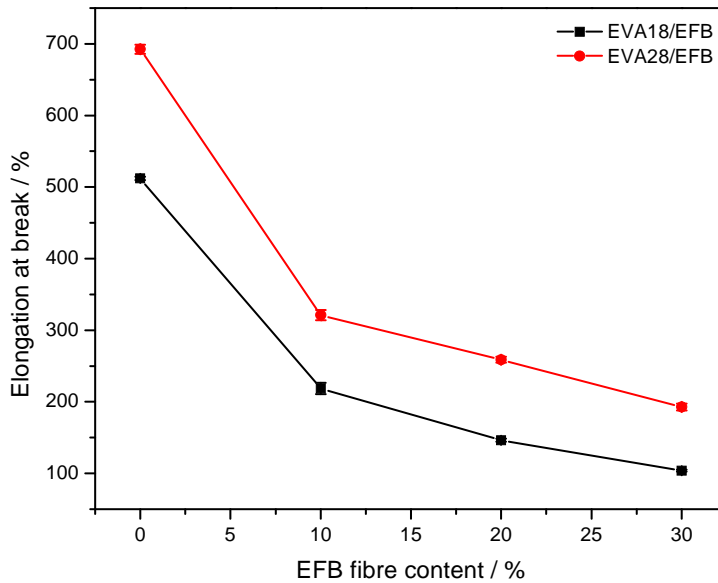


**Figure 4.25** Elongation at break of EVA18/EFB and EVA28/EFB as a function of EFB fibre loading

The elongation at break shows a similar dependence on the EFB fibre content in the composites for both EVA18 and EVA28 (Figure 4.25, Table 4.6). It seems as if the possible improved interaction between EVA28 and the EFB fibre does not give rise to significantly improved stress transfer between the polymer and the fibre. The elongation at break decreases noticeably with increasing fibre content. The reason for this is the same as those discussed above for the decreasing tensile stress at break with increasing fibre content.

Figure 4.26 shows the Young's modulus of the different samples as function of EFB content. It is evident that EVA18 has a higher modulus than EVA28. Since Young's modulus of neat polymers depends on the degree of crystallinity, it is expected that the EVA28 should have a lower modulus. The modulus of the EVA28 samples increases significantly with increasing EFB content, most probably because of an improved interaction between EVA28 and EFB, while that of the EVA18 samples increases only slightly. However, it seems as if the improvement in the interaction between EVA28 and EFB was not significant enough to overcome the inherent weak properties of EVA28. The most probable reasons for the slight increase in the case of EVA18 is (i) the insufficient wetting of the fibre by the polymer, and (ii) the already high modulus of EVA18 as a result of its higher crystallinity.

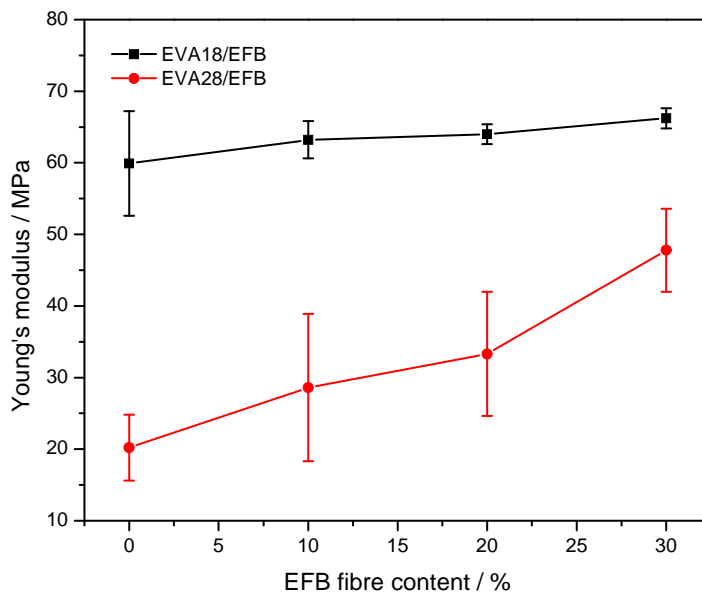


**Figure 4.26** Young's modulus of the different composites as a function of EFB fibre content

In summary it may be pointed out that the presence and amount of EFB fibre influenced the stress and strain at break of EVA18 and EVA28 in a similar way. Although EVA28 should interact more strongly with the fibre than EVA18, it cannot be seen in the influence of the fibre on these properties. The influence of EFB on the Young's modulus is more significant in the case of EVA28. It seems as if the improved interaction between EVA28 and EFB allowed enough stress transfer for the Young's modulus to improve more significantly in this case.

#### 4.7 References

1. S.K. Nayak, S. Mohanty, S.K. Samal. Influence of interfacial adhesion on the structural and mechanical behaviour of PP-banana/glass hybrid composites. *Polymer Composites* 2010; 31:1247-1257.  
DOI: 10.1002/pc.20914
2. H.D. Rozman, A.R. Rozyanty, G.S. Tay, R.N. Kumar. The effect of glycidyl methacrylate treatment of empty fruit bunch (EFB) on the properties of ultra-violet radiation cured EFB-unsaturated polyester composite. *Journal of Applied Polymer Science* 2010; 115:2677-2682.  
DOI: 10.1002/app.29791
3. P. Antich, A. Vázquez, I. Mondragon, C. Bernal. Mechanical behaviour of high impact polystyrene reinforced with short sisal fibres. *Composites: Part A* 2006; 37:139-150.  
DOI: 10.1016/j.compositesa.2004.12.002
4. G. Canché-Escamilla, G. Rodríguez-Trujillo, P.J. Herrera-Franco, E. Mendizábal, J.E. Puig. Preparation and characterization of henequen cellulose grafted with methyl methacrylate and its application in composites. *Journal of Applied Polymer Science* 1997; 66:339-346.  
DOI: 0021-8995/97/020339-08
5. M.Z.M. Yusoff, M.S. Salit, N. Ismail, R. Wirawan. Mechanical properties of short random oil palm fibre reinforced epoxy composites. *Sains Malaysian* 2010; 39:87-92.
6. H.P.S. Abdul-Khalil, S. Hanida, C.W. Kang, N.A. Nik-Fuaad. Agro-hybrid composite: the effects on mechanical and physical properties of oil palm fibre (EFB)/glass hybrid reinforced polyester composites. *Journal of Reinforced Plastics and Composites* 2007; 26(2):203-217.

- DOI: 10.1177/0731684407070027
7. H.D. Rozman, G.S. Tay, A. Abubakar, R.N. Kumar. Tensile properties of oil palm empty fruit bunch polyurethane composites. *European Polymer Journal* 2001; 37:1759-1765.  
DOI: S0014-3057(01)00063-5
  8. R.M.N. Arib, S.M. Sapuan, M.M.H.M. Ahmad, M.T. Paridah, H.M.D. Khairul-Zaman. Mechanical properties of pineapple leaf fibre reinforced polypropylene composites. *Materials and Design* 2006; 27:391-396.  
DOI: 10.1016/j.matdes.2004.11.009
  9. S.M. Lee, D. Cho, W.H. Park, S.G. Lee, S.O. Han, L.T. Drzal. Novel silk/poly(butylene succinate) biocomposites: The effect of short fibre content on their mechanical and thermal properties. *Composites Science and Technology* 2005; 65:647-657.  
DOI: 10.1016/j.compscitech.2004.09.023
  10. C.T. Ratnam, G. Raju, W.M.Z. Wan-Yunus. Oil palm empty fruit bunch (OPEFB) fibre reinforced PVC/ENR blend – electron beam irradiation. *Nuclear Instruments and Methods in Physics Research B* 2007; 265:510-514.  
DOI: 10.1016/j.nimb.2007.09.045
  11. H. Ismail, R.M. Jaffri. Physico-mechanical properties of oil palm wood flour filled natural rubber composites. *Polymer Testing* 1999; 18:381-388.  
DOI: S0142-9418(98)00031-2
  12. P.J. Herrera-Franco, A. Valadez-González. Mechanical properties of continuous natural fibre-reinforced polymer composites. *Composites: Part A* 2004; 35:339-345.  
DOI: 10.1016/j.compositesa.2003.09.012
  13. H.D. Rozman, K.W. Tan, R.N. Kumar, A. Abubakar, Z.A. Mohd. Ishak, H. Ismail. The effect of lignin as a compatibilizer on the physical properties of coconut fibre-polypropylene composites. *European Polymer Journal* 2000; 36:1483-1494.  
DOI: S0014-3057(99)00200-1
  14. L.Y. Mwaikambo, M.P. Ansell. Hemp fibre reinforced cashew nut shell liquid composites. *Composites Science and Technology* 2003; 63:1297-1305.  
DOI: 10.1016/S0266-3538(03)00101-5
  15. S. Chen, J. Zhang, J. Su. Effect of damp-heat aging on the properties of ethylene vinyl acetate copolymer and ethylene acrylic acid copolymer blends. *Journal of Applied Polymer Science* 2009; 114:3110-3117.



- DOI: 10.1002/app.30859
16. S.P. Tambe, S.K. Singh, M. Patri, D. Kumar. Ethylene vinyl acetate and ethylene vinyl alcohol copolymer for thermal spray coating application. *Progress in Organic Coatings* 2008; 62:382-386.  
DOI: 10.1016/j.porgcoat.2008.02.006
  17. N.S. Allen, M. Edge, M. Rodriguez, C.M. Liauw, E. Fontan. Aspects of the thermal oxidation of ethylene vinyl acetate copolymer. *Polymer Degradation and Stability* 2000; 68:363-371.  
DOI: S0141-3910(00)00020-3
  18. M.M.U. Haque, M. Pracella. Reactive compatibilization of composites of ethylene-vinyl acetate copolymers with cellulose fibres. *Composites: Part A* 2010; 41:1545-1550.  
DOI: 10.1016/j.compositesa.2010.07.001  
DOI: S0924-2031(97)00010-6
  19. L.Y. Mwaikambo, M.P. Ansell. Chemical modification of hemp, sisal, jute, and kapok fibres by alkalization. *Journal of Applied Polymer Science* 2002; 84:2222-2234.  
DOI: 10.1002/app.10460
  20. D.S. Marathe, P.S. Joshi. Characterization of highly filled wood flour-PVC composites: Morphological and thermal studies. *Journal of Applied Polymer Science* 2009; 114:90-96.  
DOI: 10.1002/app.30452
  21. D.G. Dikobe, A.S. Luyt. Morphology and properties of polypropylene/ethylene vinyl acetate copolymer/wood powder blend composites. *eXPRESS Polymer Letters* 2009; 3(3):190-199.  
DOI: 10.3144/expresspolymlett.2009.24
  22. M. Pracella, M.M.-U. Haque, V. Alvarez. Compatibilization and properties of EVA copolymers containing surface-functionalized cellulose microfibers. *Macromolecular Materials and Engineering* 2010; 295:949-957.  
DOI: 10.1002/mame.201000175
  23. G. Takidis, D.N. Bikiaris, G.Z. Papageorgiou, D.S. Achilias, I. Sideridou. Compatibility of low density polyethylene/poly(ethylene-co-vinyl acetate) binary blends prepared by melt mixing. *Journal of Applied Polymer Science* 2003; 90:841-852.

24. X.M. Shi, J. Zhang, J. Jin, S.J. Chen. Non-isothermal crystallization and melting of ethylene vinyl acetate copolymers with different vinyl acetate contents. *eXPRESS Polymer Letters* 2008; 2(9):623-629.  
DOI: 10.3144/expresspolymlett.2008.75
25. H.A. Khonakdar, U. Wagenknecht, S.H. Jafari, R. Hässler, H. Eslami. Dynamic mechanical properties and morphology of polyethylene/ethylene vinyl acetate copolymer blends. *Advances in Polymer Technology* 2004; 23:307-315.  
DOI: 10.1002/adv.20019
26. J. Jin, S.J. Chen, J. Zhang. Non-isothermal crystallization kinetics of partially miscible ethylene-vinyl acetate copolymer/low density polyethylene blends. *eXPRESS Polymer Letters* 2010; 4(3):141-152.  
DOI: 10.3144/expresspolymlett.2010.19
27. M.E. Malunka, A.S. Luyt, H. Krump. Preparation and characterization of EVA sisal fibre composites. *Journal of Applied Polymer Science* 2006; 100:1607-1617.  
DOI: 10.1002/app.23650
28. G.D. Vilakazi, A.K. Mishra, S.B. Mishra, B.B. Mamba, J.M. Thwala. Influence of TiO<sub>2</sub>-modification on the mechanical and thermal properties of sugarcane bagasse-EVA composites. *Journal of Inorganic and Organometallic Polymers and Materials* 2010; 20:802-808.  
DOI: 10.1007/s.10904-010-9398-x
29. A. Arsac, C. Carrot, J. Guillet. Determination of primary relaxation temperatures and melting points of ethylene vinyl acetate copolymers. *Journal of Thermal Analysis and Calorimetry* 2000; 61:681-685.  
DOI: 1418-2874/2000
30. R.C.L. Dutra, B.G. Soares. Determination of the vinyl mercaptoacetate content in poly(ethylene-co-vinyl acetate-co-vinyl mercaptoacetate) (EVASH) by TGA analysis and FTIR spectroscopy. *Polymer Bulletin* 1998; 41:61-67.  
DOI: 10.1007/s002890050333
31. B. Rimez, H. Rahier, G. Van-Assche, T. Artoos, M. Biesemans, B. Van-Mele. The thermal degradation of poly(vinyl acetate) and poly(ethylene-co-vinyl acetate), Part I: Experimental study of the degradation mechanism. *Polymer Degradation and Stability* 2008; 93:800-810.  
DOI: 10.1016/j.polymdegradstab.2008.01.010

32. D.G. Dikobe, A.S. Luyt. Effect of filler content and size on the properties of ethylene vinyl acetate copolymer wood fibre composites. *Journal of Applied Polymer Science* 2007; 103:3645-3654.  
DOI: 10.1002/app.25513
33. M.F. Rosa, B.-S. Chiou, E.S. Medeiros, D.F. Wood, T.G. Williams, L.H.C. Mattoso, W.J. Orts, S.H. Imam. Effect of fibre treatments on tensile and thermal properties of starch/ethylene vinyl alcohol copolymers/coir biocomposites. *Bioresource Technology* 2009; 100:5196-5202.  
DOI: 10.1016/j.biortech.2009.03.085
34. B. Li, J. He. Investigation of mechanical property, flame retardancy and thermal degradation of LLDPE-wood fibre composites. *Polymer Degradation and Stability* 2004; 83:241-246.  
DOI: 10.1016/S0141-3910(03)00268-4
35. W. Zhang, D. Chen, Q. Zhao, Y. Fang. Effects of different kinds of clay and different vinyl acetate content on the morphology and properties of EVA/clay nanocomposites. *Polymer* 2003; 44:7953-7961.  
DOI: 10.1016/j.polymer.2003.10.046
36. R.R.N. Sailaja. Mechanical and thermal properties of bleached kraft pulp-LDPE composites: Effect of epoxy functionalized compatibilizer. *Composites Science and Technology* 2006; 66:2039-2048.  
DOI: 10.1016/j.compscitech.2006.01.029
37. N.C. Das, T.K. Chaki, D. Khastgri. Effect of filler treatment and crosslinking on mechanical and dynamic mechanical properties and electrical conductivity of carbon black-filled ethylene vinyl acetate copolymer composites. *Journal of Applied Polymer Science* 2003; 90:2073-2082.  
DOI: 10.1002/app.12811
38. M. Sethi, N.K. Gupta, A.K. Srivastava. Dynamic mechanical analysis of polyethylene and ethylene vinyl acetate copolymer blends irradiated by electron beam. *Journal of Applied Polymer Science* 2002; 86:2429-2434.  
DOI: 10.1002/app.10940
39. B. John, K.T. Varughese, Z. Oommen, P. Pötschke, S. Thomas. Dynamic mechanical behaviour of high-density polyethylene/ethylene vinyl acetate copolymer blends: The effects of the blend ratio, reactive compatibilization, and dynamic vulcanization. *Journal of Applied Polymer Science* 2003; 87:2083-2099.

- DOI: 10.1002/app.11458
40. D. Ray, B.K. Sarkar, S. Das, A.K. Rana. Dynamic mechanical and thermal analysis of vinylester resin matrix composites reinforced with untreated and alkali treated jute fibres. *Composites Science and Technology* 2002; 62:911-917.  
DOI: S0266-3538(02)00005-2
  41. O. Grigoryva, A. Fainleib, O. Starostenko, A. Tolstov, W. Brostow. Thermoplastic elastomers from rubber and recycled polyethylene: Chemical reactions at interphases for property enhancement. *Polymer International* 2004; 53:1693-1703.  
DOI: 10.1002/pi.1530
  42. D.F. Caulfield, D. Feng, S. Prabawa, R.A. Young, A.R. Sanadi. Interphase effects on the mechanical and physical aspects of natural fibre composites. *Die Angewandte Makromolekulare Chemie* 1999; 272:57-64.  
DOI: 0003-3146/99/0112-0057
  43. H.S. Kim, S. Kim, H.J. Kim, H.S. Yang. Thermal properties of bio-flour-filled polyolefin composites with different compatibilizing agent type and content. *Thermochimica Acta* 2006; 451:181-188.  
DOI: 10.1016/j.tca.2006.09.013
  44. V.G. Geethamma, G. Kalaprasad, G. Groeninckx, S. Thomas. Dynamic mechanical behaviour of short coir fibre reinforced natural rubber composites. *Composites: Part A* 2005; 36:1499-1506.  
DOI: 10.1016/j.compositesa.2005.03.004
  45. M. Behzad, M. Tajvidi, G. Ehrahimi, R.H. Falk. Dynamic mechanical analysis of compatibilizer effect on the mechanical properties of wood flour-high density polyethylene composites. *International Journal of Engineering Transactions B: Applications* 2004; 17(1):95-104.
  46. E. Passaglia, S. Coiai, G. Giordani, E. Taburoni, L. Fambri, V. Pagani, M. Penco. Modulated crosslinking of polyolefins through radical processes in the melt. *Macromolecular Materials and Engineering* 2004; 289:809-817.  
DOI: 10.1002/mame.200400155
  47. K.P. Menard. *Dynamic Mechanical Analysis: A Practical Introduction*. CRC Press LLC, Boca Raton, Florida (1999).  
ISBN: 0-8493-8688-8
  48. F.W. Billmeyer. *Textbook of Polymer Science*, 3<sup>rd</sup> edition, John Wiley & Sons, Inc., Canada (1976).

## CHAPTER 5

### CONCLUSIONS

The objective of this study was to investigate composites based on EVA copolymers and Malaysian EFB fibre, and to study the effects of the fibre content and the vinyl acetate (VA) contents of the EVA copolymers on the thermal and mechanical properties of the composites. Another objective was to explain these observations in terms of the morphology and possible interactions between the Malaysian EFB fibre and the EVA copolymer.

#### 5.1 Comparison of the EVA copolymers

The peak temperatures of melting and crystallization, as well as the melting and crystallization enthalpies decreased considerably with an increase in VA content. The EVA18 generally showed higher melting and crystallization temperatures than EVA28. The EVA18 has a significantly higher crystallinity than the EVA28, indicating that the presence of VA groups inhibits the crystallization of EVA. Since EVA18 had better resolved melting and crystallization peaks than EVA28, it has a narrower crystal size distribution than EVA28. EVA18 is more thermally stable than EVA28, due to its higher crystallinity. Both these copolymers showed no residue remaining after heating to 600 °C in nitrogen. The storage modulus and loss modulus for both neat EVA18 and EVA28 samples decreased with an increase in the temperature. EVA18 showed higher storage modulus values than EVA28. EVA28 showed a third relaxation, probably an  $\alpha'$ -relaxation around 50 °C in both the E' and E'' curves, which is related to slippage between the crystallites of the sample. The EVA28 had a more resolved  $\beta$ -relaxation peak than the EVA18, but a less intense  $\alpha$ -peak. There was an observed shift in the  $T_g$  to lower temperatures with an increase in the VA content.

The stress-strain curves of both these polymers showed strain hardening, but that of EVA18 was more significant. EVA18 has a better toughness than EVA28, and thus absorbed more energy before breakage. Both the EVA copolymers did not display a clear yield point and also no neck formation during stretching. EVA18 showed higher stress at break and Young's modulus values, but lower elongation at break, than EVA28.

## 5.2 EVA/EFB composites

For EVA/EFB composites, there seems to be quite intimate contact between the EVA18 and the EFB, although some fibre pull-outs creating holes with smooth walls in the EVA matrix were observed. The presence of a very small void around the fibre was noticed in the case of the EVA18 samples, while for EVA28 there were no fibre pull-outs resulting from the fracturing of the composites and no voids around the fibres. The FTIR spectra of the EVA/EFB composites show all the characteristic peaks for both pure EVA and EFB, and despite a slight shift in the carbonyl peaks, it was not possible to conclusively confirm interactions between the polymer and the fibre from the FTIR results.

The incorporation of EFB fibre had very little influence on the melting and crystallization behaviour of both EVA18 and EVA28. Although EVA28 seems to interact more strongly with the fibre than EVA18, it cannot be seen in the influence of the fibre on the melting and crystallization behaviour of these two copolymers. The crystallinity values of the EVA18 composites were higher than those of the EVA28 composites. The EVA copolymers were more thermally stable than their respective composites. The fibre decomposition seems to be impeded when mixed with EVA due to the higher thermal stability of the matrix. No real difference was observed between EVA28 and its composites in the decomposition rate of the last step, while in the case of EVA18 there was a clear decrease in the decomposition rate with increasing EFB content. The amount of char residue formed increased with an increase in the EFB fibre content.

The storage modulus values below  $T_g$  were different for the different samples, and there was no trend with respect to the presence and amount of fibre in both EVA copolymers. Above the  $T_g$  the  $E'$  values increased with increasing fibre content, but decreased with increasing temperature. The loss modulus curves showed the same trend as was observed for the storage modulus. The glass transition temperature of the EVA copolymers observably increased with an increase in EFB content. The intensity of the  $\beta$ -relaxation peak decreased with increasing EFB content in both EVA18 and EVA28 composites. There was also a decrease in the total damping during the transitions with an increase in the EFB fibre content for both the EVA copolymers. The  $\alpha$ -relaxation peak for EVA28 and its composites was less intense than the  $\beta$ -relaxation peak, compared to the curves for EVA18 and its composites. The temperature of the  $\alpha$ -peak, which is related to relaxations of the interlamellar amorphous polymer chains,

was observably lower for the 30% fibre containing sample. There was a third relaxation peak, which may have been related to the  $\alpha'$ -relaxation at 50 °C. This was observable in both the loss modulus and the  $\tan \delta$  curves.

The stress-strain curves for both polymers showed a decreasing ductility with an increase in EFB content. The curves of EVA18 showed more pronounced strain hardening than the EVA28 samples. The incorporation of the EFB fibres observably reduced the strain hardening of the materials. The tensile stress and elongation at break decreased significantly with the incorporation of EFB fibre for both polymers. The presence and amount of EFB fibre influenced the stress and strain at break of EVA18 and EVA28 in a similar way. The EVA18 composites had higher modulus values than the EVA28 composites. The Young's modulus of the EVA28 samples increased significantly with increasing EFB content, while in the case of EVA18 there was a much less significant increase.

### **5.3 Final conclusion**

In summary it may be concluded that EVA18 seems to have better mechanical and thermal properties than EVA28. Although better interaction between EVA28 and EFB was expected, and observed in the SEM pictures, this interaction was not significant enough to produce composites with better properties than the comparable EVA18 composites, because of the inherent weak properties of EVA28. In this case it is probably better to recommend the use of EVA18 for the preparation of EVA/natural fibre composites.

## ACKNOWLEDGEMENTS

First and foremost I would like to offer my unreserved gratitude and praises to **Almighty God** for His kind blessings and the undying strength bestowed upon me during the course of this study.

I would like to extend the sense of appreciation to my supervisor, **Prof. Adriaan Stephanus Luyt**, for his great efforts, constant encouragement, guidance and assistance during my research period. My special acknowledgement to him for being so inspirational and understanding with regard to all research aspects or focus areas. His unwavering support and hard work was amazing throughout the entire period of my study. I sincerely express my deepest gratitude for his availability coupled with the greatest ideas and fresh thoughts for this project to become a massive success. Throughout my thesis-writing period, he emphasized on the project insight and knowledge, sound advice, and a high-quality research work.

I wish to highly acknowledge the support from the University of the Free State (Qwa-Qwa Campus) for providing the golden opportunity to undertake this work.

My utmost acknowledgement goes to the **National Student Financial Aid Scheme (NSFAS) and National Research Foundation (NRF)** for their financial support throughout my entire undergraduate and postgraduate studies.

My greatest thanks to **TATA in Africa** for their prestigious scholarship award as a financial support for this study.

All special thanks to the entire Chemistry department crew for the collective efforts, maximum co-operation, and help displayed during the whole research project.

In the **Polymer Institute, Slovak Academy of Sciences**, I basically want to thank Dr. I. Novák, Dr. Igor Krupa in collaboration with Prof. A.S. Luyt, Mr. Marek, and all other individuals for their hospitality and financial support during my stay in Slovakia for ChemiZi (Chemistry conference in High Tatras Mountains Slovakia ) 2009 and the research visit.



During this work I managed to interact with many polymer scientists for whom I have great regard, and I wish to extend my warmest thanks to all those who have helped me with my work, especially Dr. Vladimir Djokovic (from Serbia), Prof. Pasch (Germany, Stellenbosch), Dr. I. Novák, Dr. Igor Krupa (both from Slovakia) , Dr. Kovacs (Hungry-Budapest), Dr. J.A. Molefi (Sasol), Dr. Mamale Hato (CSIR), Dr. P.E. Mallon (Stellenbosch), for their research insights.

Sense of gratitude to all my fellow polymer science research group and colleagues (Dr. S. Ochigbo, Mr. Mohammad Essa Ahmad, Mr. Mfiso Mngomezulu, Mr. Tshwafo Motaung, Mr. Samson Lulu Mohomane, Mr. Lefu Nhlapo, Ms. Julia Puseletso Mofokeng, Mr. Thabang Hendrica Mokhothu, Mr. Thabo Oscar Phelephe, Mr. Bongani Amos Tshabalala, Mr. Bongani Msibi, Mr. Lucky Dlamini, Mr. Jonas Mochane, Mr. Tladi Mofokeng, Mr. Moeketsi Mangwaela, Ms. N. Nhlapo, Ms. Zanele Clarke, Mr. Tsietsi Tsotetsi, Mrs Nomampondomise Molefe and Neo Moji), for all their help, support, interest and valuable inputs.

All special appreciation goes to Mrs. M. Mokoena and Mrs. D.G. Masiangaoko for being inspirational and supportive mentors inside as well as outside the research box, particularly during the NRF internship duration.

I would also like to appreciate the sensational work done by Ms Julia Puseletso Mofokeng (Research Assistant) and Mr Mohammad Essa Ahmad by ensuring I have the thorough comprehensive operation of various analytical techniques in the research lab.

I would also like to thank Bo-mama in the Faculty of Natural and Agricultural Sciences for their moral support in ensuring clean research labs as well as helping us with the master-key and roll papers: Mme Malehlonolo Moremi, Mme Madibusing Lemeko and Mme Maani Motaung.

For the job well-done, heads off for the maintenance personalities particularly Mr. Motaung, Songemame and his colleagues for taking care of the lawn next to the research Lab and the Staff parking outside.

I am grateful to the Faculty programme secretary and programme officer, Mrs Marlize Jackson and Mpho Leripa for their unself-centred service rendered and moral support.

From the Department of Information and Technology (Computer services), the credit must be given to Mr. late Charles Masondo and Mr. John Setai as well as Mr. Isaac Mokgotla for fixing my computer problems every now and then.

I would like to gratefully acknowledge the inspiration and motivation from Dr R. Ocaya, Dr Mothudi, Dr S. Dhlamini, Mr D.B. Bem, Mr. J.J. Dolo and Mr Joel Selepe Motlounge, from Physics department.

I wish to thank greatly my best friends (The Late Mr. Khambule Themba, Boitumelo Anderson Tsotetsi, Kamoho Jokolele Mokhatla, Lehlohonolo Fortune Koao, Motseki Mahlakodisane, Mahadi Mahlakodisane, Teboho Dhlamini, Ncubuka Langa, Elias Monareng, Molaudi Molefe, Doctor Motlokwa, Maqaleng Joseph Mbule, Kauwane Motaung, Mohapi Thebe, Fusi Isaac Mphuthi, Kananelo Samuel Sefadi, Kabelo Gift Sefadi, Ntebaleng Eva Molise), for helping me get through the tough times, for all the good ideas shared, acquired knowledge via strong interaction, moral support, and encouragement.

All the vibrant and capable individuals at Motheo Foundation Academy's unwavering support and positive development made in my studies.

All the sincere thanks to my former Seroali educators (Mrs Mahlakodisane, Mrs Mabe, Mrs Rakatsenyana, Mrs Ramakatane, Mrs Matlala, Mrs Molete, Mrs Mlangeni, Mr Moloi, Mr Motaung, Mr Thateng, Mr Mothwalo, Mr Mkhwanazi, The late Mr Letsoko, Principal Mr Zeche Maleka, Mr Seobi, and the SGB members) their parental support and guidance throughout the difficulties encountered in my life.

The following are the most important families with their maximum contribution in my studies: Moloi's family, Motaung's family, Mabe's family, Thateng's family, Mlangeni's family and the neighbours around my uncle's house.

Most importantly, the credit must be given to my Parents (The Late Mr. Paul Mahlaku Sefadi and Lonia Madimakatso Sefadi), my uncle (Pule Francis Sefadi) and his wife who serve as my second Mother for more than 12 years now (Limakatso Annalettah Mokoena) for raising me with their love, guidance, support, responsibility, and a lot of encouragement.

All sense of gratitude to all my grandmothers, grandfathers, the extended relatives for everything they have done for me during the tough times.

My genuine thanks to all my honourable siblings Palesa Sefadi, Pontsho Gloria Mokoena, Malefa Alice Sefadi, Telang Eric Nkosi, Tshepo Isaac Mokoena, Lebohang Ernest Mokoena, Tshidi Motwana, Mr. Enock Themba Ngwenya Mokoena, Ausi Jwana, Katlego Mokoena, Tshidiso Sefadi, Sello Sefadi, Tanki Eric Sefadi, and eventually all other people who are not included here.

## APPENDIX

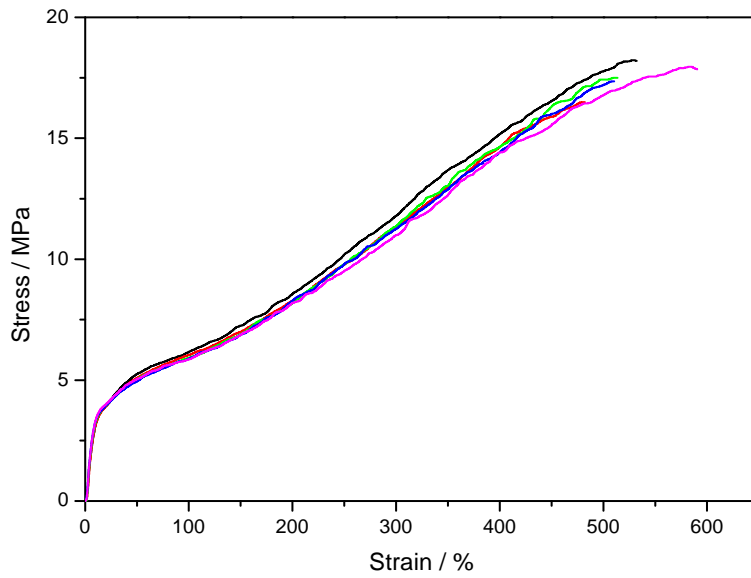


**Figure A.1** Stress-strain curves for EVA18

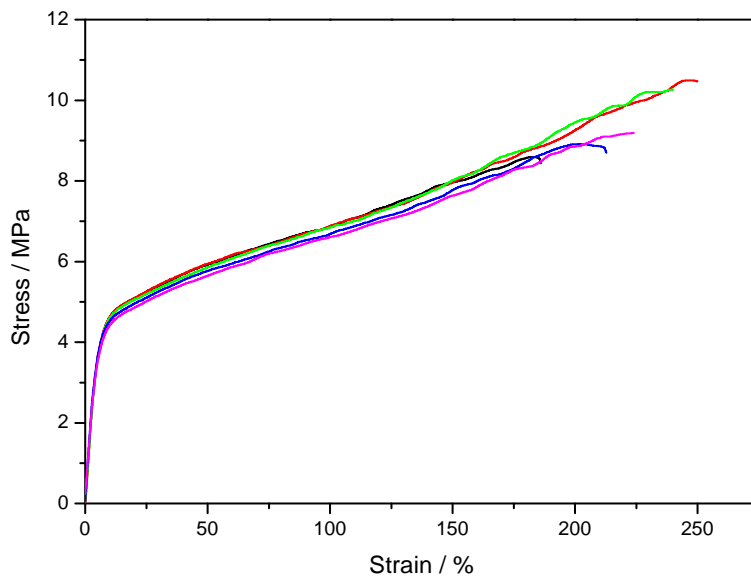


**Figure A.2** Stress-strain curves for 90/10 w/w EVA18/EFB

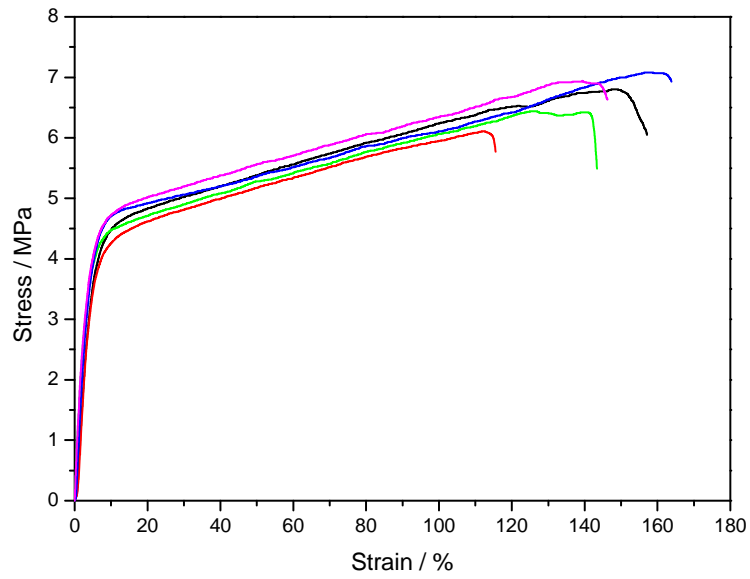


**Figure A.3** Stress-strain curves for 80/20 w/w EVA18/EFB

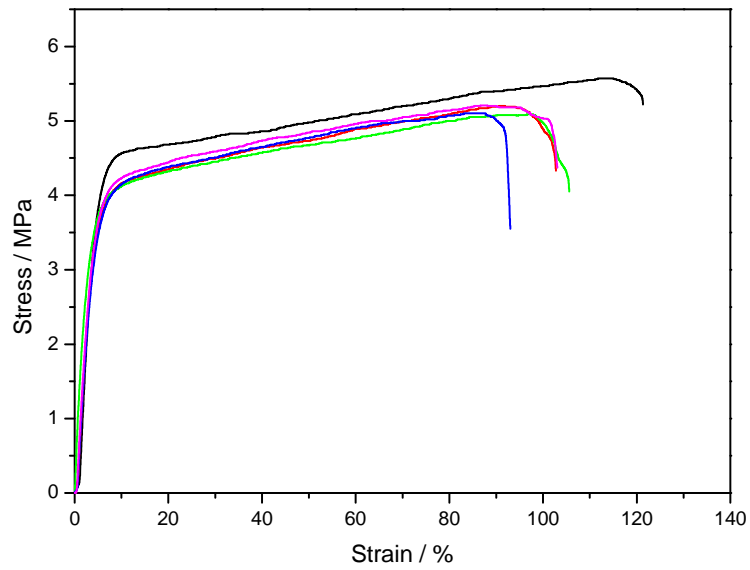


**Figure A.4** Stress-strain curves for 70/30 w/w EVA18/EFB

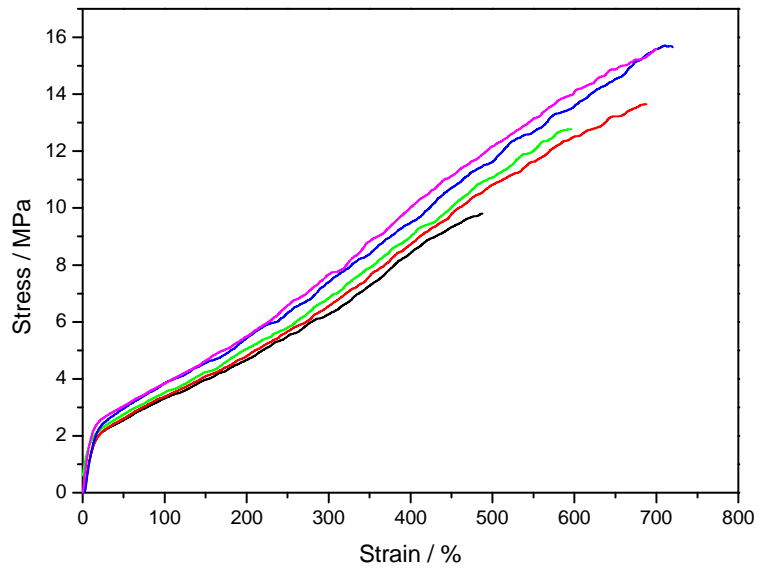


**Figure A.5 Stress-strain curves for EVA28**

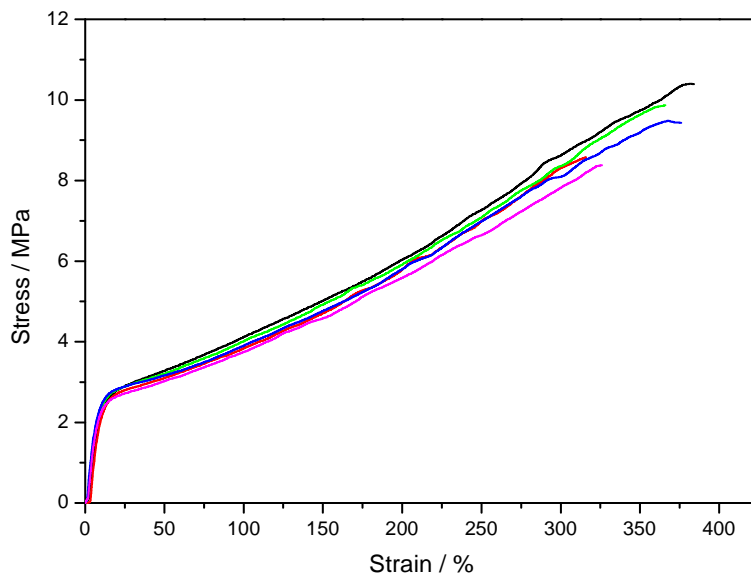


**Figure A.6 Stress-strain curves for 90/10 w/w EVA28/EFB**

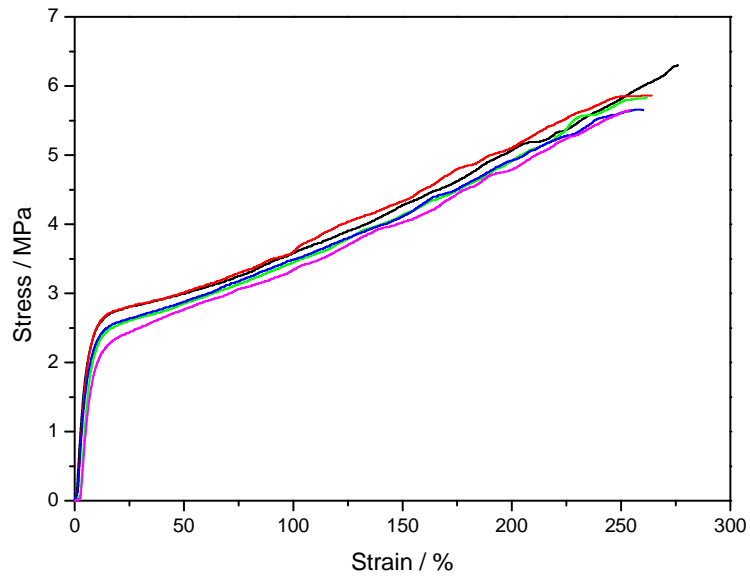


**Figure A.7** Stress-strain curves for 80/20 w/w EVA28/EFB

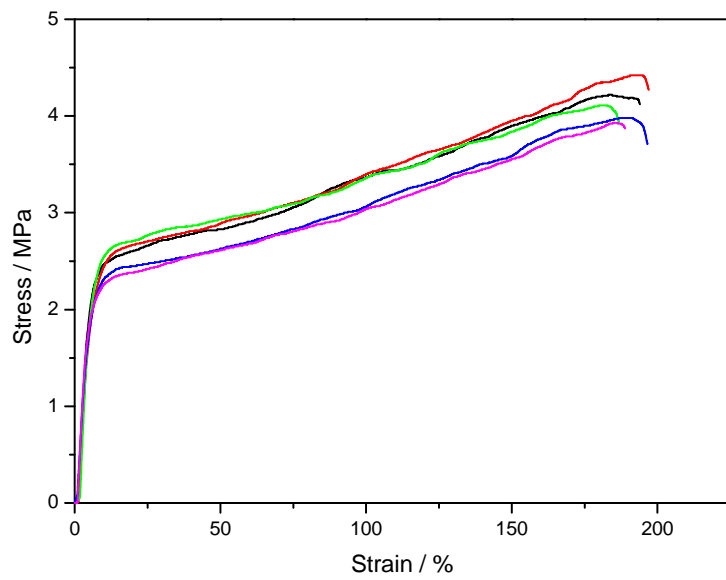


**Figure A.8** Stress-strain curves for 70/30 w/w EVA28/EFB